

On Arctic and Atlantic halocline interactions in Baffin Bay

Julie Lobb

M.Sc. (2000), B.Sc. (1997), McGill University

A thesis submitted in partial fulfillment of the requirements for the degree of

DOCTOR OF PHILOSOPHY

In the Department of Earth and Ocean Sciences

© Julie Lobb, 2004

University of Victoria

All rights reserved. This thesis may not be reproduced in whole or in part, by photocopy or other means, without permission of the author.

Supervisors: Dr. A.J. Weaver and Dr. E.C. Carmack

Abstract

Physical measurements from 1928-2001 and geochemical measurements from 1997 were used to examine water interaction and mixing in the Baffin Bay region. Interactions between inputs from the Canadian Archipelago and the North Atlantic were apparent throughout the study area, but most notably near the Lancaster Sound/North Water region and Davis Strait. The Lancaster Sound/North Water region appeared determinant in establishing the downstream structure of the Baffin Current, whereas Davis Strait regulated both exchange with the North Atlantic and the recirculation of Baffin Current waters toward central Baffin Bay. Results from an advective-diffusive model indicated that Canadian Archipelago outflow might play a dominant role in maintaining the intermediate and deep structures of central Baffin Bay. Further to this, a hypothesis was developed relating central basin structure to variations in Baffin Current flow and recirculation near Davis Strait. That is, increases in Baffin Current flow would cause the following responses within Baffin Bay: an eastward shift in the West Greenland Current/Baffin Current boundary at Davis Strait; a deepening of the warm halocline of West Greenland Current waters entering Baffin Bay; an increase in Baffin Bay recirculation below the Davis Strait sill depth; and enhanced diffusion of warm, salty properties to the deep. In contrast, relatively diminished Baffin Current flow would cause the following: a shallower warm halocline for West Greenland Current input; less recirculation below the Davis Strait sill depth; and moderate diffusion of relatively cool, fresh properties to the deep. Oscillation between these responses appears to maintain the intermediate (700-1500 m) structure of waters in the central basin.

Contents

Abstract	ii
Contents	iv
List of Tables	vi
List of Figures	viii
1 Introduction	1
2 Background	9
2.1 Baffin Bay region source waters	9
2.1.1 North Atlantic source waters	9
2.1.2 Arctic Ocean source waters	12
2.2 Waters within the Baffin Bay region	17
3 Methodology	25
3.1 Analysis Tools and Nomenclature	25
3.2 Physical Data	28
3.3 Geochemical Data	39
4 Observations	44
4.1 Geographical variations in halocline structure	44
4.2 Zone of halocline convergence	56
4.3 Transformation processes	66
4.4 Geochemical structure	79

4.5 Temporal patterns in halocline structure: Eastern Davis Strait	90
5 Discussion	105
5.1 Summary of mixing transformations	105
5.2 Advective-diffusive model	109
5.3 Recirculation and the deep halocline of the central basin: a hypothesis	119
6 Conclusions	126
Bibliography	129
Appendix	138

List of Tables

Table 2.1	General nomenclature and associated characteristics used by the literature to describe waters of the Baffin Bay region. Based on works by Bailey (1956), Muench (1971), Addison (1987) and Bourke et al (1989).	20
Table 4.1	CTD data availability for the six regions presented in Chapter 4.1. The years depicted in Figs. 4.1-4.6 are indicated in bold and were chosen because they offered the best spatial coverage for each region.	45
Table 4.2	Summary of Baffin Bay θ -S properties based on Chapter 4.1 geographical grouping.	55
Table 4.3	CTD data availability for the six frontal sections presented in Chapter 4.2. Years depicted in Figs. 4.9-4.14 are in bold.	58
Table 4.4	Comparison of CFC concentrations between 1983 (Wallace, 1985) and 1997 for Station B1.	90
Table 4.5	Comparison of WH properties for WGC waters along Davis Strait in 1987, 1988, 1990 and 1997.	104
Table 5.1	Summary of the halocline anatomy of Baffin Bay inflows (via eastern Davis Strait, and the Canadian Archipelago) and outflow (via western Davis Strait).	106
Table 5.2	Input parameters used in finite-difference approximation of	113

advective-diffusive model. θ and S values were obtained from August 1997 CTD data.

Table 5.3 Modeled θ and S values corresponding to the least combined absolute error with respect to observed θ and S values in 1997. The K value used was $7.5 \times 10^{-9} \text{ m}^2/\text{s}$ 115

List of Figures

Figure 1.1	Regional setting and place names of Baffin Bay and adjacent seas.	3
Figure 1.2	Major currents of the Baffin Bay region.	4
Figure 2.1	Schematic map showing paths for the North Atlantic components which compose the WGC.	10
Figure 2.2	Map showing bathymetry for the Arctic Ocean and circulation of its Atlantic-origin (red) and Pacific-origin (blue) waters.	13
Figure 2.3	a) Water signatures for the four Arctic basins (borrowed from McLaughlin, 1996). Arctic Surface Water features for the Canada and Makarov basins (which are the primary immediate upstream basins to the Canadian Archipelago and Baffin Bay region) are labeled in blue and green. b) Water signatures for the Canada Basin (McLaughlin, 1996), Smith Sound and Jones Sound (MEDS). Data for these curves were obtained in 1997.	14
Figure 3.1	Schematic potential temperature-salinity diagram illustrating the main nomenclature terms used throughout this dissertation.	26
Figure 3.2	a) Location of bottle data stations; b) Location of CTD data stations (obtained and retained from MEDS archive).	29
Figure 3.3	Potential temperature versus salinity scatter plots for all retained bottle (above) and CTD (below) data in a) Eastern	32

Davis Strait, b) Melville Bay, c) the North Water region, d) Lancaster Sound, e) the Baffin Island coast, and f) central Baffin Bay.

- | | | |
|------------|--|----|
| Figure 3.4 | Reconstructed source functions for CFC-11, CFC-12, CFC-113 and CCL4. From Walker et al., 2000. | 40 |
| Figure 3.5 | Station locations for August 1997 CFC and dissolved nutrient data. | 41 |
| Figure 4.1 | θ and S properties in Eastern Davis Strait in the a) summer (June, July, August) and b) fall (September, October) of 1990. | 46 |
| Figure 4.2 | θ and S properties in Melville Bay in the a) summer (June, July, August) of 1986 and b) fall (September, October) of 1987. | 47 |
| Figure 4.3 | θ and S properties for the North Water region in the a) summer (June, July, August) of 1998 and b) fall (September, October) of 1999. | 48 |
| Figure 4.4 | θ and S properties for Lancaster Sound in the a) summer (June, July, August) and b) fall (September, October) of 1979. | 51 |
| Figure 4.5 | θ and S properties along the Baffin Island coast in the a) summer (June, July, August) and b) fall (September, October) of 1978. | 52 |
| Figure 4.6 | θ and S properties in central Baffin Bay in the a) summer (June, July, August) of 1997 and b) fall (September, October) | 53 |

	of 1999.	
Figure 4.7	Detail of θ and S properties in central Baffin Bay. Data from August 1997.	54
Figure 4.8	Map of sections described in Chapter 4.2.	57
Figure 4.9	Potential temperature (Tpot-0) and potential density (sigma-0) across section A (Davis Strait). Data from August 1997.	59
Figure 4.10	Potential temperature (Tpot-0) and potential density (sigma-0) across section B (southern Baffin Bay). Data from September 1990.	60
Figure 4.11	Potential temperature (Tpot-0) and potential density (sigma-0) across section C (central Baffin Bay). Data from August 2001.	61
Figure 4.12	Potential temperature (Tpot-0) and potential density (sigma-0) across section D (northern Baffin Bay, North Water region). Data from June 1998.	62
Figure 4.13	Potential temperature (Tpot-0) and potential density (sigma-0) across section E (Lancaster Sound). Data from September 1979.	63
Figure 4.14	Potential temperature (Tpot-0) and potential density (sigma-0) across section F (Lancaster Sound). Data from September 1979.	64
Figure 4.15	a) Regional map of Baffin Bay. B) Close-up of northern Baffin Bay (aka North Water Polynya region) with stations sampled	68

in June 1998 and September 1999. Five additional stations were sampled between Stn. 68 and Stn. 70 in September 1999 (not shown). 600 (solid) and 200m (dotted) isobaths are indicated.

- Figure 4.16 Horizontal distribution of properties and potential temperature-salinity curves for a) June 1998 and b) September 1999. 72
- Figure 4.17 a) θ and b) T_u across the frontal zone in September 1999. Both graphs are plotted on a logarithmic density scale relative to the maximum density in the water column, allowing better resolution of the intrusive features at depth. Density equivalencies are indicated in italic. 75
- Figure 4.18 Estimated changes in density across the frontal zone due to cabelling in September 1999. 77
- Figure 4.19 a) θ and b) CFC-11 versus S for geochemical stations sampled in August 1997. 80
- Figure 4.20 a) Nitrate, b) Silicate, c) Dissolved oxygen, and d) Phosphate versus S for Jones Sound (J3, green) and Smith Sound (S2, purple) in August 1997. 84
- Figure 4.21 Tracer concentrations at Station B1 in central Baffin Bay. 89
- Figure 4.22 Normalized mean winter NAO indices. The top panel indices are based on the difference in normalized sea level pressure 92

between Lisbon, Portugal and Iceland. Indices in the middle panel derive from the principal component of the leading empirical orthogonal function (EOF) of Atlantic sea-level pressure. Indices in the lower panel derive from the principal component of the leading EOF of Northern Hemisphere sea level pressure. Heavy solid lines represent the indices smoothed to remove fluctuations with periods less than 4 years. Modified from Hurrell et al., 2003.

- Figure 4.23 Contoured a) S and b) θ (Tpot-0) time series for Eastern Davis Strait (1966-2000) based on available CTD and bottle data. No data was available for 1970, 1979 and 1994. Data points are indicated with black dots. 94
- Figure 4.24 Schematicized impacts to Baffin Bay of the preferential export hypothesis for Arctic outflow in response to NAO change. 98
- Figure 4.25 Properties along Davis Strait at ~ 67 N in a) 1987, b) 1988, c) 1990 and d) 1997. 99
- Figure 5.1 Waters within and below the WH core of central Baffin Bay lie within a mixing triangle between the WH core of WGC waters (AT), WH waters from the North Water/Lancaster Sound region (AR) and pre-existing Bottom Water (BW). 110
- Figure 5.2 Schematic of 3-box model 111
- Figure 5.3 Absolute error at nodes (1), (2), and (3) as a function of a) 116

theta and b) S values for AT and AR. K was kept constant at 7.5×10^{-9} m²/s. Red dots indicate the original input values for AT and AR listed in Table 5.2.

- Figure 5.4 Combined absolute error for nodes (1), (2), and (3) as a function of Tau 1 and Tau2. Above Panel indicates absolute error values for theta, below for S. K was kept constant at 7.5×10^{-9} m²/s. Red dots indicate the original input values for Tau1 and Tau2 listed in Table 5.2. Red arrows show how increasing Tau2 (via the recirculation of water in the model's middle box) would reduce absolute error. 118
- Figure 5.5 Summary of the impacts of increased Canadian Archipelago outflow on the Baffin Bay region. 121
- Figure 5.6 Potential Temperature and Salinity profiles for BC waters in a) 1979 (weakening NAO index/relatively unfavoured Canadian Archipelago export) and b) 1990 (strengthening NAO index/relatively favoured Canadian Archipelago export). The blue curves correspond to central Baffin Bay (August 1997). 122

1 Introduction

The Baffin Bay region ($690 \times 10^3 \text{ km}^2$), in the Canadian Arctic, is defined to the east by Greenland and to the west by the Islands of Ellesmere, Devon, Bylot and Baffin (Fig. 1.1). It is a significant region for bridging physical, geochemical and biological processes between the Arctic Ocean and the North Atlantic (Smith et al., 1937; Sverdrup et al., 1942; Bailey, 1956; Carmack, 2000; Melling, 2000). To its south, exchange with the Labrador Sea occurs across the 640 m deep and 300 km broad Davis Strait (Smith et al., 1937; Sverdrup et al., 1942). To its north, exchange with the Arctic Ocean occurs across 250 m deep and 55 km wide Smith Sound (via Nares Strait and Kane Basin), 1000 m deep and 55 km wide Lancaster Sound (via M'Clure Strait, Viscount Melville Sound and Barrow Strait) and 700 m deep and 12 km wide Jones Sound (via various passages between the Queen Elizabeth Islands). A 100 m sill in Barrow Strait ultimately limits upstream exchange with the Arctic Ocean via Lancaster Sound, whereas Jones Sound is bound to the east and west by sill depths of 400 m and 200 m, respectively.

The deep (2300 m) central portion of Baffin Bay is bordered on the east by a series of relatively shallow ($\sim 200 \text{ m}$) banks and east-west canyons ($\sim 500 \text{ m}$) extending roughly 400 km from the Greenland coast. To the west, Baffin Island has a 500 m deep and 200 m wide shelf cut by several deep ($\sim 1000 \text{ m}$) trenches. North of 75°N (commonly referred to

as the 'North Water region' or simply 'North Water'), waters extend to 200-400 m with the exception of a 600 m deep north-south canyon that shoals to 250 m in Smith Sound.

Circulation in the Baffin Bay region is driven by two components: a northern-flowing branch of the West Greenland Current (WGC) and a continuation of Arctic Ocean throughflow that is called the Baffin Current (BC) (Fig. 1.2). The WGC originates at the southwestern tip of Greenland with the convergence of waters from the East Greenland Current and the Irminger Current (Smith et al., 1937; Lazier, 1973 & 1988; Lee, 1968; Clarke, 1984; Bourke et al., 1989; Buch, 1990 & 1993, Lazier and Wright, 1993). While most of the WGC branches westward near Davis Strait to join the Labrador Current, a significant portion continues northward along the Greenland coast into Baffin Bay. As it approaches the North Water region, it is augmented by Arctic outflow through Smith, Jones and Lancaster Sounds and turns southward along the Baffin Island coast as the BC, which ultimately exits into the Labrador Sea along the western side of Davis Strait (Rudels, 1986).

The Baffin Bay region has remained largely understudied by the scientific community despite its long-standing history in human whaling/exploration and the recent recognition of its role in regulating downstream convection events in the North Atlantic (Rudels, 1986; Carmack, 2000; Melling, 2000). As a result, several aspects of its oceanography remain unresolved:

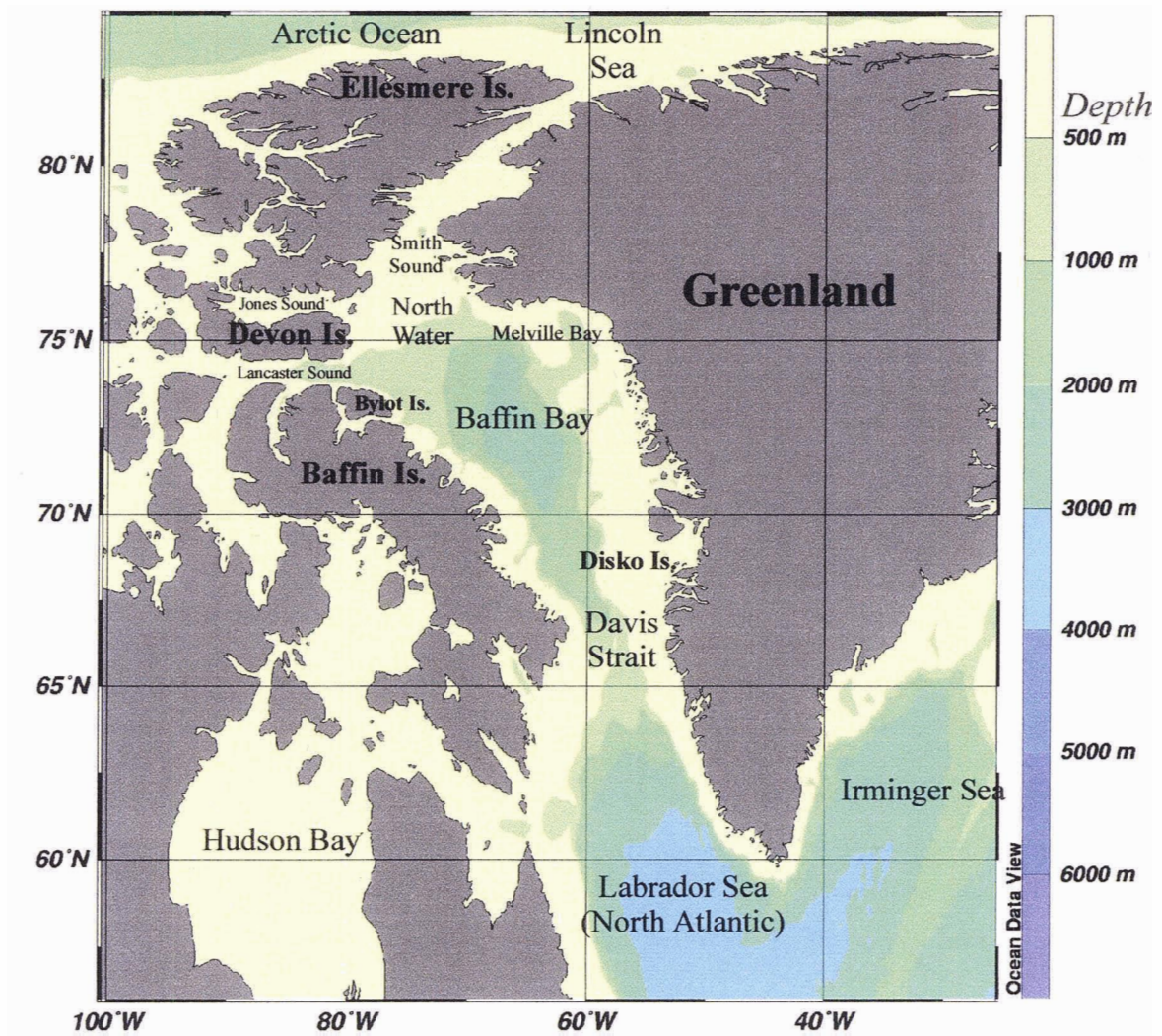


Figure 1.1: Regional setting and place names of Baffin Bay and adjacent seas.

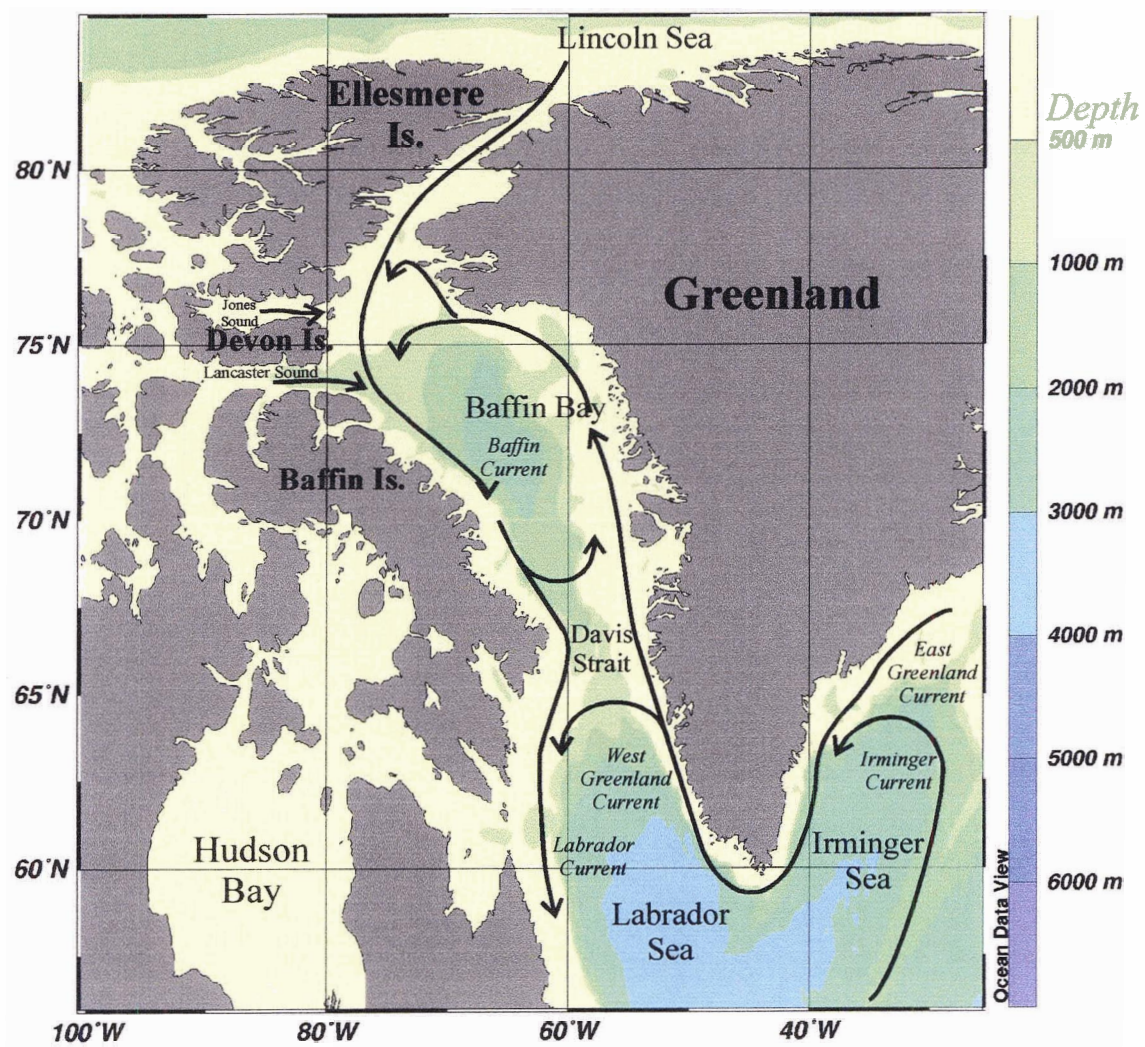


Figure 1.2: Major currents of the Baffin Bay region.

- 1) Although descriptions of water masses and circulation have been made in northern Baffin Bay (Bailey, 1956; Muench, 1971; Sadler, 1976; Bâcle et al., 2002; Melling et al., 2001) and northwestern Baffin Bay (Lemon and Fissel, 1982; Fissel et al., 1981&1982), very few data have been published over the remainder of Baffin Bay (Bailey, 1956; Muench, 1971). This has resulted in the absence of a generally accepted water nomenclature for the region (Tomczak and Godfrey, 1994), as well as a limited understanding of the mixing processes, spatial variability, climatology, and intermediate/near-bottom circulation of its Arctic- and Atlantic-derived components (Addison, 1987; Bâcle et al, 2002; Rudels, 1986);

- 2) Mechanisms leading to the formation of Baffin Bay Deep Water (> 1200 m) and Baffin Bay Bottom Water (> 1800 m) remain speculative. Unresolved hypotheses involving both Atlantic (Sverdrup et al., 1942) and Arctic (Bailey, 1956; Collin, 1965; Palfrey and Day, 1968; Muench, 1971; Sadler, 1976; Bourke et al., 1989; Bourke and Paquette, 1991) sources, and their geochemical implications (Top et al., 1980; Redfield and Friedman, 1969; Tan and Strain, 1980; Coote and Jones, 1982; Jones et al., 1984; Campbell and Yeats, 1982; Jones and Levy, 1981; Ostlund and Hut, 1984, Wallace, 1985) have lead to a limited understanding of Baffin Bay's heat, salt, and geochemical cycles;

- 3) Unlike the adjacent Labrador Sea (Rätz and Stein, 1999; Crawford, 1992; Buch and Hansen, 1988; Hansen and Buch, 1986; Hansen and Hermann, 1965; Buch et al, 1994; Hansen, 1949), few of the relationships between physics and biology have been studied within Baffin Bay. This has lead to an incomplete understanding of regional fisheries.

Thus, there is a need for a complete oceanographic synthesis of the physical, geochemical and biological environment of the Baffin Bay region, not only to further knowledge of local oceanic processes, but to assess Baffin Bay's interdependence on the oceanography of adjacent seas and determine its response to variability in Arctic and Atlantic source properties. In response, this dissertation presents a retrospective analysis of the Baffin Bay region, its water column structures, their sources, their spreading pathways and modifications *en route*, by interrogating physical (conductivity, temperature, depth) data collected between 1928 and 2001 and geochemical (dissolved nitrate, phosphate, silicate, oxygen, CFC-11, CFC-12, CFC-113 and CCl₄) data from August 1997. Specifically, the questions of this dissertation are:

- 1) What are the water column structures over the larger Baffin Bay region as a whole? This question is intended to establish a primary understanding of the relative presence of Arctic and Atlantic-derived waters within the region and the modifications they have undergone from their source regions.

- 2) How are Arctic and Atlantic-derived waters locally modified within the Baffin Bay region? That is, what are the mechanisms responsible for the spreading and mixing of water structures within Baffin Bay.

- 3) How do changes in the relative proportion or characteristics of Arctic- and Atlantic-derived waters impact the characteristics of Baffin Bay's surface, intermediate and deep water structures, and ultimately the characteristics of outflow to the North Atlantic? That is, to develop a hypothesis which illustrates the sensitivity of local mixing mechanisms to variability in Arctic and Atlantic input.

This dissertation will provide a physical oceanographic synthesis of a largely understudied oceanic region. Its findings will contribute to the understanding of high latitude ocean fluxes and mixing processes, questions of critical importance for the development of Global Ocean Models (Griffies et al., 2000). In addition, it will provide a framework for the understanding of advective and vertical fluxes of nutrients, and the exchange of particulate matter and plankton between Arctic and Atlantic basins.

Chapter 2 presents an overview of current Baffin Bay oceanography, including the upstream characteristics of its Arctic and Atlantic inputs, its local circulation, and existing studies of its regional water structures. Chapter 3 outlines the methodology of the thesis, including analysis tools and criteria for the selection, evaluation and synthesis of the data used. Chapter 4 then synthesizes observations made from the data set. These include water

structure descriptions made in terms of geographical variation, frontal interaction, small-scale mixing, geochemical signature, and climatological variability. Together, these descriptions lead to a conceptual summary of water structure transformations within the Baffin Bay region, presented in Chapter 5. Chapter 5 also includes an evaluation of the relative importance of Arctic- and Atlantic-derived waters in maintaining local transformations based on an advection-diffusion model. It concludes with a discussion of the potential impact of large-scale climatic variations in Arctic and Atlantic source waters on the maintenance of local Baffin Bay transformations.

2 Background

2.1 Baffin Bay region source waters

Waters entering the Baffin Bay region through Davis Strait and the Canadian Archipelago take their origin from two upstream basins, the North Atlantic and the Arctic Ocean. Each of these basins contain waters that are unique due to their bathymetry, climatology, current advection, surface exchanges, and mixing history. As a result, the signature of these waters and the modifications they incur *en route* to the Baffin Bay region are also very distinct.

2.1.1 North Atlantic source waters

North Atlantic waters enter the Baffin Bay region from the southwest with the WGC. As the WGC approaches the eastern side of Davis Strait, it bifurcates such that its main branch diverts west to join the Labrador Current and only a minor branch continues northward. Although the vertical volume flow for the WGC across Davis Strait reaches a depth of 500 m, its strongest baroclinic flow¹ occurs in the top 100 m (Muench, 1971) and is estimated at 1 Sv² (Smith et al, 1937).

¹ Circulation associated with horizontal gradients in seawater density.

² 1 Sv = 10⁶ m³/s

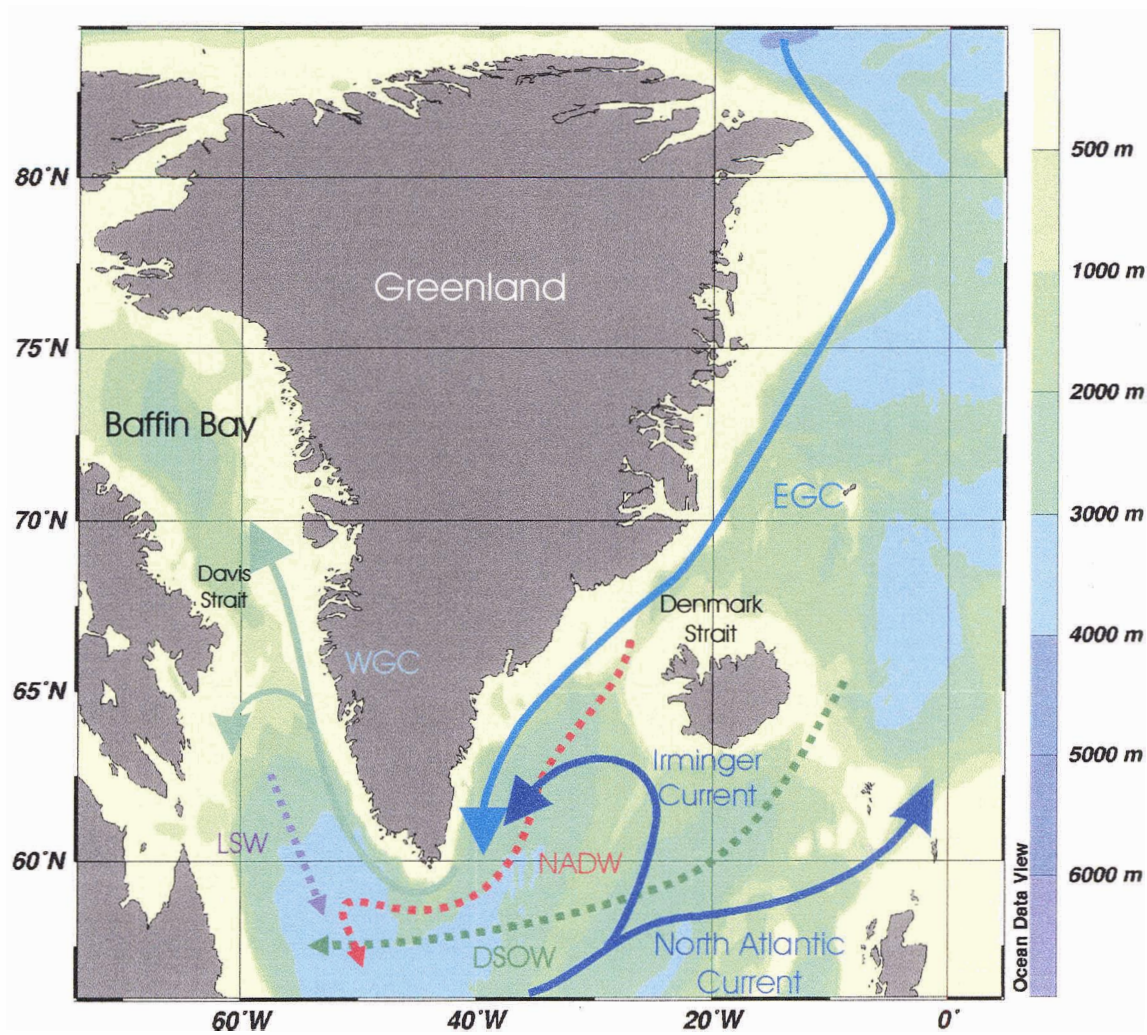


Figure 2.1: Schematic map showing paths for the North Atlantic components which compose the WGC.

Various nomenclatures have been developed to describe North Atlantic waters carried with the WGC (Smith et al., 1937; Killerich, 1943; Lazier, 1973 & 1988; Lee, 1968; Clarke, 1984; Bourke et al., 1989; Buch, 1990 & 1993; Lazier and Wright, 1993). The top 500 m of the WGC is comprised of two components (Fig. 2.1). The upper component originates from the cold *East Greenland Current (EGC)*, the main conduit for waters exiting the Arctic Ocean and the Nordic Seas into the North Atlantic (Rudels et al., 2002). Waters of this component are characterised by $3.0 < \theta < 5.5$ °C, and $34.4 < S < 35.0$ (Lazier, 1973). The lower component is from the *Irminger Current*, which is an eastward side-branch of the North Atlantic Current. This water (classically referred to as 'Irminger Water'; Smith et al., 1937; Killerich, 1943) is characterised at its top by $\theta \sim 5.5$ °C and $S \sim 35.0$ and at its bottom by $\theta \sim 3.5$ °C and $S \sim 34.9$.

Below 500 m, WGC waters consist of three other components. Their entry into the Baffin Bay region are prohibited, however, by the 500 m sill depth in eastern Davis Strait. The upper component is *Labrador Sea Water (LSW)*, which is formed within the Labrador Sea via deep convection and is defined by $S < 34.95$ and $3.0 < \theta < 3.5$ °C (Gascard and Clarke, 1983; Talley and McCartney, 1982; Lazier, 1973 & 1988; Lazier and Wright, 1993). Below this, lies *North Atlantic Deep Water (NADW)* which is defined as a layer of relatively high salinity (above 34.9) with $2.0 < \theta < 3.0$ °C. It consists of deep water from the Greenland and Norwegian Seas that has overflowed into the Labrador Sea and undergone mixing with LSW and *Denmark Strait Overflow Water (DSOW)*. Also referred

to as Northwest Atlantic Bottom Water (Mann, 1969), DSOW is the deepest component of WGC waters. Formed over a 600 m sill in the Denmark Strait (Dickson and Brown, 1994), its characteristics are defined as $S > 34.90$ and $1.0 < \theta < 2.0$ °C.

2.1.2 Arctic Ocean source waters

Steep ridges and shallow continental shelves divide the Arctic Ocean into four main basins: the Nansen Basin, the Amundsen Basin, the Makarov Basin and the Canada Basin (Fig. 2.2). The circulation and hydrography of these basins is shaped by several inputs, including Atlantic-origin waters via Fram Strait and the Barents Sea, and Pacific-origin waters via Bering Strait. Subsequent outflows from the Arctic Ocean follow two routes to reach the North Atlantic: Fram Strait (via the Greenland Sea) and the Canadian Archipelago (via the Baffin Bay region).

The structure of Arctic Ocean waters (Fig. 2.3a) is typically described in three layers: an *Upper Layer*, an *Atlantic Layer* and a *Deep Layer* (McLaughlin et al., 2002). The Upper Layer consists of two components: a *polar mixed layer* (0-50 m) and a *halocline layer* (50-250 m). The Atlantic Layer also comprises two components. The upper component enters through Fram Strait and is identified by a warm core (i.e. temperature maximum). The lower component is from the Barents Sea and is relatively fresher than the Fram Strait component. Finally, the Deep Layer originates primarily as Greenland Sea Deep Water, but may be augmented by dense waters formed through ice formation along the Arctic Ocean's shallow shelves (Aagaard et al, 1985).

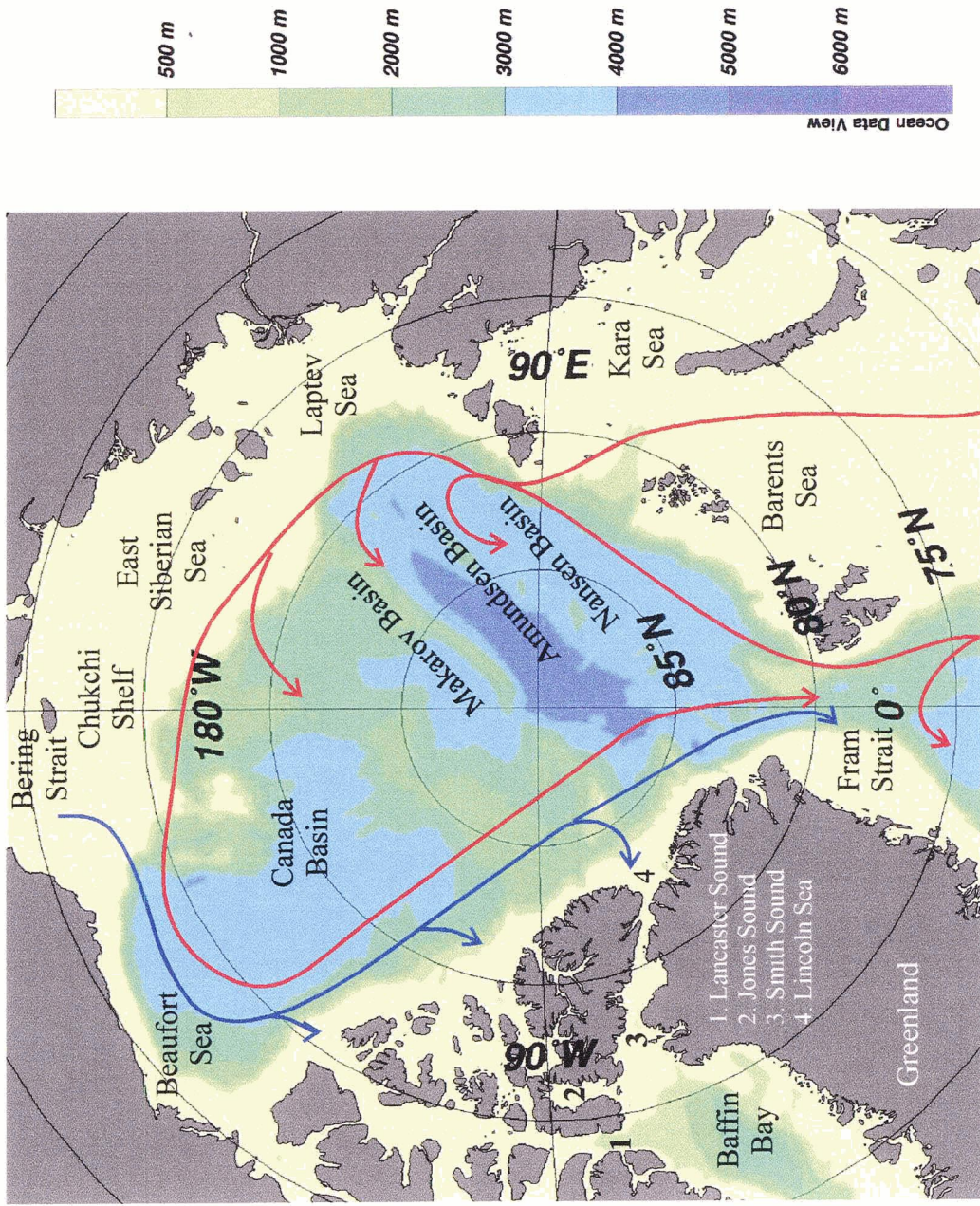


Fig. 2.2: Map showing bathymetry for the Arctic Ocean and circulation of its Atlantic-origin (red) and Pacific-origin (blue) waters.

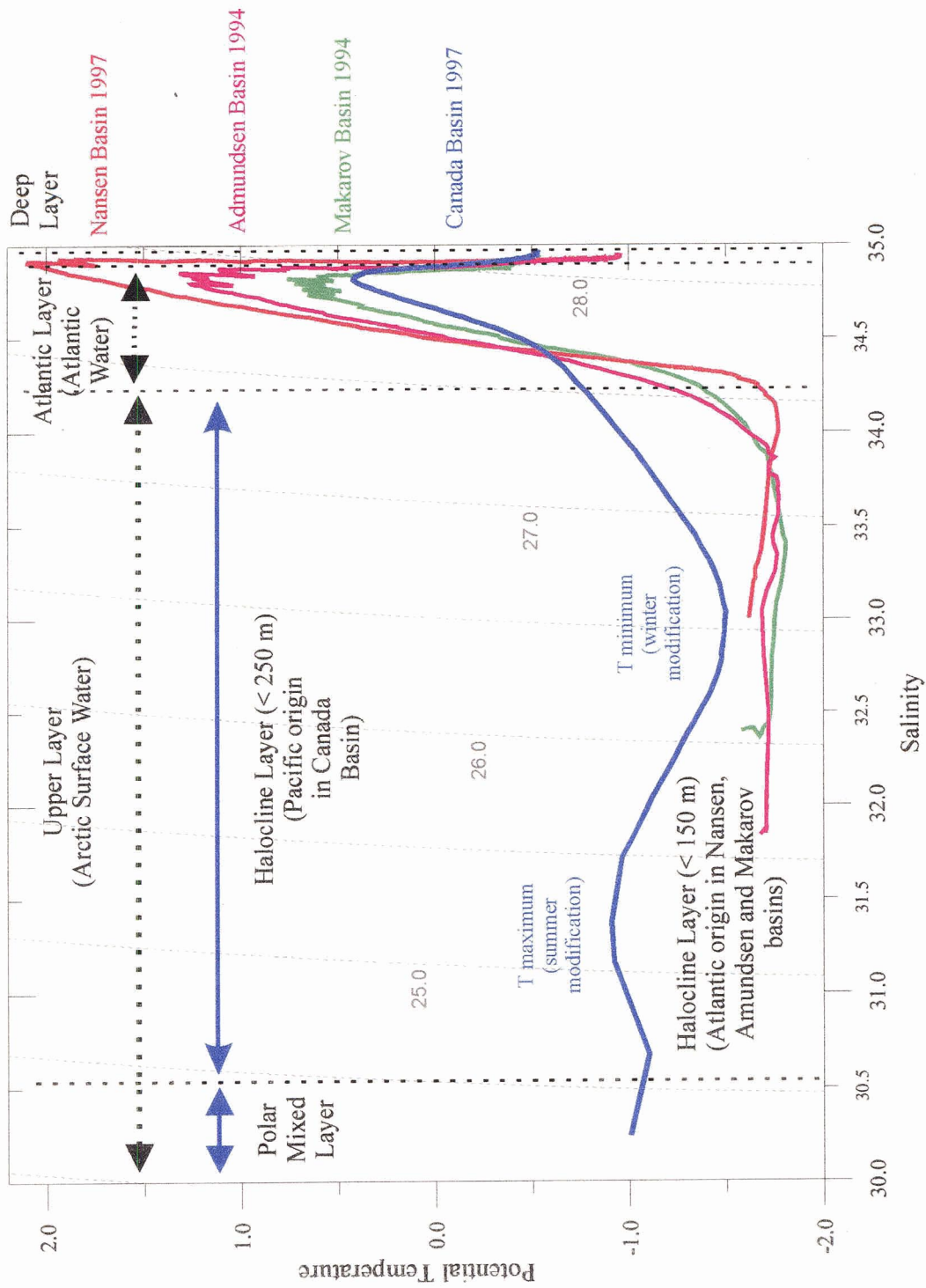


Fig. 2.3: a) Water signatures for the four Arctic basins (borrowed from McLaughlin, 1996). Upper Layer features for the Canada and Makarov basins (which are the primary upstream basins to the Canadian Archipelago and Baffin Bay region) are labeled in blue and green.

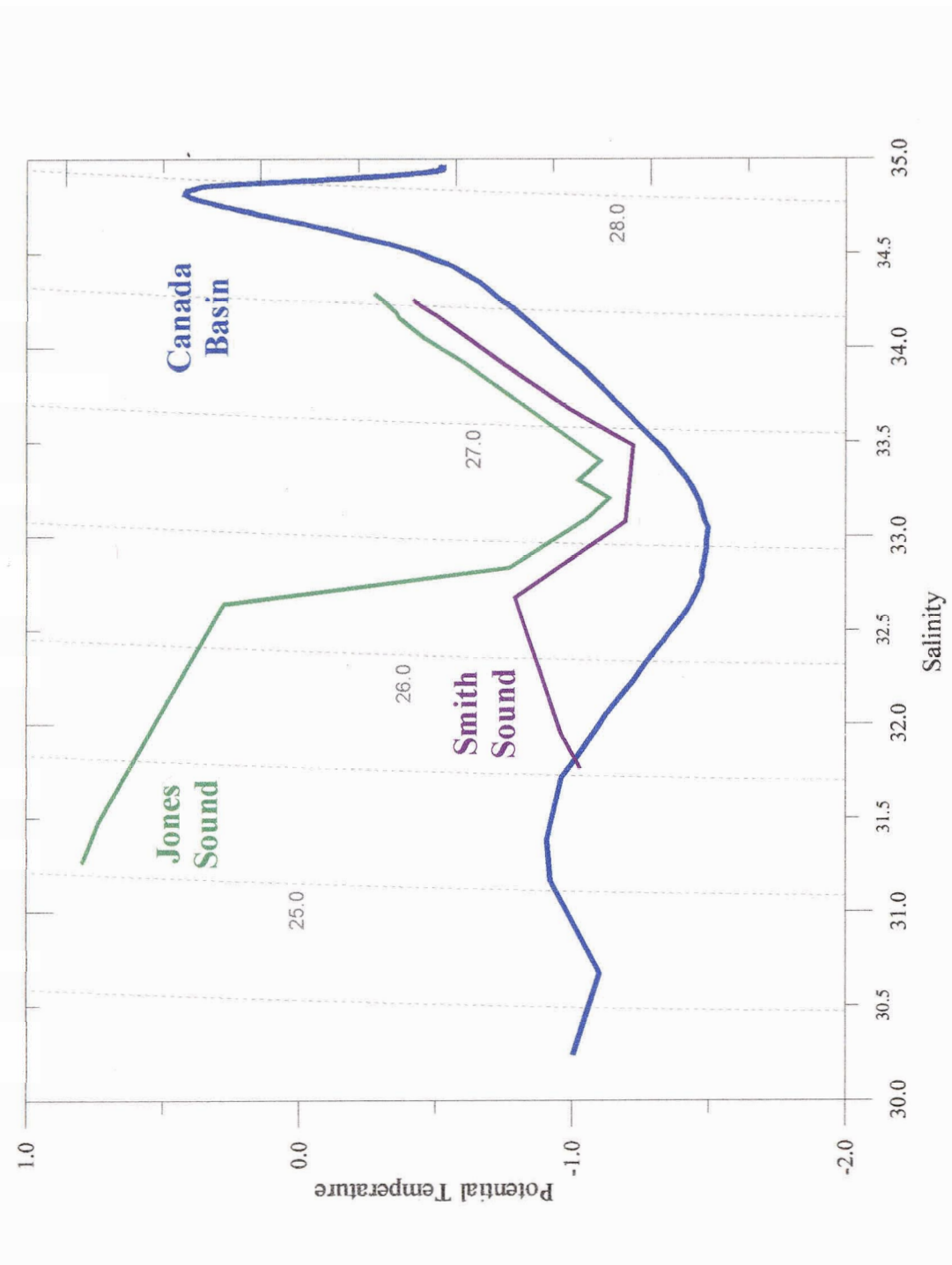


Fig. 2.3:b) Water signatures for the Canada Basin (McLaughlin, 1996), Smith Sound and Jones Sound (MEDS). Data for these curves were obtained in 1997.

Properties of the polar mixed layer reflect the seasonal ice formation/melt cycle and river runoff. Properties of the halocline layer depend on three things: its origin (Pacific or Atlantic), modification on shelves, and the extent of mixing with ambient waters. Within the Canada and Makarov basins, which are the immediate upstream basins to the Baffin Bay region, the origin of the halocline layer was likely the Pacific Ocean until the early 1990's. After that, the presence of Pacific-origin waters was observed to shift to the Canada Basin only (McLaughlin et al., 1996), possibly in response to large-scale shifts in atmospheric patterns (McLaughlin et al., 1996 & 2002; Morison et al., 1998; Proshutinsky and Johnson, 1997; Steele et al., 2004). As Pacific-origin waters enter the Arctic Ocean over the Chukchi Shelf, they inherit two features by means of seasonal processes. The first is a temperature maximum (with associated low nutrient and high oxygen concentrations) for $31.0 < S < 32.0$ related to summer warming. The second is a temperature minimum (with associated high nutrient and low oxygen concentrations) near 33.1 related to inflow during winter (Coachman and Barnes, 1961; McLaughlin et al., 1996).

Properties of the halocline layer are also greatly determined by mixing with the underlying Atlantic Layer (Jones and Anderson, 1986; Melling, 1998). This occurs through the production of ice along the Arctic Ocean's shelves, which releases cold, salty plumes that are sufficiently dense to drain from the shelves and mix with ambient waters. Despite the small overall volume of the halocline layer throughout the Arctic Ocean, this kind of

mixing causes significant cooling and freshening of the Atlantic Layer (Aagaard et al., 1981).

Canada Basin and Makarov Basin waters exported toward the Baffin Bay region through the Canadian Archipelago are subject to several modifications (Melling et al., 1984). First, shallow sills prevent the temperature maximum associated with the Atlantic Layer from entering these regions. This does not mean that input to the Baffin Bay region from the Arctic does not contain any Atlantic-origin water, but that it only contains Atlantic-origin water modified by mixing with the Arctic halocline layer. Second, because the Canadian Archipelago is covered with land-fast ice for approximately 6 months per year, ice growth and the production of cold, salty plumes is limited, such that significant entrainment into deeper waters cannot occur. This results in an overall warming of the water column as it travels through the Canadian Archipelago, due to upward vertical heat diffusion from underlying Atlantic-origin waters. Finally, energetic flows over shoaling or narrow topography cause turbulent mixing which acts to further enhance upward heat flux in the water column. Fig. 2.3b illustrates these modifications by comparing properties in the Canada Basin to those of waters exiting the Canadian Archipelago into Baffin Bay across Smith Sound and Jones Sound.

2.2 Waters within the Baffin Bay region

The hydrography and dynamics of the Baffin Bay region are relatively understudied. However from what is known, it is a region that is similar to its northern source basin: the

Arctic Ocean. This is because, like the Arctic Ocean, Baffin Bay is a mediterranean sea (Tomczak and Godfrey, 1994). That is, sills bind its topography, and thermohaline differences rather than wind forcing primarily drive its circulation and dynamics. For Baffin Bay, shallow sill depths at Davis Strait, Smith Sound, Jones Sound and Lancaster Sound restrict exchange with the deep waters of the North Atlantic and the Arctic. As for its thermohaline-driven dynamics, they are mainly dominated by salinity (as is the case in high latitudes). This implies that, like the Arctic Ocean, freshwater transport and sea-ice formation and melting largely influence its surface circulation and water characteristics.

The sea-ice cycle for the Baffin Bay region begins in October with winter freeze-up (Wang et al., 1994). This occurs firstly in the North Water region and spreads southward and eastward, covering Davis Strait by the end of November. As winter progresses, the southern ice edge along the Greenland coast moves north, such that a narrow (< 60 km) ice-free zone reaches Disko Island by the end of June. To the north, channelled northerly winds and currents tend to form an ice bridge near Smith Sound in March-April. This bridge blocks ice flow from the north while allowing ice to the south to be advected away by winds and currents, resulting in a low ice concentration within the North Water region (Melling et al., 2001). By late June, the North Water's ice edge expands southward into the mouth of Lancaster Sound. By the end of July, all of the North Water region, Melville Bay, Davis Strait and the eastern half of Baffin Bay are ice-free. Any remaining ice found at the center of Baffin Bay and along the Baffin Island coast is cleared by the end of

September (Fraser, 1983). At this time, ice bridges in Smith Sound and Barrow Strait generally break, and a strong pulse of sea ice empties into Baffin Bay.

Similar to the Arctic Ocean, the Baffin Bay region has traditionally been described in terms of three layers: an *Arctic Layer*, and *Atlantic Intermediate Layer* and a *Deep Layer* (Table 2.1). Baffin Bay's Arctic Layer (extending 100-300 m deep) consists of two sub-layers: *Surface Water* (which obtains its characteristics seasonally from solar heating and meltwater addition) and *Arctic Water* (which is not modified by surface processes). The latter is characterised by a prominent temperature minimum (Muench, 1971) maintained by convective overturning via cold winter temperatures and the release of brine through ice formation. Addison (1987) further made the distinction between *Arctic Basin Arctic Water* ($\theta < 0\text{ }^{\circ}\text{C}$; $S < 34.5$) and *WGC Arctic Water* ($\theta < 0\text{ }^{\circ}\text{C}$; $S < 34.25$). Both of these take their source in the Arctic Ocean. However Arctic Basin Arctic Water enters Baffin Bay directly from the Canadian Archipelago whereas WGC Arctic Water flows clockwise around the southern tip of Greenland with the EGC before entering Baffin Bay with the WGC.

Layer	Water mass	Physical Characteristics	Renewal time (years)	Residence time (years)	Comments
Arctic Layer	Surface Water ⁱ	$-1 < \theta < 6 \text{ }^\circ\text{C}$ $S < 33.5$ $< 75 \text{ m}$		0-1 ^v	Derived seasonally through meltwater admixture and solar heating
	Arctic Basin Arctic Water ⁱⁱ	$\theta < 0 \text{ }^\circ\text{C}$ $S < 34.5$ $< 250 \text{ m}$		2 ^{v, vi}	Originates in the Arctic Ocean and enters Baffin Bay through Jones, Smith, and Lancaster sounds.
	WGC Arctic Water ⁱⁱ	$\theta < 0 \text{ }^\circ\text{C}$ $S < 34.25$ $< 250 \text{ m}$			Originates in the Arctic Ocean and enters Baffin Bay through Davis Strait
Atlantic Intermediate Layer ⁱⁱⁱ	Baffin Bay Intermediate Water ^{iv}	$\theta > 0 \text{ }^\circ\text{C}$ $33.8 < S < 34.45$ $200-1200 \text{ m}$		8 ^v 20 ^{vi}	Enters Baffin Bay via the WGC
Deep Layer	Baffin Bay Deep Water	$-0.23 < \theta < -0.46 \text{ }^\circ\text{C}$ $34.45 < S < 34.48$ $1200-1800 \text{ m}$	77-455 ^v 20 ^{vii} 125- 1450 ^{viii}	?	Only present in central Baffin Bay
	Baffin Bay Bottom Water	$-0.46 < \theta < -0.5 \text{ }^\circ\text{C}$ $S > 34.48$ $> 1800 \text{ m}$?	?	Only present in central Baffin Bay

Table 2.1: General nomenclature and associated characteristics used by the literature to describe waters of the Baffin Bay region. Based on works by Bailey (1956), Muench (1971), Addison (1987) and Bourke et al (1989).

ⁱ Also called *Arctic Surface Water* or *Baffin Bay Surface Water*

ⁱⁱ Also called *Arctic Intermediate Water*, *Arctic Ocean Intermediate Water*, *Polar Water* or *Cold Water*

ⁱⁱⁱ Also called *Warm Water Layer* or *Atlantic Layer*

^{iv} Also called *Atlantic Intermediate Water*, *WGC Atlantic Water*, *WGC Atlantic Intermediate Water*, or *Polar Atlantic Water*

^v Top et al. (1980)

^{vi} Rudels (1986)

^{vii} Sadler (1976)

^{viii} Wallace (1985)

The term “Atlantic Intermediate Layer” in Baffin Bay refers to Atlantic-origin waters of $\theta > 0$ °C and $33.8 < S < 34.45$. The term is ambiguous for several reasons. Firstly, because it has endured more variations than any other Baffin Bay water definition (such that it is sometimes called “Atlantic Intermediate Water”, “WGC Atlantic Water”, “WGC Atlantic Intermediate Water” and even “Polar Atlantic Water”). Secondly, because the use of the term “Intermediate” in Baffin Bay relates strictly to position in the water column, with no relation to the traditional definition characterising water formed by subduction near the Antarctic Polar Front (Tomczak and Godfrey, 1994). Finally, because shallow sill depths along the Canadian Archipelago prohibit waters of such characteristics from entering the Baffin Bay region. The definition of Atlantic Intermediate Layer thus implies that Atlantic-origin water in Baffin Bay only originates from inflow via the WGC. (This shortcoming will be addressed in Chapter 3 with the introduction of a more inclusive nomenclature system for Baffin Bay waters, which recognises modified Atlantic-origin waters from the Arctic Ocean across Smith Sound, Jones Sound and Lancaster Sound).

Baffin Bay’s Deep Layer, found only in the deep central portion of its basin, is generally described in terms of *Baffin Bay Deep Water (BBDW)* and *Baffin Bay Bottom Water (BBBW)* (Muench, 1971). BBDW is characterised as water between 1200 and 1800 m with $-0.23 < \theta < -0.46$ °C and $34.45 < S < 34.48$. Below it, BBBW is nearly uniform in temperature ($-0.46 < \theta < -0.5$ °C) and salinity ($S \sim 34.48$). Where this Deep Layer takes its origin and how it is maintained is the subject of much speculation. The earliest theory placed its origin in the Labrador Sea (Sverdrup et al., 1942), where it was described as a

mixing product between LSW and Baffin Bay Surface Water whose salinity had been sufficiently increased by brine rejection to cause it to sink. Other theories place its origin in the north, via: 1) the pulsing of dense water of appropriate characteristics through Smith Sound during winter (Bailey, 1956; Collin, 1965; Palfrey and Day, 1968; Muench, 1971); 2) deep convection involving the cooling and mixing of brine-enriched Surface Water from Smith Sound with Baffin Bay Intermediate Water (Sadler, 1975); or 3) the sinking of plumes of cold, brine-enriched Smith Sound shelf water that are modified by entrainment with ambient waters (Bourke et al., 1989; Bourke and Paquette, 1991). Stable isotope studies (Redfield and Freidman, 1969; Tan and Strain, 1980; Ostlund and Hut, 1984) assessing the relative contribution of meteoric³ water and sea-ice meltwater to Baffin Bay's Deep Layer have been used to examine the feasibility of these hypotheses. In particular, Tan and Strain's (1980) analysis of oxygen isotope ratios proved to be consistent with the southern hypothesis of Sverdrup et al. (1942) and the northern pulsing hypothesis of Muench (1971), while being inconclusive for the northern convection hypotheses (Sadler, 1975).

Analyses of non-conservative tracers, such as nutrients, dissolved oxygen, and trace metal concentrations (Jones et al., 1984; Coote and Jones, 1982; Campbell and Yeats, 1982, Wallace, 1985) have indicated homogenous distributions throughout Baffin Bay's Deep Layer. Using CFC data, Wallace (1985) estimated a renewal time for the Deep Layer of 125-1450 years, based on the assumption of a steady-state renewal process. However he

³ From precipitation or runoff.

noted that renewal of the Deep Layer could potentially be intermittent, complicating his estimates which were based on data collected at a single point in time.

While little is known about the circulation of Baffin Bay's Atlantic Intermediate and Deep layers, Smith et al. (1937) proposed an extensive recirculation for these waters near Davis Strait. This would result in mixing between newly entered WGC waters and recirculated BC waters, and subsequent rapid cooling of WGC input. Under such conditions, Rudels (1986) estimated that the Atlantic Intermediate Layer along the Greenland coast would be composed of 1/6 water from the WGC and 5/6 recirculated water, which itself would be dominated by Arctic Archipelago outflow. This was corroborated by Tan and Strain (1980), who found a correspondence in oxygen isotope ratio levels between the Atlantic Intermediate Layer and waters below 250 m in Nares Strait. Rudels (1986) concluded that the contribution of Arctic Archipelago outflow to Baffin Bay potentially increased from 50 % in the Arctic Layer to more than 80 % in the Atlantic Intermediate Layer (and presumably greater in the Deep Layer), and that the formation of the Deep Layer likely originated from the north.

In contrast to limited data reported in Baffin Bay's central basin, extensive surveys relating to hydrography and currents have been made in the North Water region (Muench, 1971, Addison, 1987, Melling et al., 2001, Bâcle et al., 2002) and in Lancaster Sound (Lemon and Fissel, 1982; Fissel et al., 1982). In terms of circulation, only a minor branch of the WGC follows the Greenland Coast all the way to Smith South (Melling et al., 2001; Bâcle

et al., 2002); most of the flow veers westward, entering the mouth of Lancaster Sound as a narrow (10 km), swift (70 cm/s) 'intrusive current' (Fissel et al., 1982) before flowing back into Baffin Bay along the coast of Bylot Island. This intrusive current has been associated with strong horizontal density gradients postulated as a mean for enhanced vertical motion due to reduced stratification (Fissel et al., 1982).

3 Methodology

3.1 Analysis Tools and Nomenclature

A widely used tool for the study of water properties is the temperature-salinity (T-S) diagram (Mamayev, 1975). This is where values of T and S for a given oceanographic station are plotted against each other and joined in order of depth. On such a plot, a water body whose characteristics can be described by a point is referred to as a 'water type', while a line is referred to as a 'water mass'. In this dissertation, a variation of the T-S diagram called the potential temperature-salinity diagram was used. The choice of potential temperature (θ) rather than T was made due to the adiabatic warming of seawater at depth. For deep regions like Baffin Bay, the difference between θ (temperature as affected by adiabatic compression), and T can be quite significant, such that the θ -S diagram becomes a much better observation of property conservation.

While Baffin Bay's θ -S properties have traditionally been described in terms of water masses (see Table 2.1), this dissertation focused on describing prominent features in halocline structure (i.e. features in property distributions associated with salinity gradients). This approach avoids arbitrary θ -S delineations that limit descriptions of *en route* water modifications and local mixing. This technique may also be transferable to other regions and facilitate future studies of inter-basin exchanges.

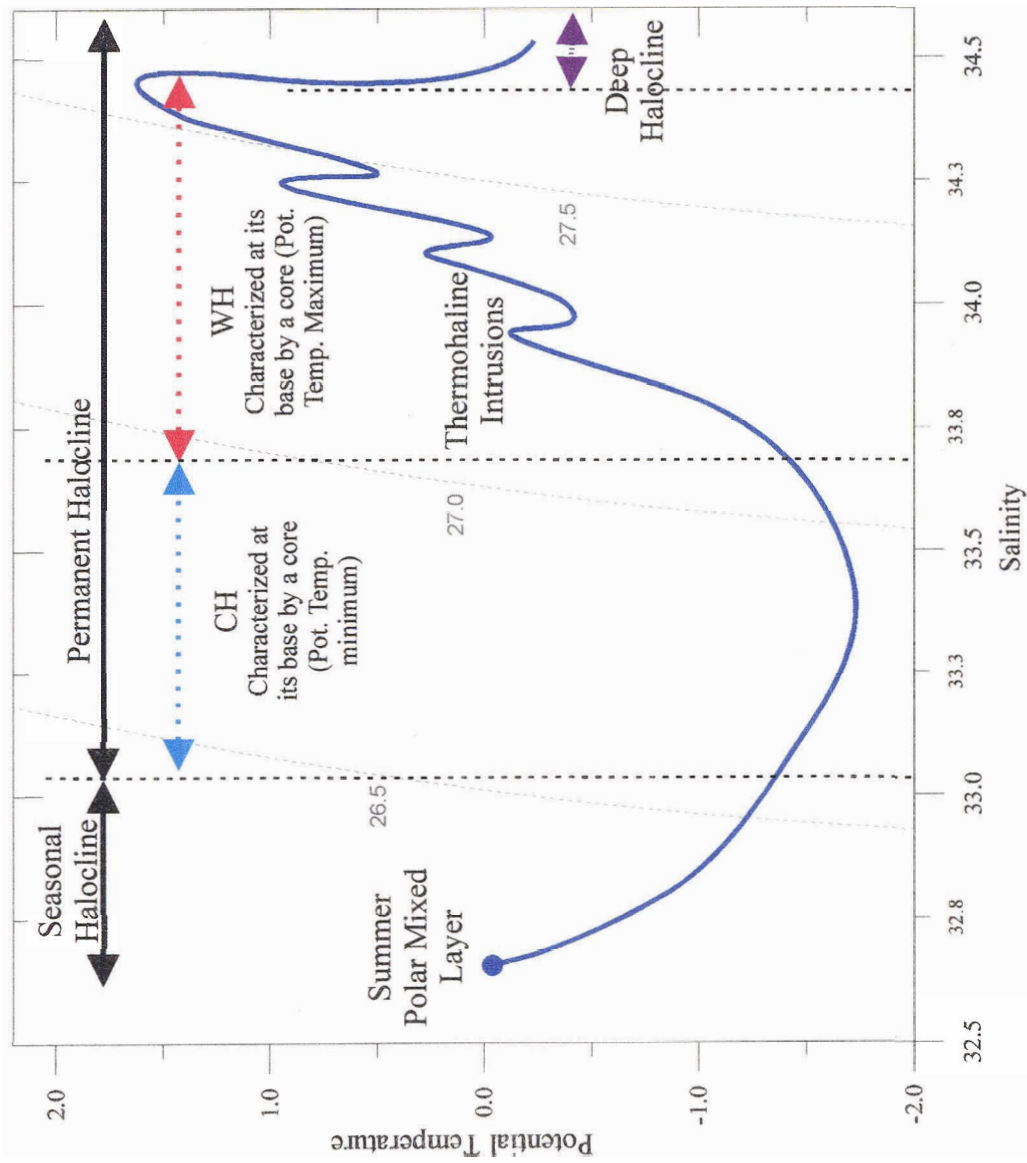


Fig. 3.1: Schematic potential temperature-salinity diagram illustrating the main nomenclature terms used throughout this dissertation.

The main θ -S features studied in this dissertation were prominent extrema (maxima or minima), or cores, and thermohaline intrusions (Fig. 3.1). Use of the term “core” differed from that originally developed by Wüst (1936) as part of the “core method” for the analysis of θ -S diagrams. Wüst’s definition referred to an extrema in the θ -S diagram situated at the mid-depth of a water mass. Here, “core” represented an extrema in θ -S space delineating the base of a halocline section of specific convective and/or advective origin (see below). A “thermohaline intrusion” referred to an inversion in θ and S (resembling a ‘saw-tooth’ on the θ -S diagram) resulting from the lateral shear advection of dissimilar water bodies. Interest in thermohaline intrusions came from the fact that they form at the confluence of differing water structures and they tend to set the stage for smaller-scale mixing processes.

Other nomenclatures used in relation to halocline structure included summer polar mixed layer, seasonal halocline, and permanent halocline. “Summer polar mixed layer” was used to refer to the upper portion of the water column subjected to wind mixing during ice-free months. This feature was nearly homogeneous in θ and S, and generally appeared as a single point on the θ -S diagram. Below this, the term “seasonal halocline” referred to a transient structure resulting from seasonal surface runoff and ice melt, while the term “permanent halocline” referred to a deeper structure maintained year-round. Distinguished within the latter were a “cold halocline” (CH) and an underlying “warm halocline” (WH). The CH signature was distinguished at its base by a “cold core” (i.e. a minimum on the θ -

S diagram) and originated as a result of wintertime convection and/or the advection of previously-formed structures from Arctic sources. The WH was generally distinguished by a “warm core” (θ maximum) and was considered to result from the admixture of Atlantic-origin water, either directly from the North Atlantic with the WGC, or circuitously via the Arctic Ocean (Bâcle et al., 2002).

3.2 Physical Data

Physical data were obtained from the Canadian Marine Environmental Data Service (MEDS), a branch of Canada's federal Department of Fisheries and Oceans (DFO) which archives ocean data collected by DFO, or acquired through national and international programs conducted in ocean areas adjacent to Canada.

Physical data obtained included profiles of T, S versus depth (D) sampled between 1928 and 2001. All profiles were collected between the months of June-October and their spatial distribution varied greatly from year to year (Figs. 3.2 and 3.3). In the late 1970s, for example, CTD⁴ data were concentrated in the northwestern portion of Baffin Bay, while those in the early 1990s were concentrated in Davis Strait and southeastern Baffin Bay, and those in the late 1990s were concentrated in the North Water region. It was therefore not possible to present a mapping of Baffin Bay's θ -S structures over the entire

⁴ Data obtained from a ‘conductivity-temperature-depth profiling system’. These systems are generally lowered through the water column from a ship and either record water properties internally or return them to the ship in real-time via conductor cable.

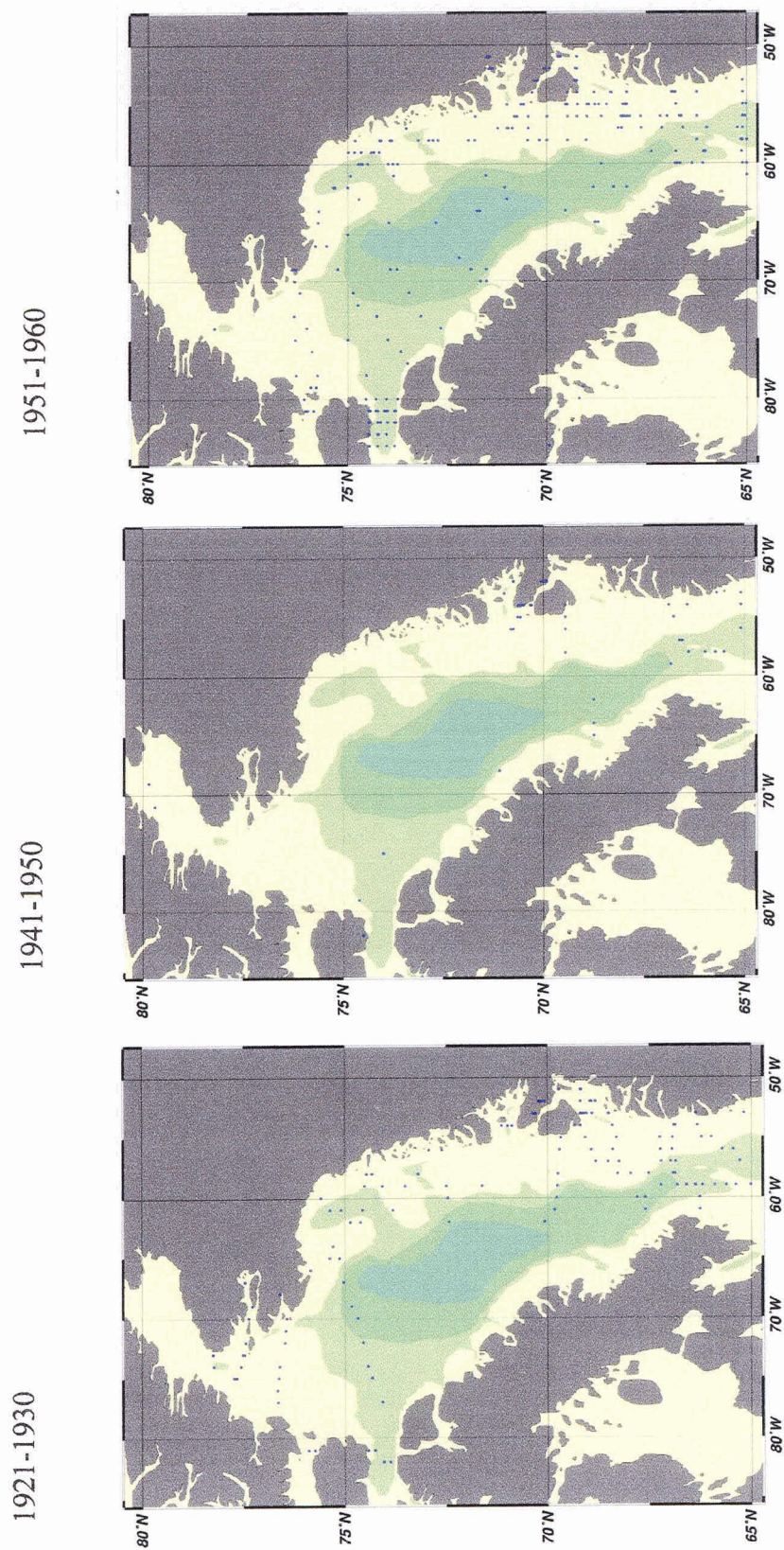


Fig. 3.2a) Location of bottle data stations (obtained and retained from MEDS archive)

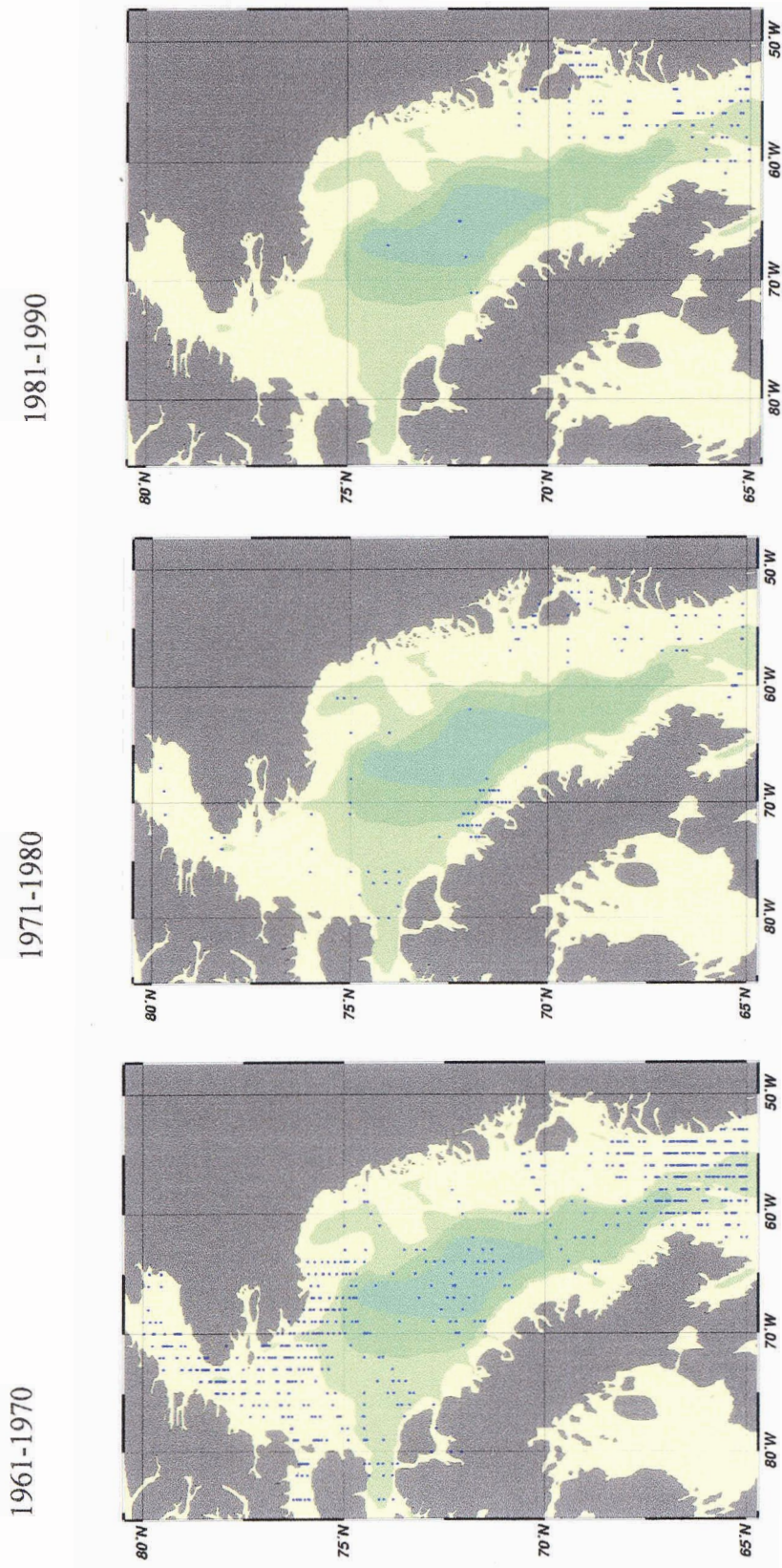


Fig. 3.2a) (continued)

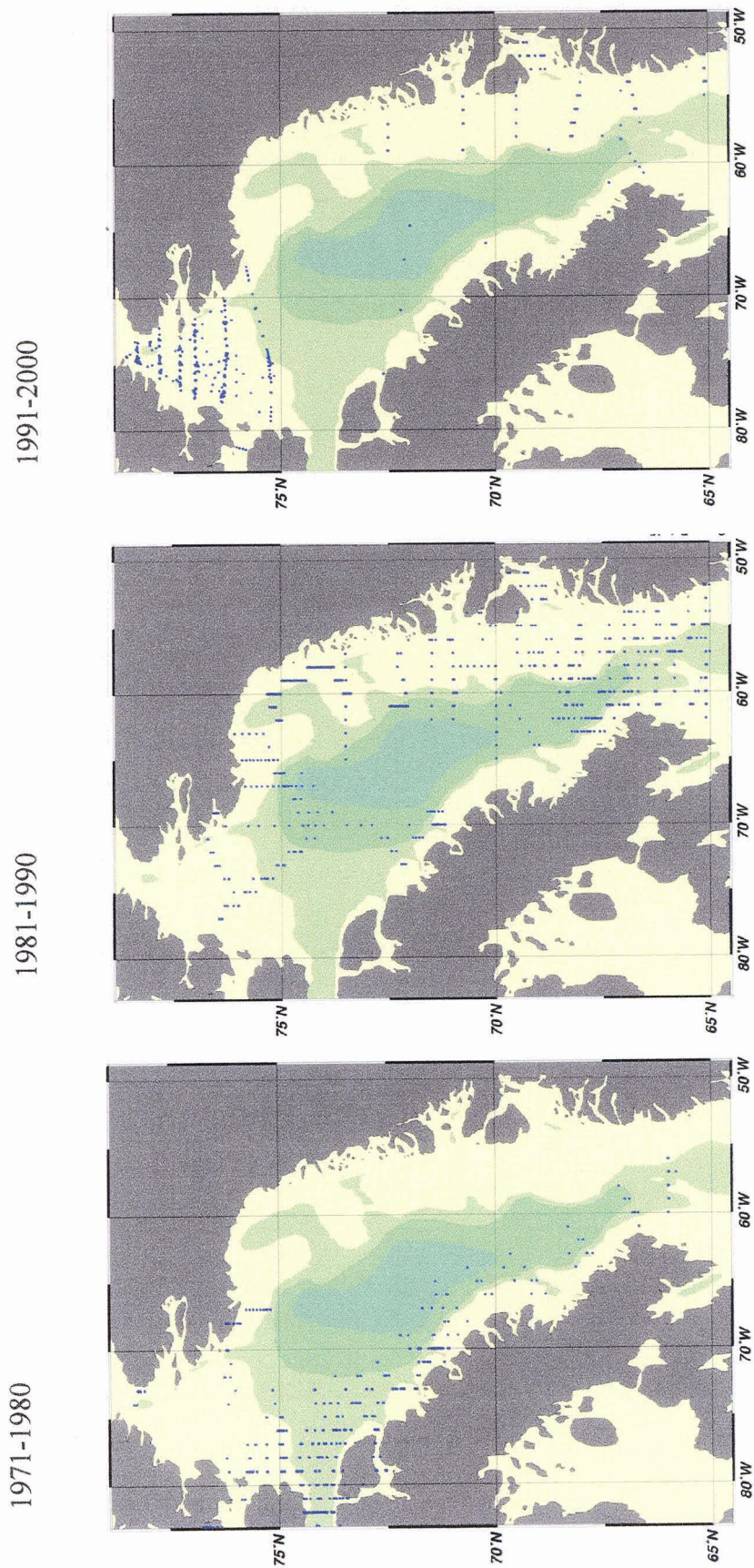


Fig. 3.2b) Location of CTD data stations (obtained and retained from MEDS archive)

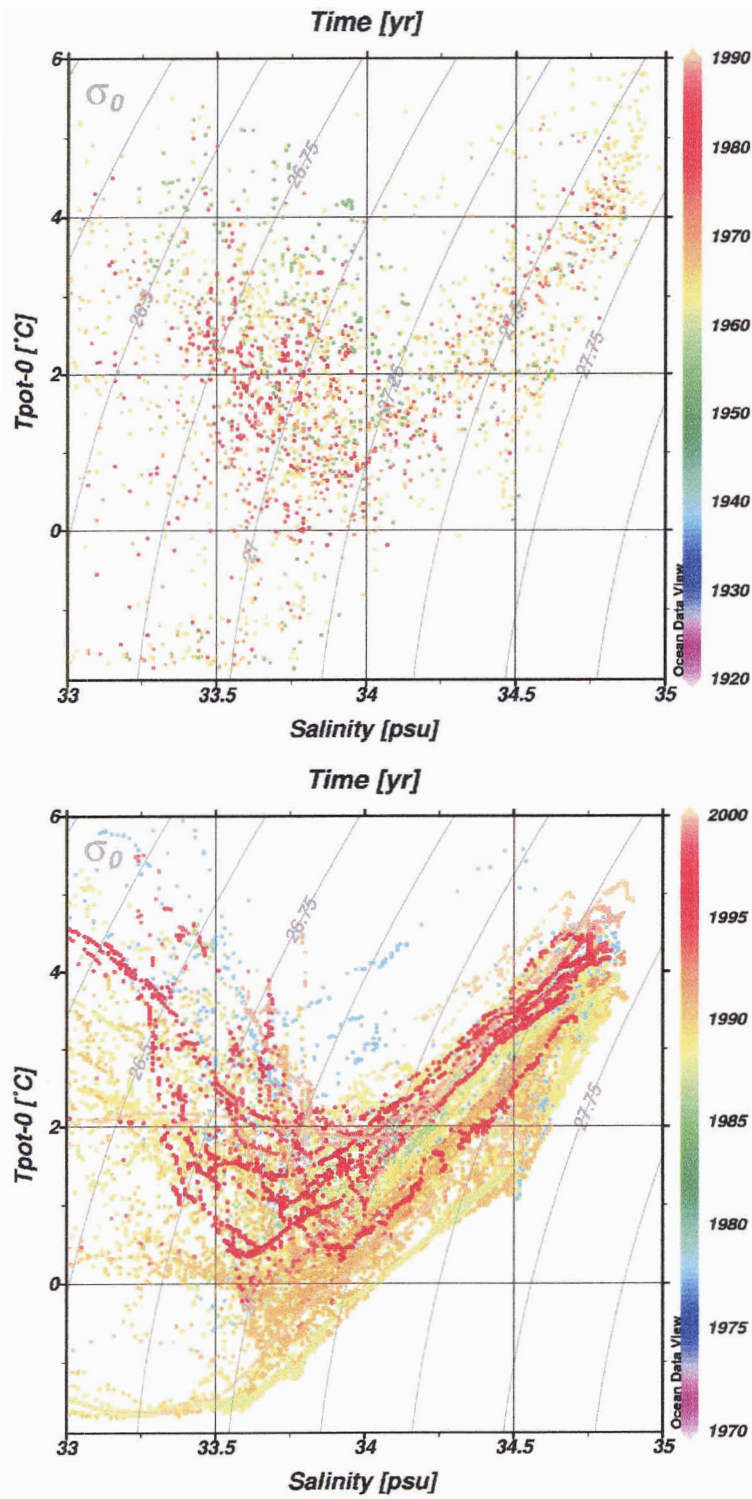


Fig. 3.3: a) potential temperature versus salinity scatter plots for all retained bottle (above) and CTD (below) data in Eastern Davis Strait.

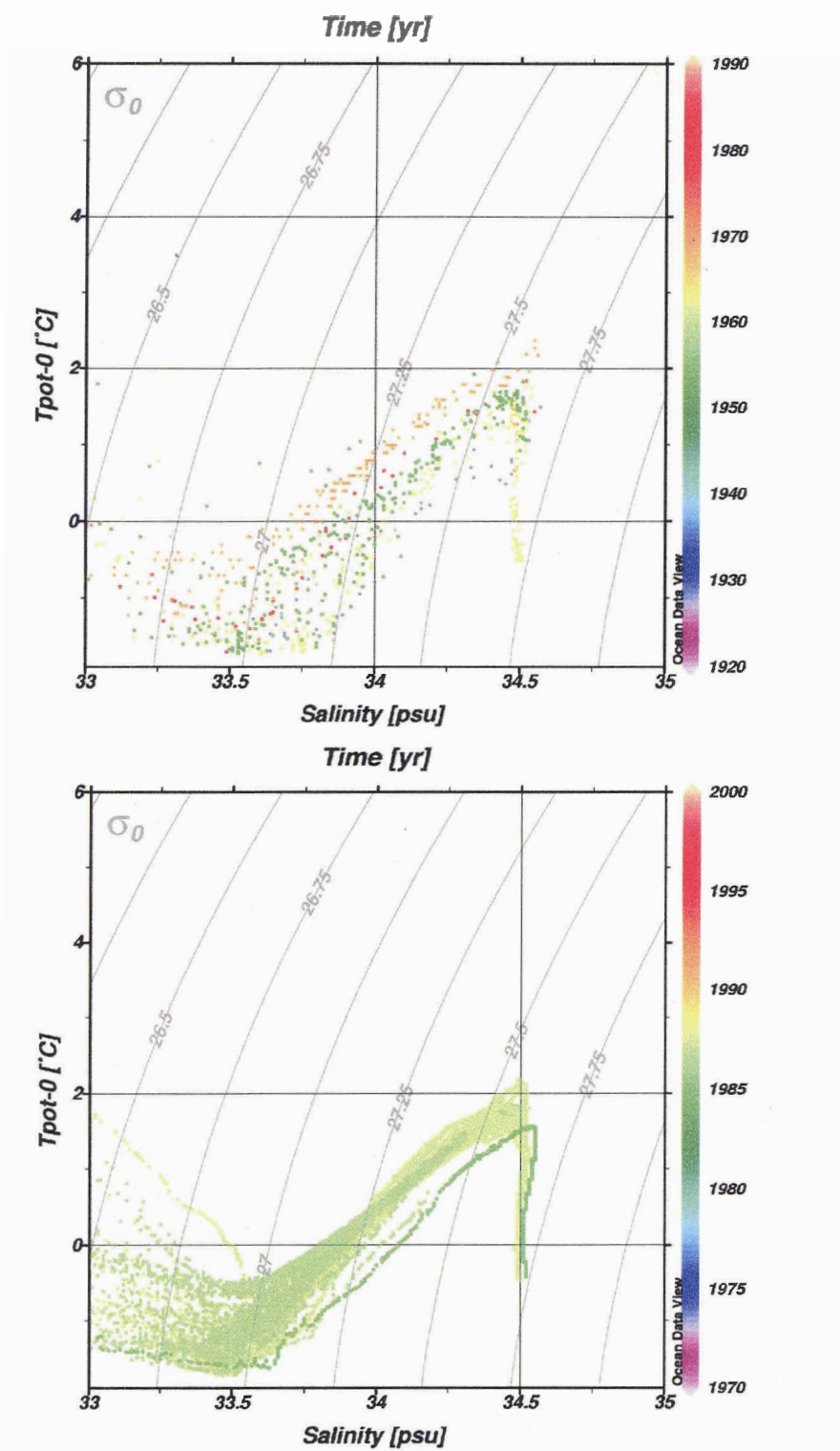


Fig. 3.3: b) Potential temperature versus salinity scatter plots for all retained bottle (above) and CTD (below) data in Melville Bay.

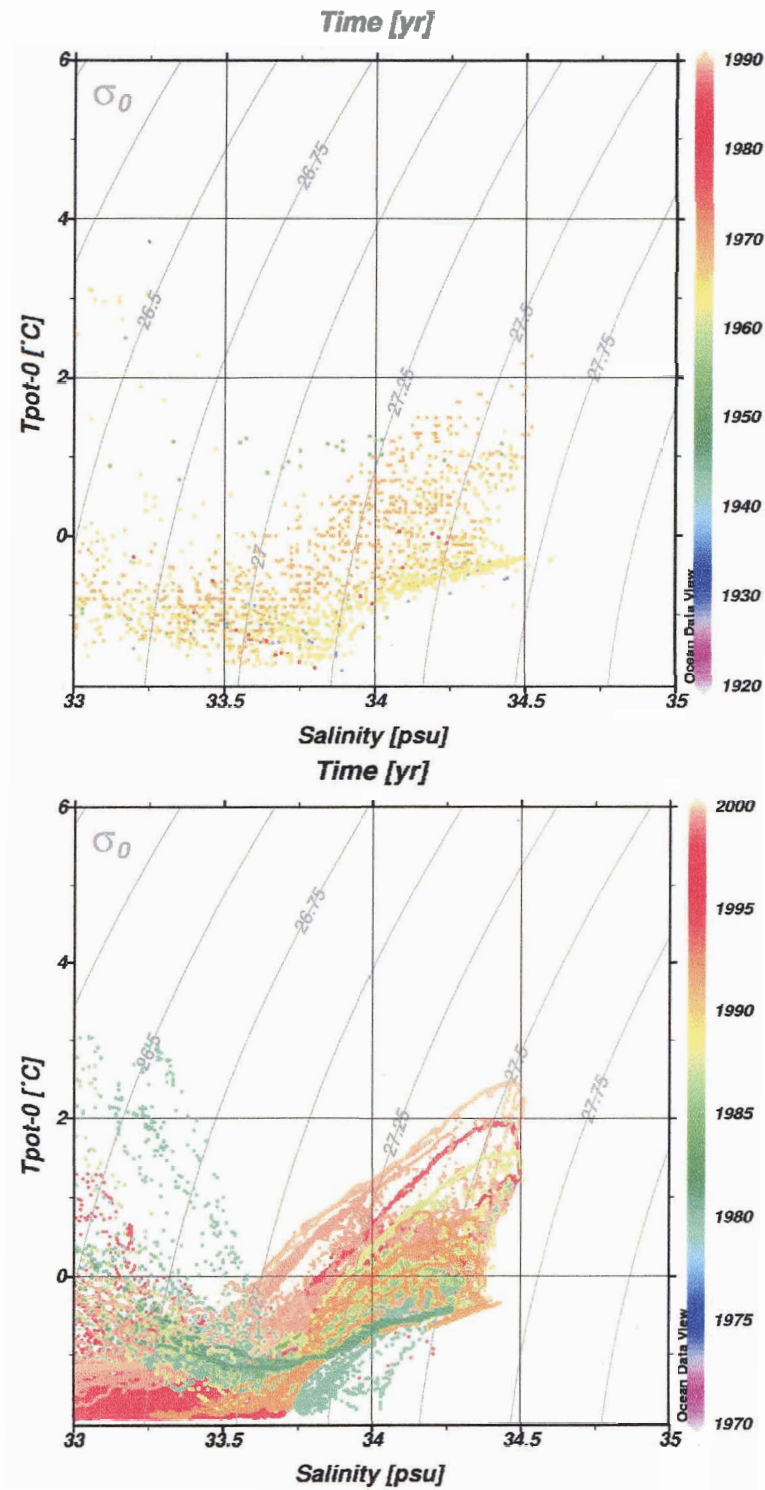


Fig. 3.3: c) Potential temperature versus salinity scatter plots for all retained bottle (above) and CTD (below) data in the North Water region.

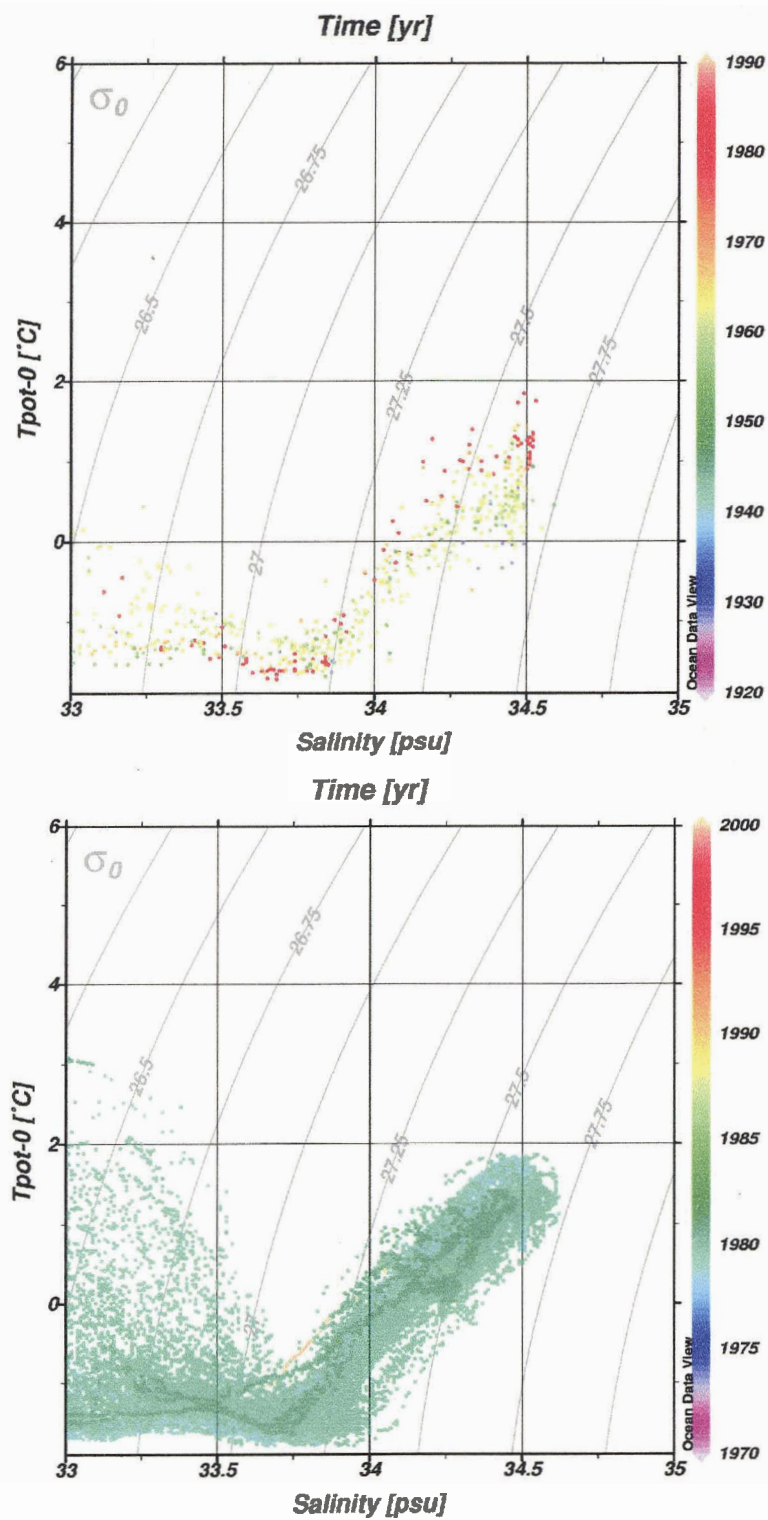


Fig. 3.3: d) potential temperature versus salinity scatter plots for all retained bottle (above) and CTD (below) data in the mouth of Lancaster Sound.

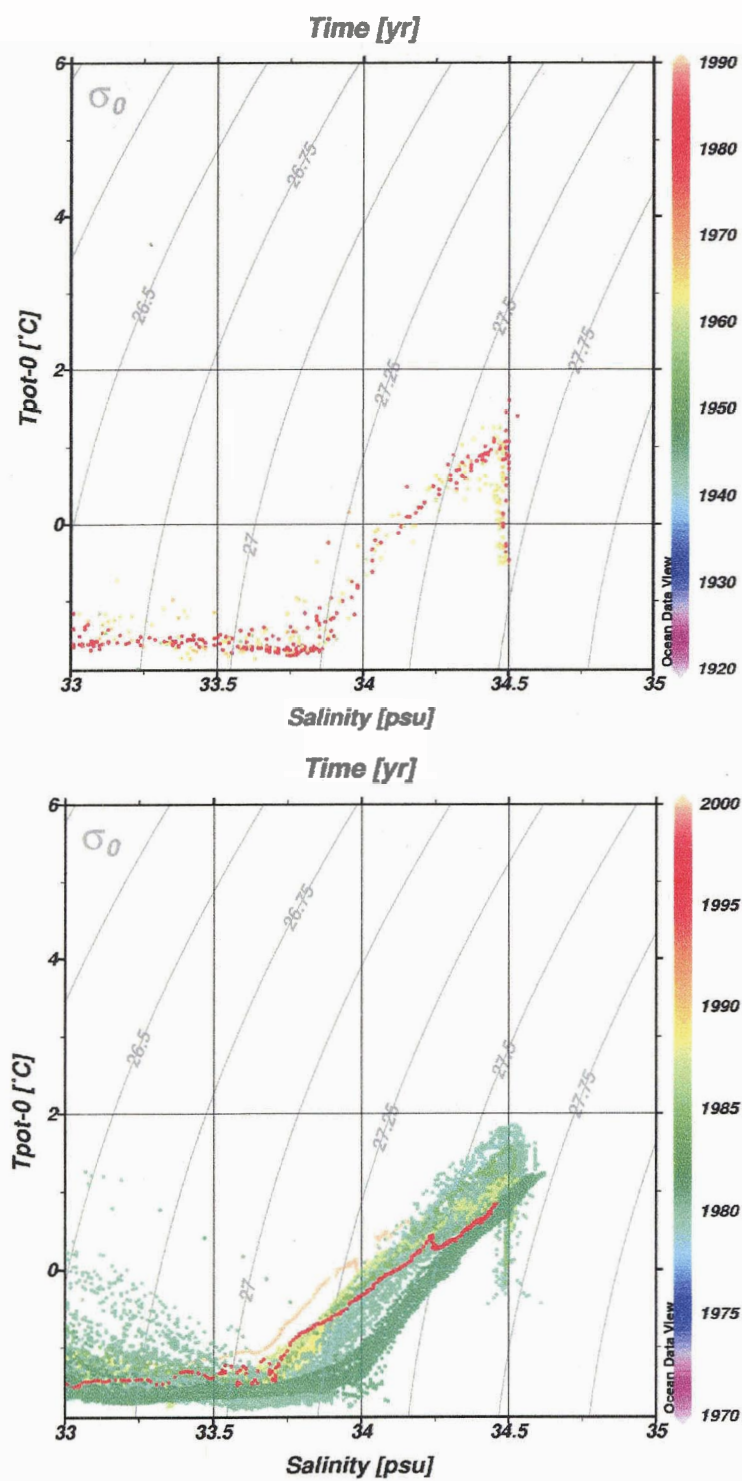


Fig. 3.3: e) potential temperature versus salinity scatter plots for all retained bottle (above) and CTD (below) data along the Baffin Island coast.

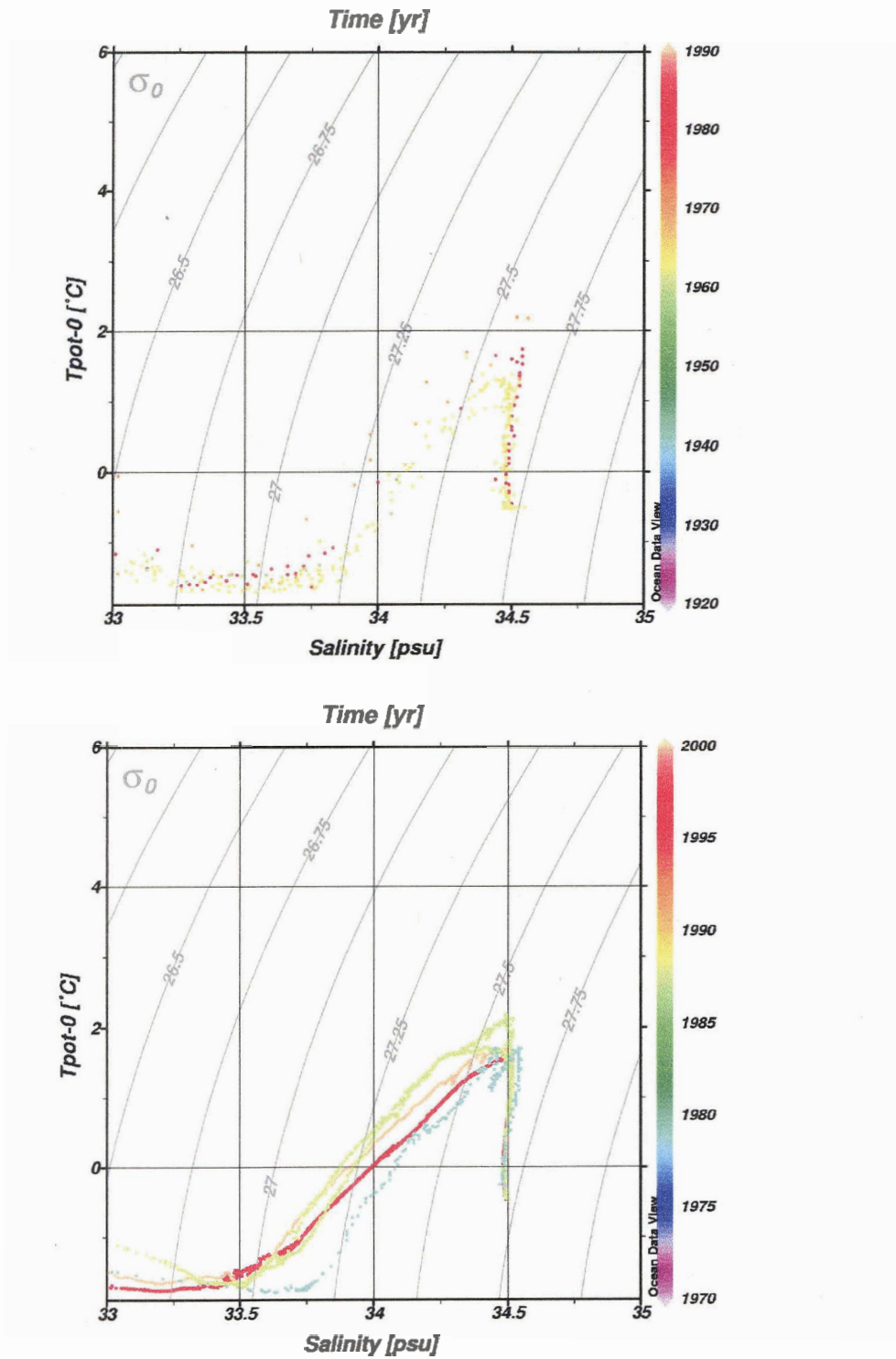


Fig. 3.3: f) potential temperature versus salinity scatter plots for all retained bottle (above) and CTD (below) data in central Baffin Bay.

region based on data from a single year. Care was taken however, to base the θ -S mapping presented in Chapter 4.1 and the frontal mapping shown in Chapter 4.2 on as few data sets and over as short a time span (1979-1997) as possible. These discussions were also based on CTD data rather than bottle⁵ data in order to allow θ -S structures to be examined under much finer resolution.

Because of limited coverage of the data both in space and time, no time series investigations were attempted on the region as a whole. However, an inter-annual comparison of data was possible for a small area (66.5 - 66.7 ° N and 56 ° W) in eastern Davis Strait and is discussed in Chapter 4.3. Both CTD and bottle data were used to generate these time series.

All MEDS-acquired data were reported to have undergone internal procedures of quality control, verification and validation. For bottle data prior to 1960, the accuracy in T was ± 0.01 °C (in accordance with the thermometer method). The precision of S was ± 0.01 ‰ prior to 1960 (via titration method) and ± 0.003 ‰ after 1960 (with the introduction of the salinometer). For CTD data (1977-2001), maximum precision for T and S was ± 0.005 °C and ± 0.005 ‰, respectively.

Further to MEDS quality control procedures, θ -S plots were examined for atypical gradients or values, using Muench's 1971 dissertation on Baffin Bay oceanography for

⁵ Data obtained from a device lowered from a ship on a cable, consisting of a water bottle and a pair of thermometers on a reversing frame.

comparison. Specifically, criteria for data dismissal included: the occurrence of density inversions, data noise which exceeded the assumed precision of the collection method used (i.e. bottle or CTD), and S values exceeding 35.0.

3.3 Geochemical Data

While the primary focus of this dissertation was Baffin Bay's physical oceanography, plots of dissolved nutrient (including nitrate, silicate, phosphate, and dissolved oxygen) and CFC (chlorofluorocarbon) concentrations were incorporated to complement observations from the physical data set. Dissolved nutrients were used to provide insight into the relative presence of source waters (eg. Pacific-origin versus Atlantic-origin) and dissolved oxygen was used to indicate ventilation events⁶ (i.e. convection). CFC concentrations provided insight into ventilation events and their time scales. This stems from the wide use of CFCs in aerosol propellants, plastic blowing agents, refrigerants and solvents until the Montreal Protocol of 1987 (which put controls on their release). Each CFC (e.g. CFC-11, CFC-12 or CFC-113) has a unique atmospheric concentration history starting the year they were introduced into the environment (Fig. 3.4). As a result, CFC concentration in a water body reflects atmospheric concentration at the time it was last in contact with the surface of the ocean (i.e. prior to processes like subduction, advection, convection or diffusion).

⁶ Ventilation refers to gaseous exchange with the atmosphere (that occurs when a water body is at the surface of the ocean) and its subsequent transference to subsurface waters. The period of time elapsed since a water body was last at the surface is called its 'ventilation age'.

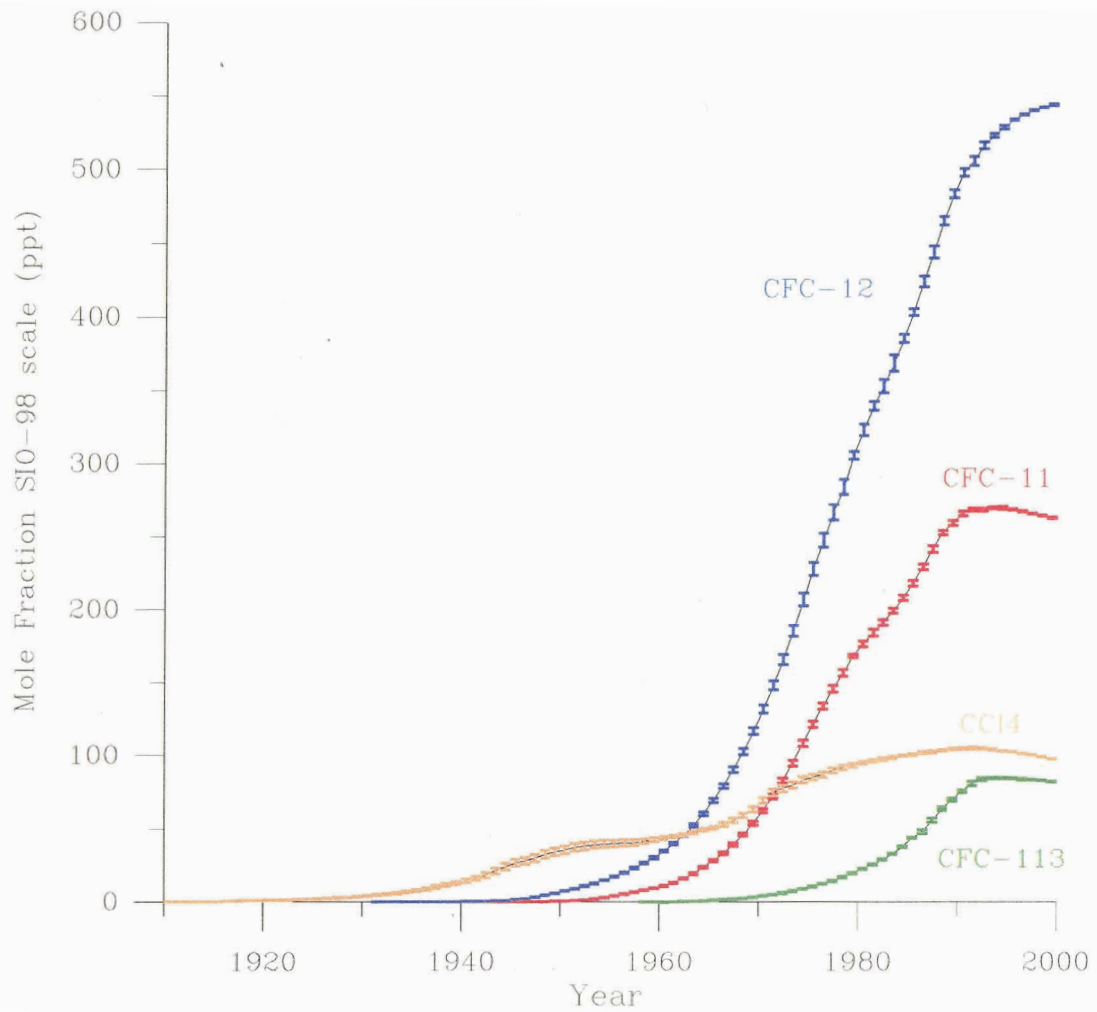


Fig.3.4: Reconstructed source functions for CFC-11, CFC-12, CFC-113 and CCl₄. From Walker et al., 2000.

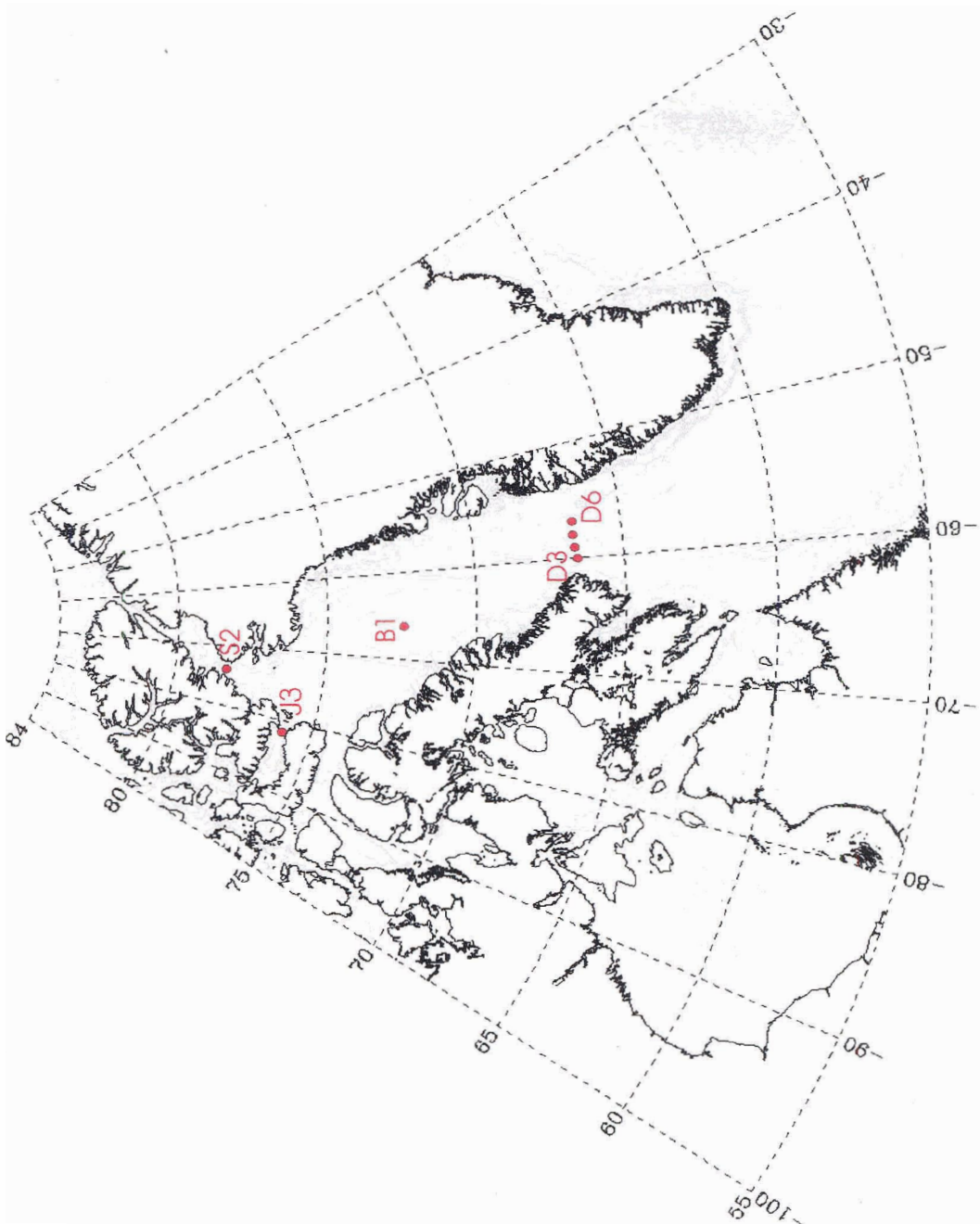


Fig. 3.5: Station locations for August 1997 CFC and dissolved nutrient data.

Although several data sets were available for Baffin Bay through MEDS, this dissertation focused on a single unpublished set of geochemical data collected in August 1997 aboard *CCGS Louis S St. Laurent* (Fig. 3.5). Dissolved nitrate, phosphate, and silicate samples were collected in replicate and analysed with an Technicon Autoanalyzer. Silicate and nitrate concentrations were determined according to Technicon Industrial Methods No. 186-71 W and 158-71 W, respectively, and phosphate was determined using a modified Technicon methodology (Barwell-Clarke and Whitney, 1996). Final concentrations were obtained by averaging values from replicate samples. The standard deviation for replicate samples was 0.08 $\mu\text{mol/L}$ (52 duplicates), 0.14 $\mu\text{mol/L}$ (52) and 0.008 $\mu\text{mol/L}$ (52) for nitrate, silicate and phosphate, respectively.

Dissolved oxygen concentrations were determined using an automated version of the Micro-Winkler Technique (Carpenter, 1965). Titration was done using a Metrohn Dosimat 665 and the end point was detected using a Brinkmann probe colorimeter PC900. The pooled standard deviation between replicate samples was 0.020 mL/L (35 duplicates).

Anthropogenic tracer data included CFC-11, CFC-12, CFC-113 and CCL₄ (carbon tetrachloride). It is to be noted that the latter halocarbon is not a CFC. However, its early introduction to the environment at the beginning of the 20th century is unique, thus providing information on the 'older' halocline structures of the deep. All chlorofluorocarbon samples were measured using two automated purge and trap systems

developed at the Bedford Institute of Oceanography (F.A. McLaughlin, pers. comm.). Separation and detection of the individual CFC components was achieved using a 60 m, 0.32 mm GasPro Gas Chromatograph fused silica column and in a Varian Electron Capture Detector. Concentrations were determined using a gas standard (S36) prepared at Brookhaven National Laboratories and standardised at Scripps Institute of Oceanography using the SIO 1993 scale. Estimated precision for this data is $\pm 2\%$.

4 Observations

This chapter intends to identify the relative presence of Arctic and Atlantic-derived waters within the Baffin Bay region and the local mechanisms responsible for their spreading and mixing. It begins with a geographical description of θ and S properties observed from the data sets. It then presents a series of sections illustrating frontal convergence and describes geochemical structure throughout the region. It ends with a temporal discussion of θ and S properties along eastern Davis Strait placed in the context of large-scale advected climatological signals.

4.1 Geographical variations in halocline structure

Due to high variability in the data's spatial and temporal distribution, the regional overview of θ -S properties presented in this section was based on data from select years based on the spatial coverage they provided. In addition, CTD data were examined rather than bottle data to allow a more detailed resolution of structure. Six areas of the Baffin Bay region were examined, including Eastern Davis Strait, Melville Bay, the North Water region, the mouth of Lancaster Sound, the Baffin Island coast and central Baffin Bay. Halocline characteristics are described starting at the surface, with the seasonal halocline, and followed by the CH and WH. The reader is asked to refer to Table 4.1 for information on the location and dates of the data depicted in Figs. 4.1-4.6.

Region	Latitude/Longitude	CTD data availability for Summer (June, July, August)	CTD data availability for Fall (September, October)
Eastern Davis Strait	65.5-68 °N / 52-57 °W	1979, 1986, 1989, 1990 , 1992, 1997, 1998, 1999	1987, 1988, 1989, 1990 , 1997, 1999
Melville Bay	73.5-76 °N / 56-66 °W	1986	1987
North Water Region	75.5-78.5 °N / 70-79 °W	1979, 1980, 1986, 1997, 1998 , 1999	1979, 1999
Lancaster Sound	72.5-74.5 °N / 75-84 °W	1978, 1979 , 1980	1978, 1979
Baffin Island coast	70-73 °N / 68-76 °W	1978 , 1979, 2001	1978 , 1979, 1980, 1987, 1988
Central Baffin Bay	71.5-74 °N / 63-69 °W	1978, 1997	1987, 1999

Table 4.1: CTD data availability for the six regions presented in Chapter 4.1. The years depicted in Figs. 4.1-4.6 are indicated in bold and were chosen because they offered the best spatial coverage for each region.

Waters in Eastern Davis Strait (Fig. 4.1) reflected θ -S properties advected into Baffin Bay with the WGC. The seasonal halocline ($S < 33.0$; $D < 50\text{m}$) was characterised by strong surface warming ($0 < \theta < 5\text{ }^\circ\text{C}$) brought on by summer ice-free conditions. The CH was characterised by a core well-above freezing ($-1.0 < \theta_{\text{core}} < 1.5\text{ }^\circ\text{C}$) and of salinity $33.4 < S_{\text{core}} < 33.8$. The core was 60-100 m thick and found between 50-150 m. Below this, the WH structure was significantly cooler and fresher ($3.0 < \theta_{\text{core}} < 4.5\text{ }^\circ\text{C}$; $34.5 < S_{\text{core}} < 34.66$) than that described in the Labrador Sea by Lazier (1973). This difference is likely explained by the strong westward topographic veering of warm, salty WGC core properties immediately south of Davis Strait. The WH core was ~ 100 m thick and found between 250 and 500 m.

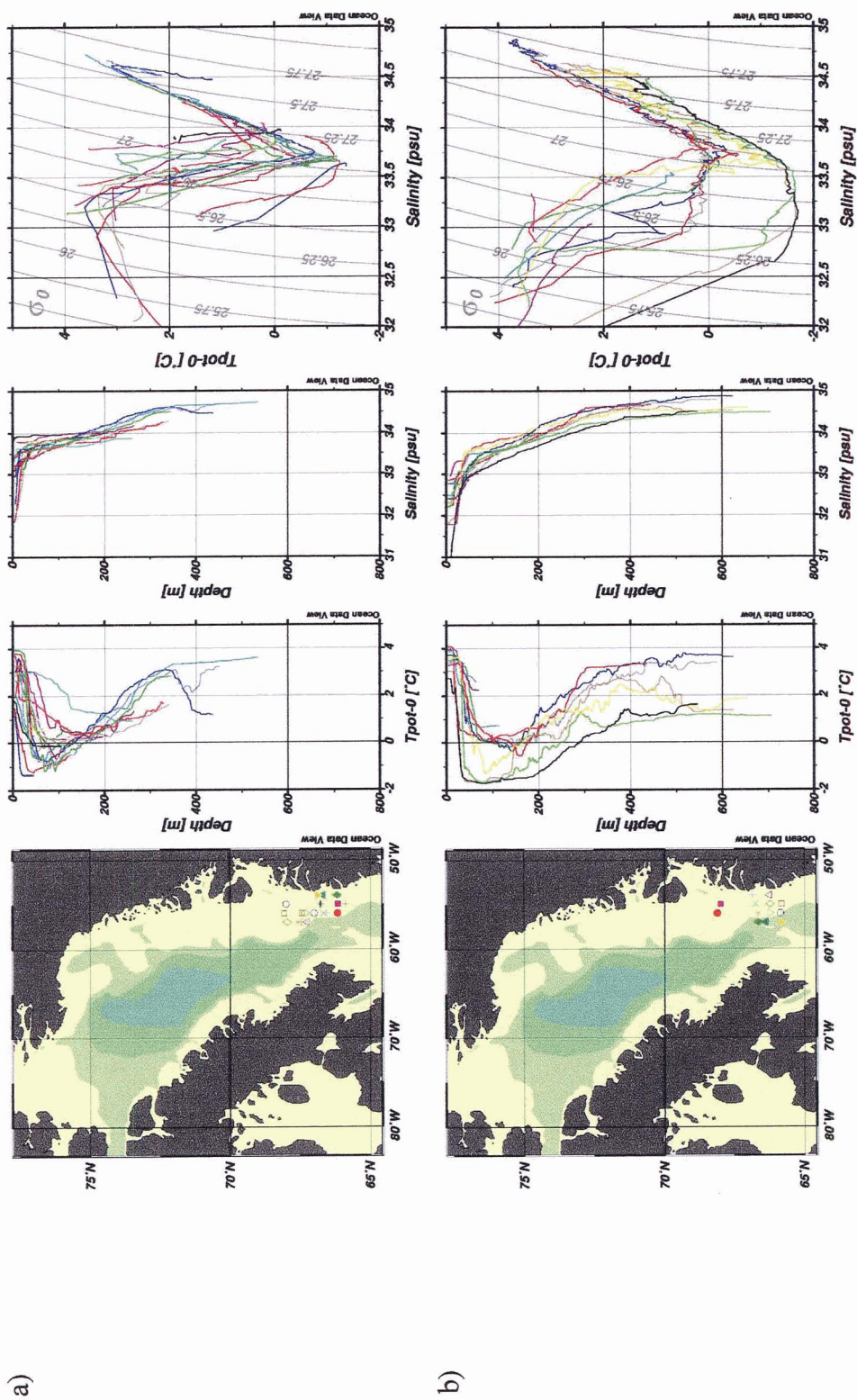


Fig. 4.1: θ and S properties in Eastern Davis Strait in the a) summer (June, July, August) and b) fall (September, October) of 1990.

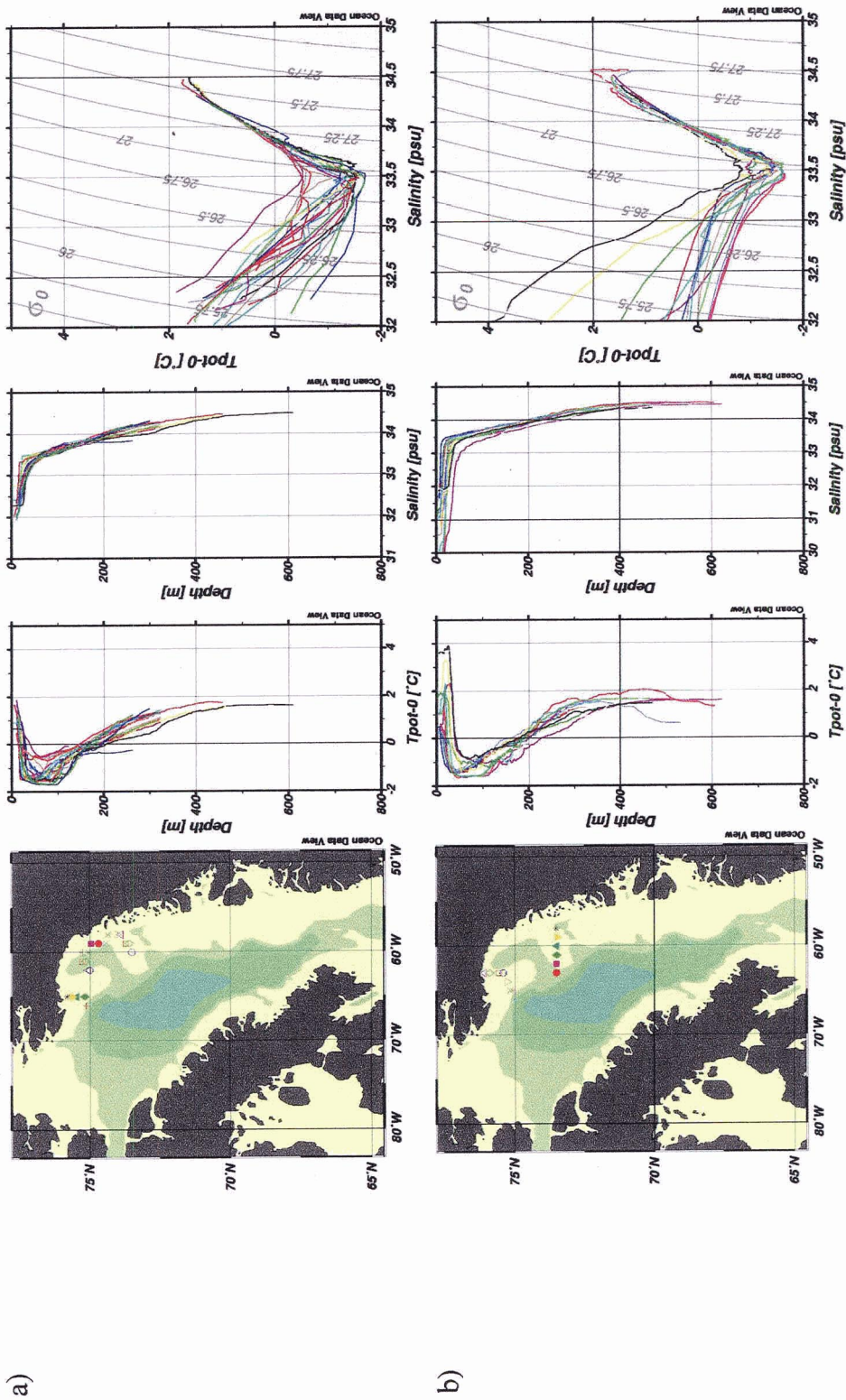


Fig. 4.2: θ and S properties in Melville Bay in the a) summer (June, July, August) of 1986 and b) fall (September, October) of 1987.

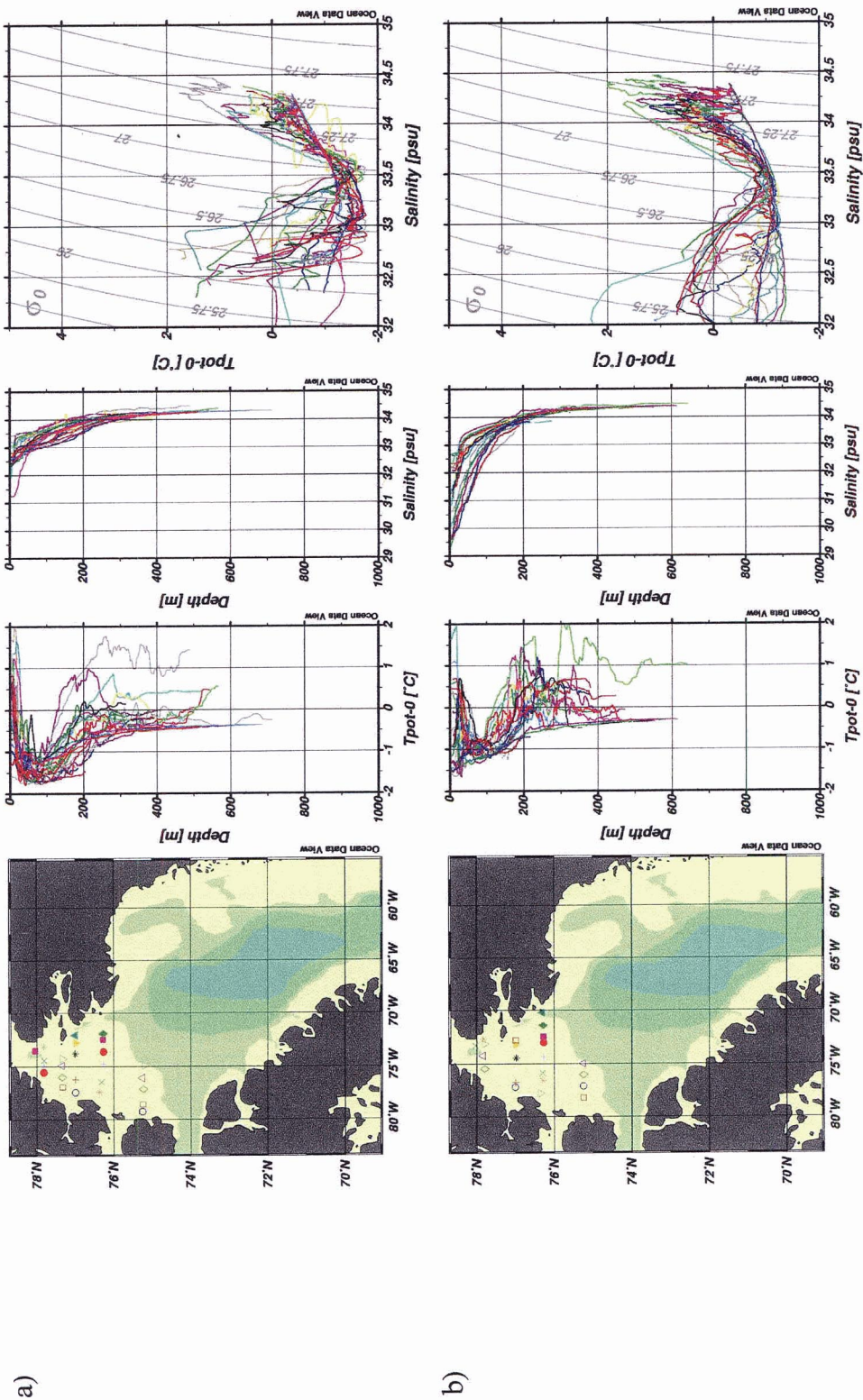


Fig. 4.3: θ and S properties for the North Water region in the a) summer (June, July, August) of 1998 and b) fall (September, October) of 1999.

Further north, WGC waters in Melville Bay (Fig. 4.2) were characterised by cooler seasonal halocline properties ($0 < \theta < 2$ °C at $S < 33.3$ and $D < 50$ m). Likewise, the CH and WH were cooler and fresher (CH: $-1.7 < \theta_{\text{core}} < -0.7$ °C; $33.3 < S_{\text{core}} < 33.55$; WH: $1.7 < \theta_{\text{core}} < 2.2$ °C; $34.3 < S_{\text{core}} < 34.5$). The depth and core thickness of the CH was similar to eastern Davis Strait, but the WH was thicker (200-300 m) and deeper (275-650 m). Differences in the properties of the seasonal halocline and CH compared to eastern Davis Strait likely resulted from cooler surface conditions and greater sea ice formation. Differences in the properties of the WH likely reflected diffusive (vertical) heat loss along the WGC's advection path.

Upon approach of the North Water region, WGC waters from Melville Bay strongly associate with the 600 m isobath leading toward Lancaster Sound (Melling et al, 2001). However, a minor portion of WGC waters enters the North Water region and undergoes intrusive mixing with waters from Smith Sound and Jones Sound. The result of this mixing, a halocline structure referred to as 'North Water Outflow' (Bâcle et al., 2002), heads southward from the North Water region west of 75°W toward Lancaster Sound. Observed seasonal halocline properties for North Water Outflow were quite variable ($-1.8 < \theta < 2.0$ °C and $32.25 < S < 32.75$; Fig. 4.3) and likely related to variations in sea-ice distribution and surface warming associated with the North Water's recurring polynya (Bâcle et al., 2002). CH properties for North Water Outflow included $-1.7 < \theta_{\text{core}} < -1.1$ °C, $33.3 < S_{\text{core}} < 33.65$, a core thickness of 50-70 m and a core depth of 25-100 m. WH

characteristics included $1.5 < \theta_{\text{core}} < 1.8$ °C, $34.35 < S_{\text{core}} < 34.5$, a core thickness of ~100 m and a core depth of 375-500 m. The WH was also characterised by the strong presence of thermohaline intrusions and an inflection in θ at $34.0 < S < 34.25$ ($-0.2 < \theta < 1.4$ °C).

The seasonal halocline in the mouth of Lancaster Sound was cool ($-1.8 < \theta < 1.0$ °C), fresh ($30.5 < S < 32.5$) and found in the upper 20 m (Fig. 4.4). Below this, CH properties reflected the influence of heavy local ice formation (cf. Melling et al., 1984) ($-1.65 < \theta_{\text{core}} < -1.55$ °C; $32.5 < S_{\text{core}} < 33.7$; core thickness: ~150 m; core depth: 35-200 m). WH characteristics ($1.2 < \theta_{\text{core}} < 1.8$ °C; $34.4 < S_{\text{core}} < 34.5$; core thickness: ~200 m; core depth: 400-800 m) included significant thermohaline intrusions as well as a θ inflection ($0.2 < \theta < 1.1$ °C; $34.2 < S < 34.3$) corresponding to that of the North Water Outflow.

Seasonal halocline conditions along the Baffin Island coast (Fig. 4.5) were $0 < \theta < 3$ °C and $30.0 < S < 32.5$ ($D < 20$ m). CH and WH properties were similar to those of Lancaster Sound (CH: $-1.65 < \theta_{\text{core}} < -1.55$ °C, $32.5 < S_{\text{core}} < 33.7$; WH: $0.9 < \theta_{\text{core}} < 1.8$ °C, $34.42 < S_{\text{core}} < 34.5$), but with thicker and deeper cores (CH core thickness: 200-250 m, CH core depth: 35-300 m; WH core thickness: 200-300 m, WH core depth: 400-900 m). The θ inflection noted in the WH of Lancaster Sound waters was also observed here for $0.8 < \theta < 1.1$ °C and $34.25 < S < 34.35$.

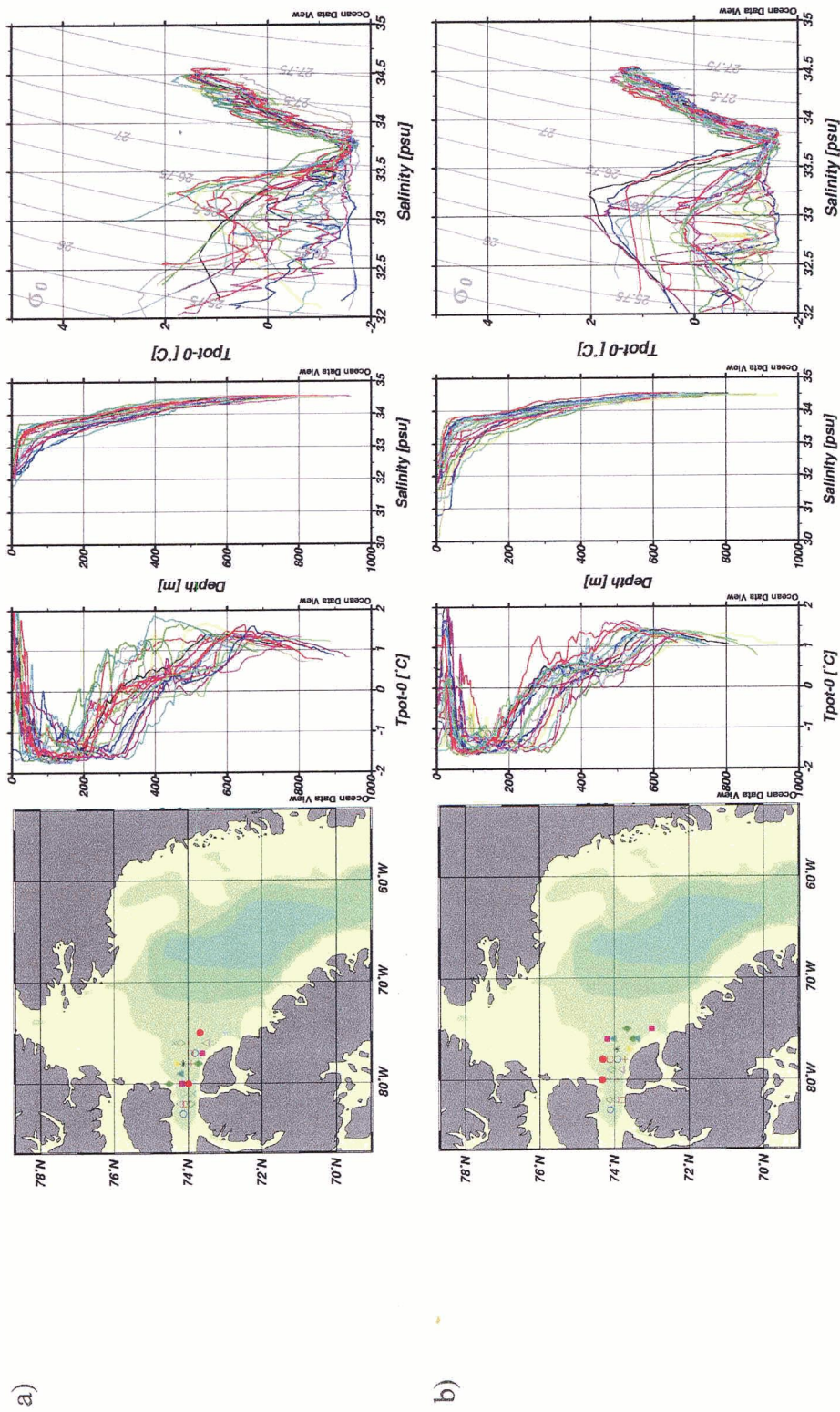


Fig. 4.4: θ and S properties for Lancaster Sound in the a) summer (June, July, August) and b) fall (September, October) of 1979.

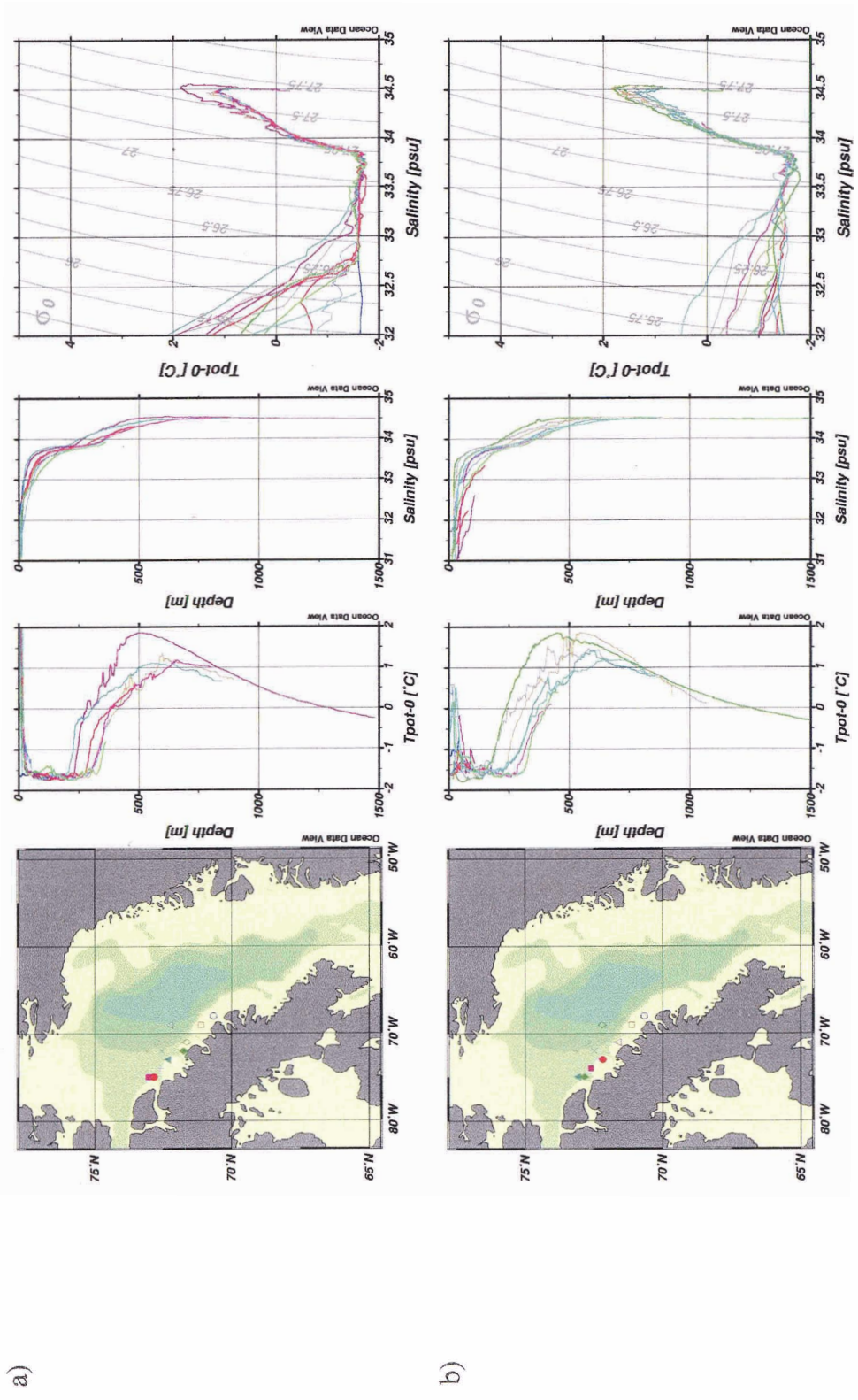


Fig. 4.5: θ and S properties along the Baffin Island coast in the a) summer (June, July, August) and b) fall (September, October) of 1978.

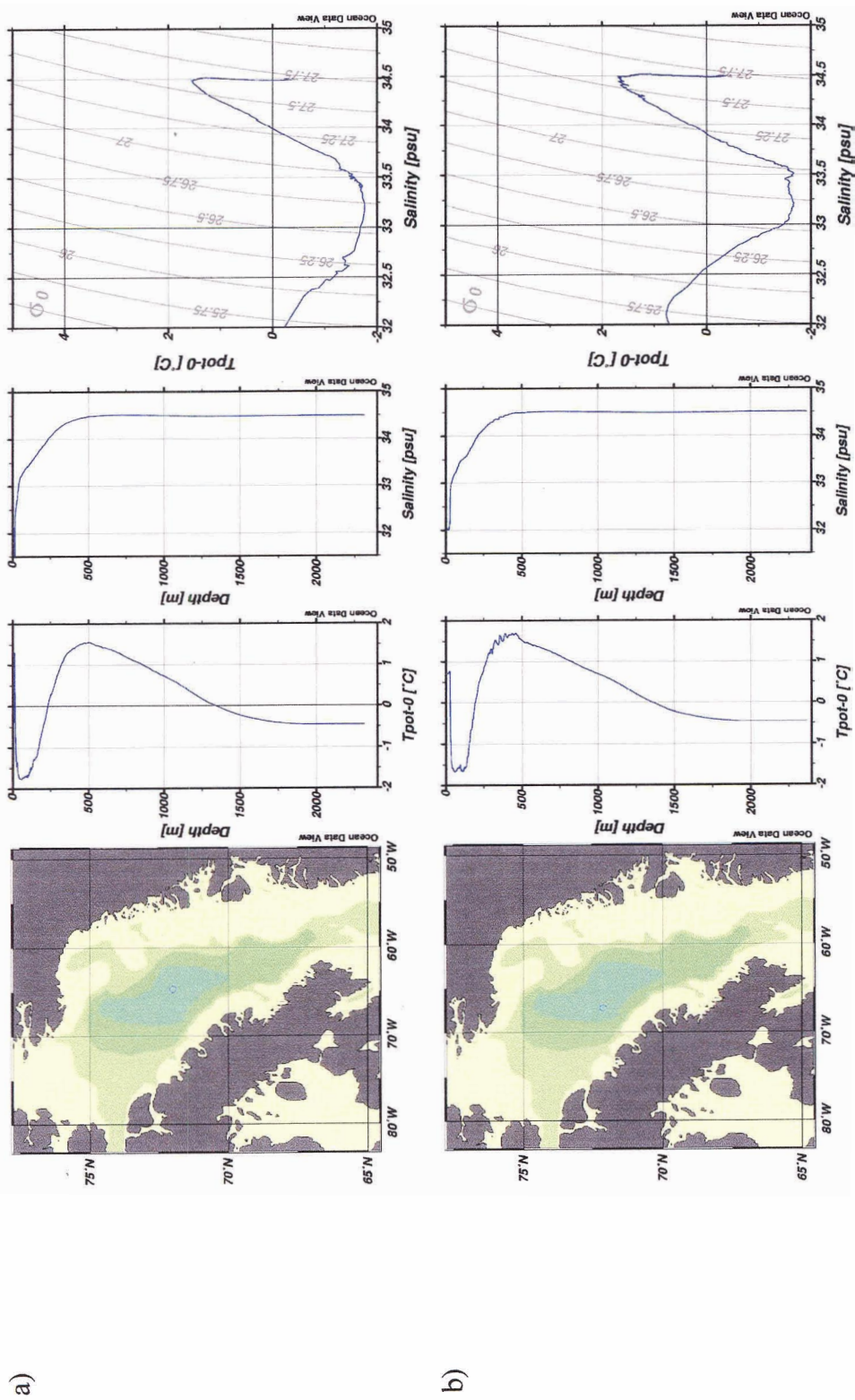


Fig. 4.6: θ and S properties in central Baffin Bay in the a) summer (June, July, August) of 1997 and b) fall (September, October) of 1999.

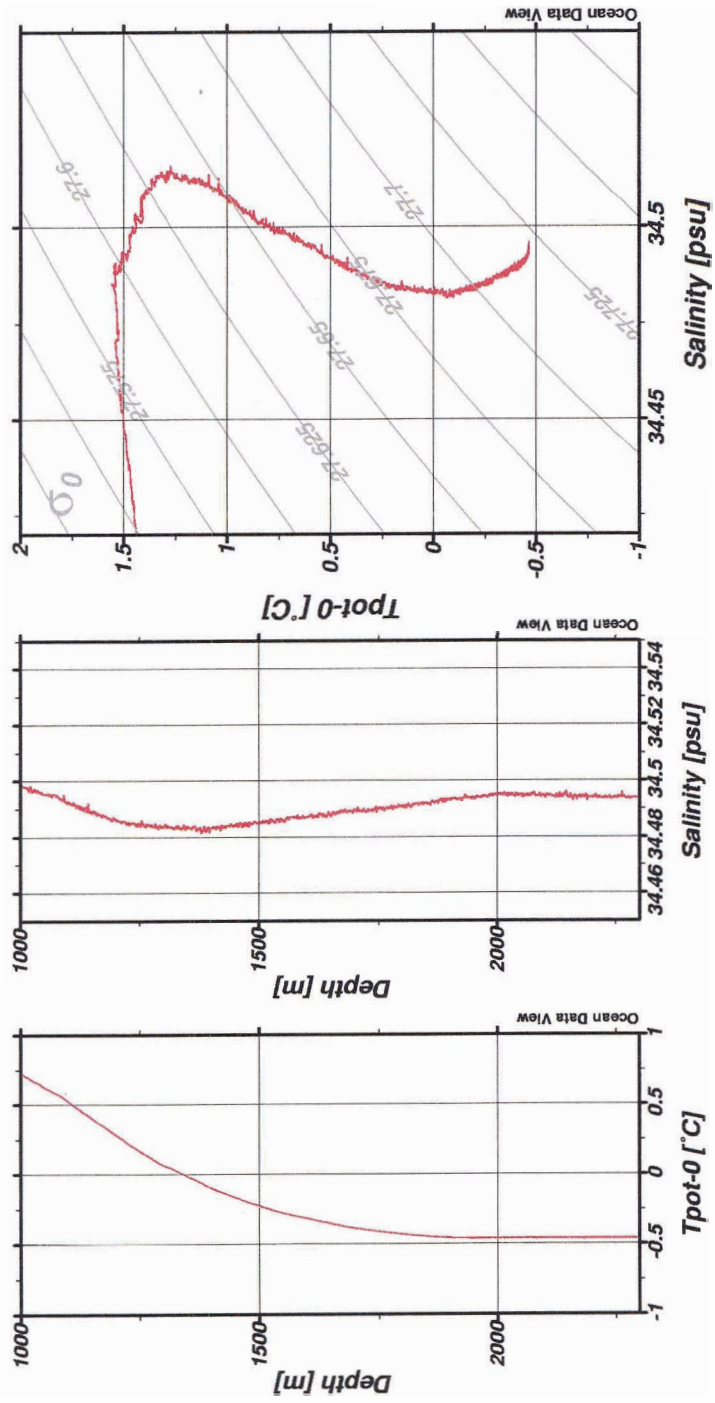
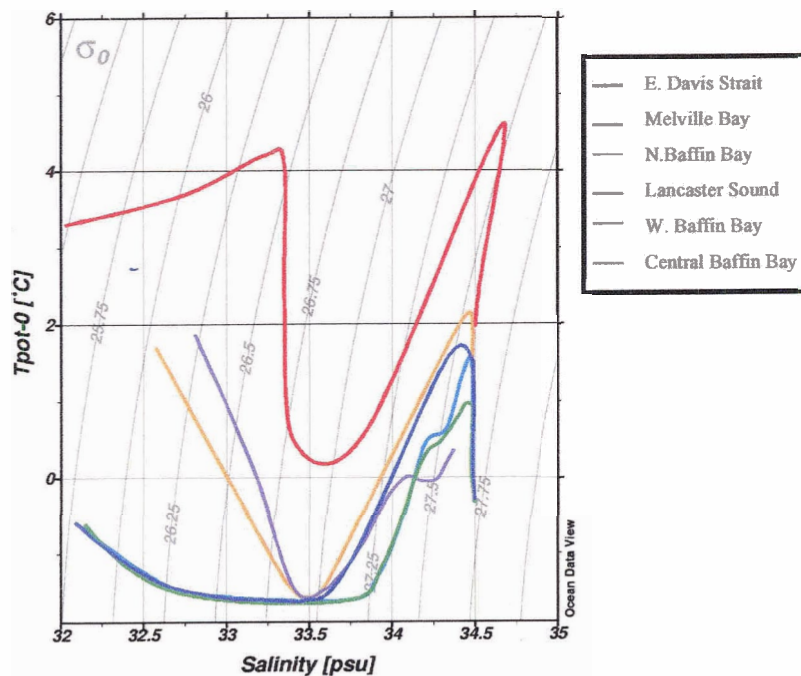


Fig. 4.7: Detail of θ and S properties in central Baffin Bay. Data from August 1997.



Region	CH core	WH core
Eastern Davis Strait	θ : -1 to 1.5°C S: 33.4-33.8 Thickness: ~60-100m Depth: 50-150m	θ : >3°C S: 34.5-34.66 Thickness: ~100m Depth: 250-500m
Melville Bay	θ : -1.7 to -0.7°C S: 33.3-33.55 Thickness: ~60-100m Depth: 50-150m	θ : 1.7 to 2.2°C S: 34.3-34.5 Thickness: ~200-300m Depth: 275-650m
'North Water Outflow' from the North Water region	θ : -1.7 to -1.1°C S: 33.3-33.65 Thickness: ~50-70m Depth: 25-100m	θ : 1.5 to 1.8°C S: 34.35-34.5 Thickness: ~100m Depth: 375-500 m
Lancaster Sound	θ : -1.65 to -1.55°C S: 32.5-33.7 Thickness: ~150m Depth: 35-200m	θ : 1.2 to 1.8°C S: 34.4-34.5 Thickness: ~200m Depth: 400-800m
Baffin Island Coast	θ : -1.65 to -1.55°C S: 32.5-33.7 Thickness: ~200-250m Depth: 35-300m	θ : 0.9 to 1.8°C S: 34.42-34.5 Thickness: ~200-300m Depth: 400-900m
Central Baffin Bay	θ : -1.65 to -1.55°C S: 32.5-33.7 Thickness: ~100-200m Depth: 35-250m	θ : 1.2 to 1.7°C S: 34.3-34.5 Thickness: ~250-400m Depth: 300-900m

Table 4.2: Summary of regional Baffin Bay θ -S properties.

Finally, structure in central Baffin Bay (Fig. 4.6) consisted of a seasonal halocline with $0 < \theta < 1$ °C and $30.0 < S < 33.5$ ($D < 50$ m). CH properties ($-1.65 < \theta_{\text{core}} < -1.55$ °C, $32.5 < S_{\text{core}} < 33.7$) were comparable to those of the Baffin Island coast, but with a thinner and shallower core (thickness: 100-200 m, depth: 35-250 m). WH properties ($1.2 < \theta_{\text{core}} < 1.7$ °C, $34.3 < S_{\text{core}} < 34.5$) were comparable to those of Melville Bay, but with a thicker, deeper core (thickness: 250-400 m, depth: 300-900 m). Below the WH core (> 900 m), the deeper halocline consisted of a monotonic decrease in θ to -0.46 °C. The signature of S exhibited a minimum (first noted by Muench, 1971) ($S_{\text{min}} \sim 34.48$) around 1400 m before converging to 34.49 at 2000 m (Fig. 4.7).

4.2 Zones of halocline convergence

Flow of the northbound WGC and southbound BC sets the stage for convergence between Arctic and Atlantic water components in the Baffin Bay region. Such convergence was found to occur throughout the region and appeared to be a significant mechanism for controlling both local mixing and downstream structures. The following table and discussion presents six sections of frontal convergence which were examined for their θ and σ_{θ} (potential density) characteristics.

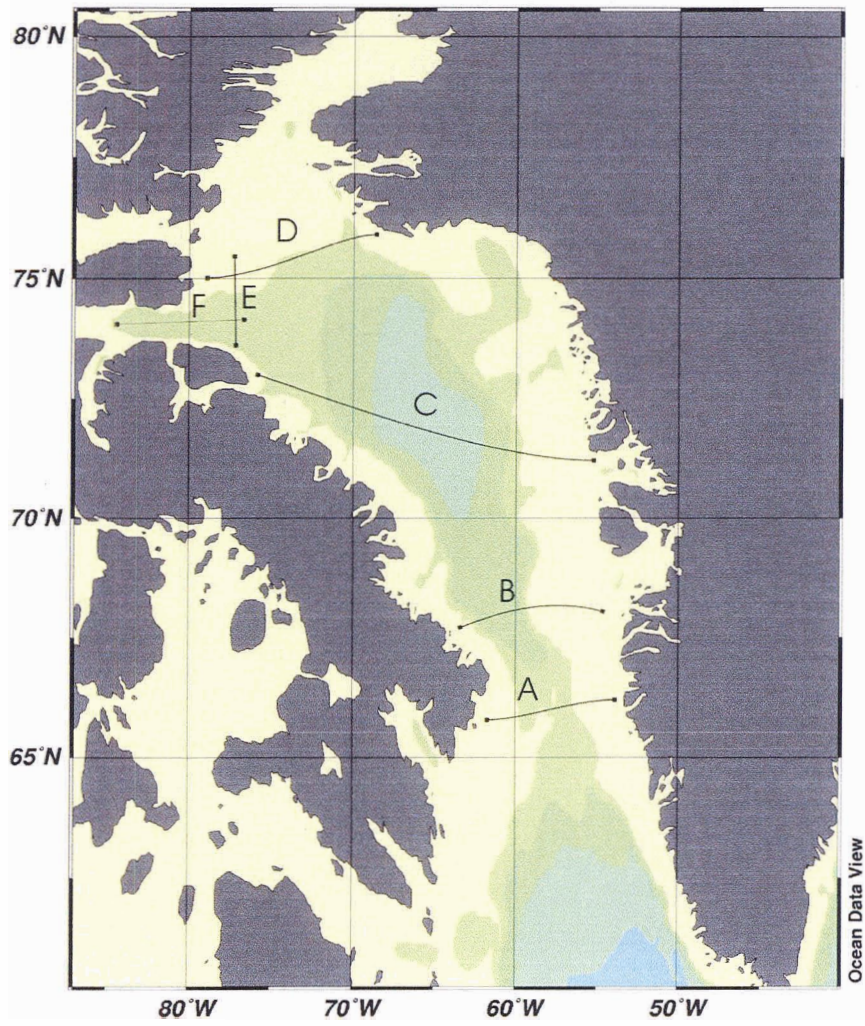


Fig. 4.8: Map of sections described in Chapter 4.2.

Section Label	Description	Location	CTD data availability
A	Davis Strait (east-west)	~ 66.5 °N	1987, 1988, 1990, 1997
B	Southern Baffin Bay (east-west)	~ 68 °N	1990
C	Central Baffin Bay (east-west)	~ 71 °N	2001
D	Northern Baffin Bay—North Water region (east-west)	~ 75.5 °N	1998, 1999
E	Lancaster Sound (north-south)	~ 74 °N	1978, 1979
F	Lancaster Sound (east-west)	~ 77 °W	1978, 1979

Table 4.3: CTD data availability for the six frontal sections presented in Chapter 4.2. Years depicted in Figs. 4.9-4.14 are in bold.

Sections A, B and C (Figs. 4.9-4.11) reflected WGC-BC convergence across Davis Strait, southern Baffin Bay and central Baffin Bay, respectively. These sections showed that as the WGC travelled northward into the Baffin Bay region, its WH core gradually eroded. That is, it cooled, freshened, thickened and deepened with increasing latitude (e.g. $\Delta \theta_{\text{core}} \sim 0.7$ °C and $\Delta S_{\text{core}} \sim 0.17$ between Section A and C), likely due to diffusion along its advection path. Core properties for the WGC also appeared constrained by shelf depths < 600 m as well as deep landward canyons (e.g. Section C at 55 °W). In contrast, properties for the BC (west) between Sections A and C remained similar to those observed along the Baffin Island coast in Chapter 4.1 (CH: $-1.7 < \theta_{\text{core}} < -1.4$ °C; $S_{\text{core}} < 33.8$; core thickness: ~200 m; core depth: 35-300m; WH: $0.9 < \theta_{\text{core}} < 1.8$ °C ; $34.4 < S_{\text{core}} < 34.5$; core thickness: 200-300 m; core depth: 400-900 m). Overall, σ_{θ} gradients across these three sections were quite small below the CH core (i.e. below 200 m) indicating that θ and S were density-compensating within the WH. This density-compensation was evidenced by the strong presence of thermohaline intrusions in WH waters, particularly where

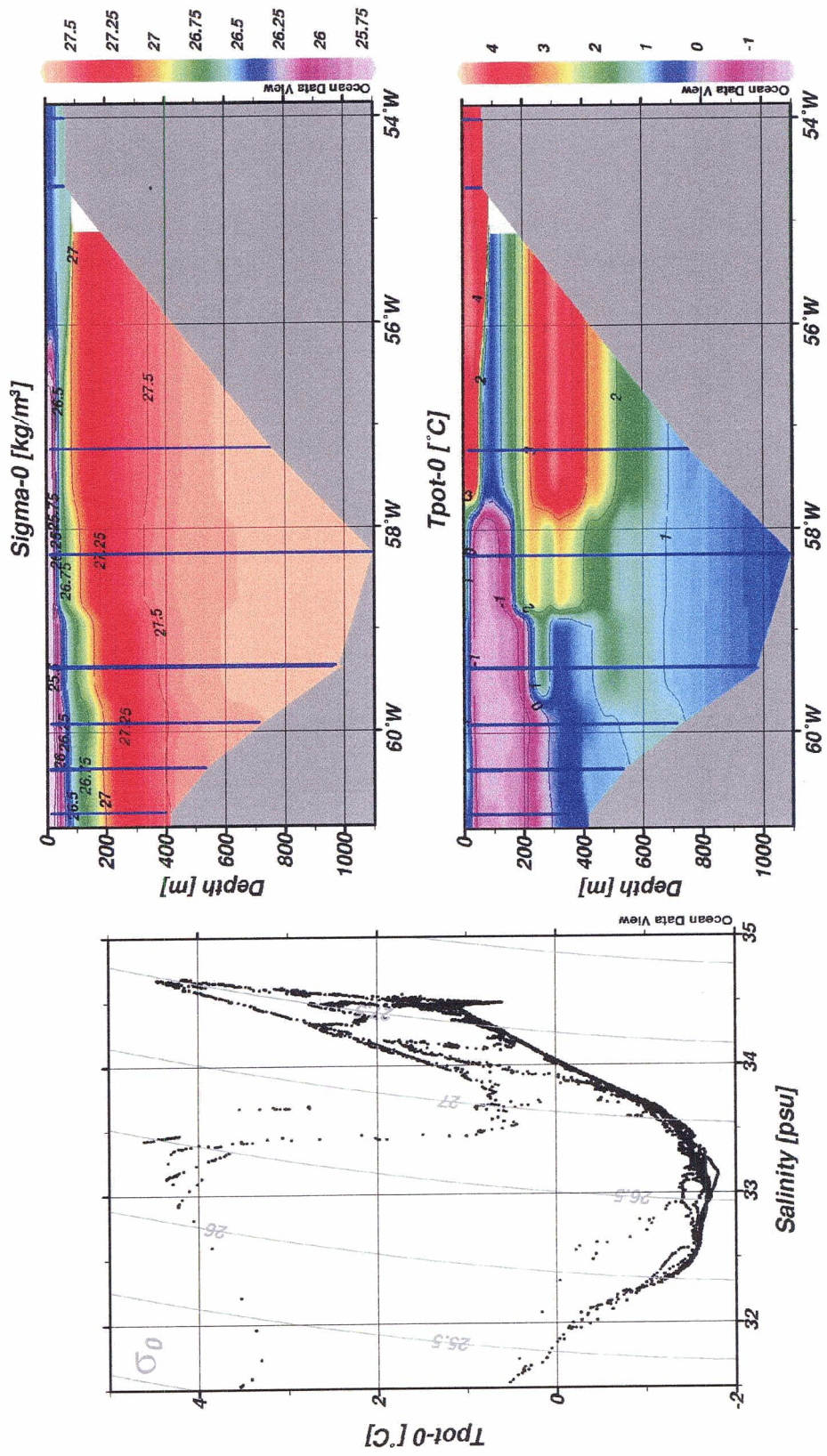


Fig. 4.9: Potential temperature (T_{pot-0}) and potential density ($\Sigma_{\theta-0}$) across section A (Davis Strait). Data from August 1997.

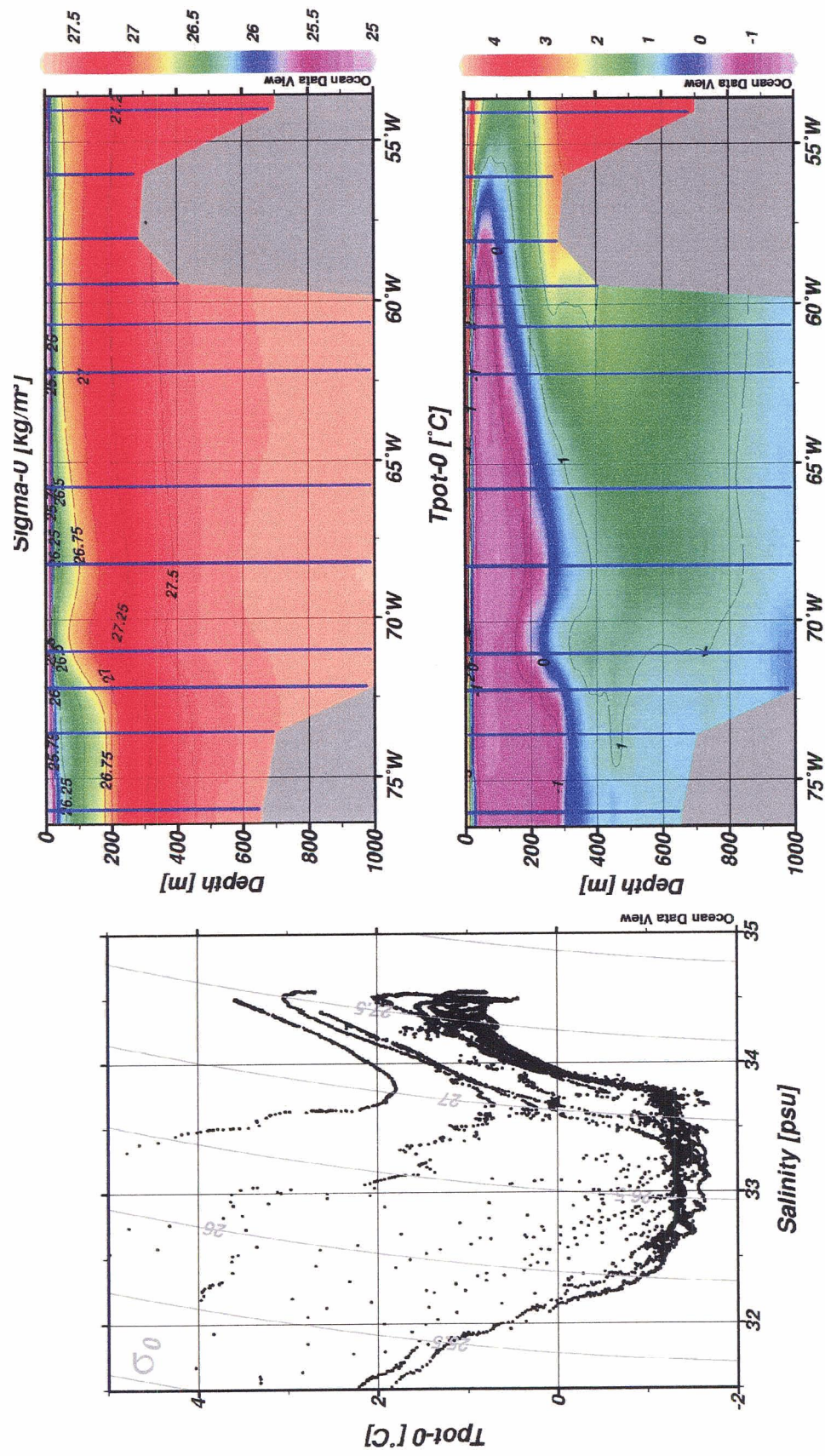


Fig. 4.11: Potential temperature (T_{pot-0}) and potential density (sigma-u) across section C (central Baffin Bay). Data from August 2001.

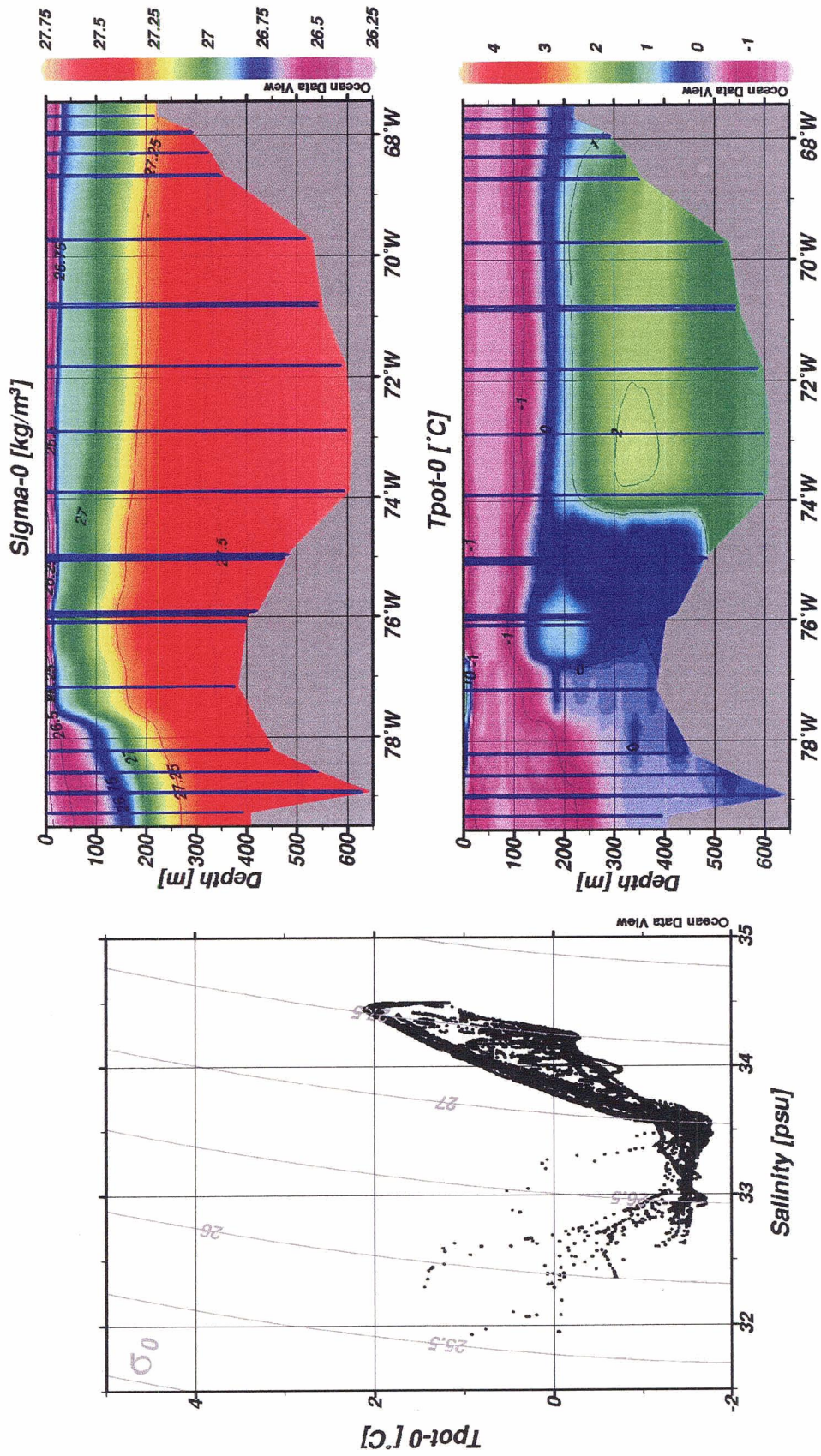


Fig. 4.12: Potential temperature (Tpot-0) and potential density (sigma-0) across section D (northern Baffin Bay, North Water region). Data from June 1998.

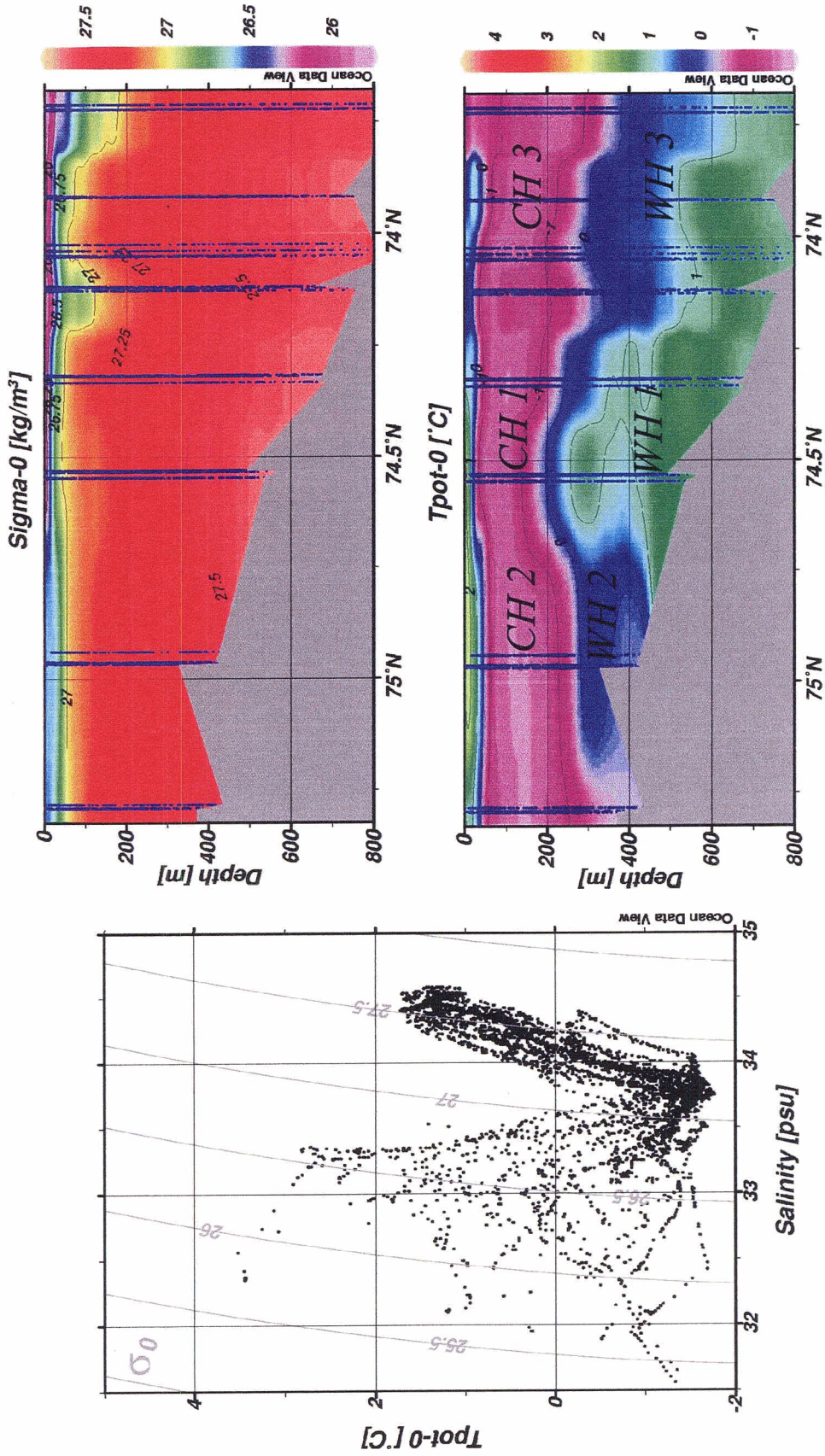


Fig. 4.13: Potential temperature (T_{pot-0}) and potential density (σ_0) across section E (Lancaster Sound). Data from September 1979.

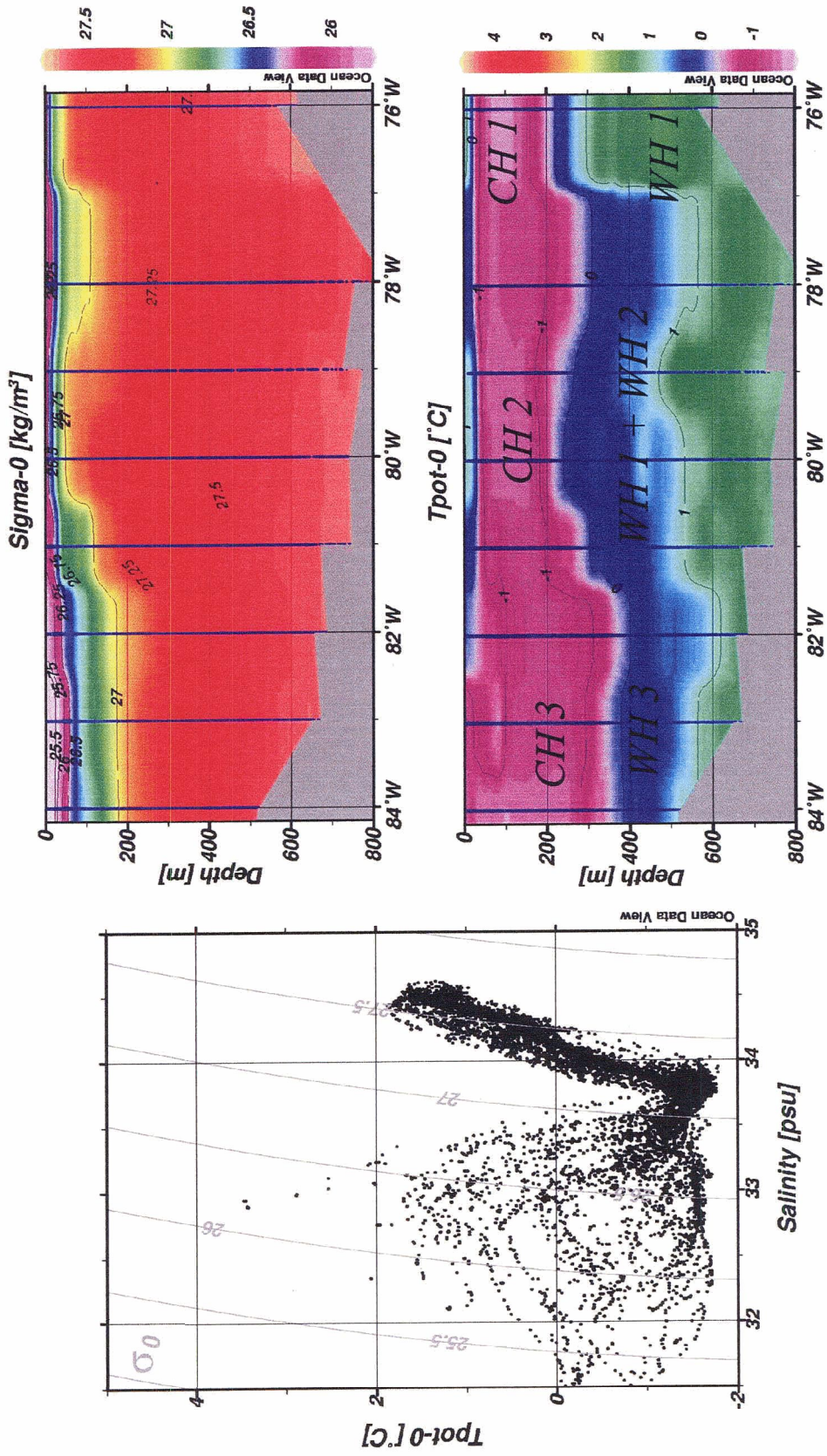


Fig. 4.14: Potential temperature (T_{pot-0}) and potential density (sigma-0) across section F (Lancaster Sound). Data from September 1979.

topography gradients were extreme (e.g. at 62° W and 59° W for Section B and at 72° W and 60° W for Section C).

Section D reflected convergence along the southern boundary of the North Water region (Fig. 4.12) between 600 m-bound WGC waters and southbound North Water Outflow. Frontal transition in θ across this section occurred roughly over ~ 40 kms with strong cross-frontal gradients of ~ 0.050 °C·km⁻¹ (at 400 m). In contrast, lateral density gradients were remarkably weak ($\sigma_\theta \sim 0.00075$ km⁻¹ at 400 m), allowing again the significant presence of thermohaline intrusions, particularly between $27.0 < \sigma_\theta < 27.66$ (or 100–600 m). Such intrusions can create conditions conducive to mixing via double-diffusion and cabelling. The possible impacts of these mixing mechanisms across Section D, as well as a more detailed description of its CH/WH structure are presented in Chapter 4.3.

Sections E and F showed north-south and east-west interactions in the mouth of Lancaster Sound (Fig. 4.13 & 4.14). Here, convergence was observed between WGC waters from Melville Bay (denoted in Figs. 4.13 and 4.14 as CH1 and WH1) and North Water Outflow (CH2 and WH2). Waters from the WGC (CH1: $-1.7 < \theta_{\text{core}} < -0.7$ °C ; $33.3 < S_{\text{core}} < 33.55$; core thickness: 60-100m; core depth: 50-150 m; WH1: $1.7 < \theta_{\text{core}} < 1.9$ °C ; $34.3 < S_{\text{core}} < 34.5$; core thickness: 200-300m; core depth: 275-650 m) were observed to approach from the north-east approximately along the 600 m isobath. North Water Outflow (CH2: $-1.7 < \theta_{\text{core}} < -1.1$ °C ; $33.3 < S_{\text{core}} < 33.65$; core thickness: 50-70 m; core depth: 25-100 m; WH2: $1.5 < \theta_{\text{core}} < 1.8$ °C ; $34.35 < S_{\text{core}} < 34.5$; core thickness: ~ 100 m;

core depth: 375-500 m) approached the region from the north. A third component for convergence was direct Canadian Archipelago outflow via Lancaster Sound (< 100 m). This latter component was not observable with CTD data, but its convergence with North Water Outflow likely occurred near 82 °W according to sharp variations in CFC structure reported by Wallace (1985). Downstream CH characteristics for the BC (CH3: $-1.6 < \theta_{\text{core}} < -1.55$ °C ; $32.5 < S_{\text{core}} < 33.7$; core thickness: ~200 m; core depth: 35-300 m) likely reflected mixing between North Water Outflow (CH1) and direct Canadian Archipelago outflow, as well as local modification via sea-ice formation. WH characteristics for the BC (WH3 : $0.9 < \theta_{\text{core}} < 1.8$ °C ; $34.42 < S_{\text{core}} < 34.5$; core thickness: 200-300 m; core depth: 400-900 m) possibly reflected intrusive mixing between WCG waters (WH1) and North Water Outflow (WH2), coupled with turbulent mixing associated with rough topography within the mouth of the sound.

4.3 Transformation processes

Chapter 4.2 discussed convergence between WGC and BC waters at six locations within the Baffin Bay region. Common features to each of these zones were weak lateral density gradients and the presence of numerous thermohaline intrusions. Such intrusions can create conditions conducive to mixing via double-diffusion and cabelling. The following section is a paper that presents a discussion of the possible impacts of these mechanisms along section D. The paper, "Structure and mixing across an Arctic/Atlantic front in Northern Baffin Bay" by J. Lobb, E.C. Carmack, A.J. Weaver and R.G. Ingram, was published in *Geophysical Research Letters*, Vol. 30, No. 16, 1833-1836, 2003.

Abstract

A front forms in northern Baffin Bay ($\sim 75.25^\circ\text{N}$) between Atlantic-derived water carried by the West Greenland Current and Arctic-derived waters exiting southward through Nares Strait and Jones Sound via the Baffin Current. Subsurface waters (e.g. below 100 m) of the West Greenland Current are as much as 2°C warmer than those of the Baffin Current. Confluence of these waters leads to a frontal transition between 100-500 m wherein cross-frontal gradients of potential temperature ($\Delta\theta/\Delta L \sim 0.06\text{-}0.07^\circ\text{C}\cdot\text{km}^{-1}$) and salinity ($\Delta S/\Delta L \sim 0.005\text{-}0.007\text{ km}^{-1}$) are largely density compensating ($\Delta\sigma_\theta/\Delta L \sim 0.001\text{ km}^{-1}$). Subsequent thermohaline interleaving establishes conditions conducive to mixing via cabelling and double-diffusion. The front's location would allow it to play a contributing role in the formation of Baffin Current water structure and eventual export of freshwater to the North Atlantic.

Introduction

Oceanic fronts in the polar regions regulate the distribution of heat, salt and mass budgets, exert control over the location of ice edges, and often play significant roles in setting ecosystem boundaries (Muench 1990). Such fronts differ in forcing and mode of formation, spatial and temporal persistence, associated mixing processes, and impacts on downstream water columns. During expeditions in 1998 and 1999 aboard the *CCGS Pierre Radisson* to northern Baffin Bay (a.k.a. North Water region), a sharp front was identified along a transect between the southern shore of Jones Sound and Cape York

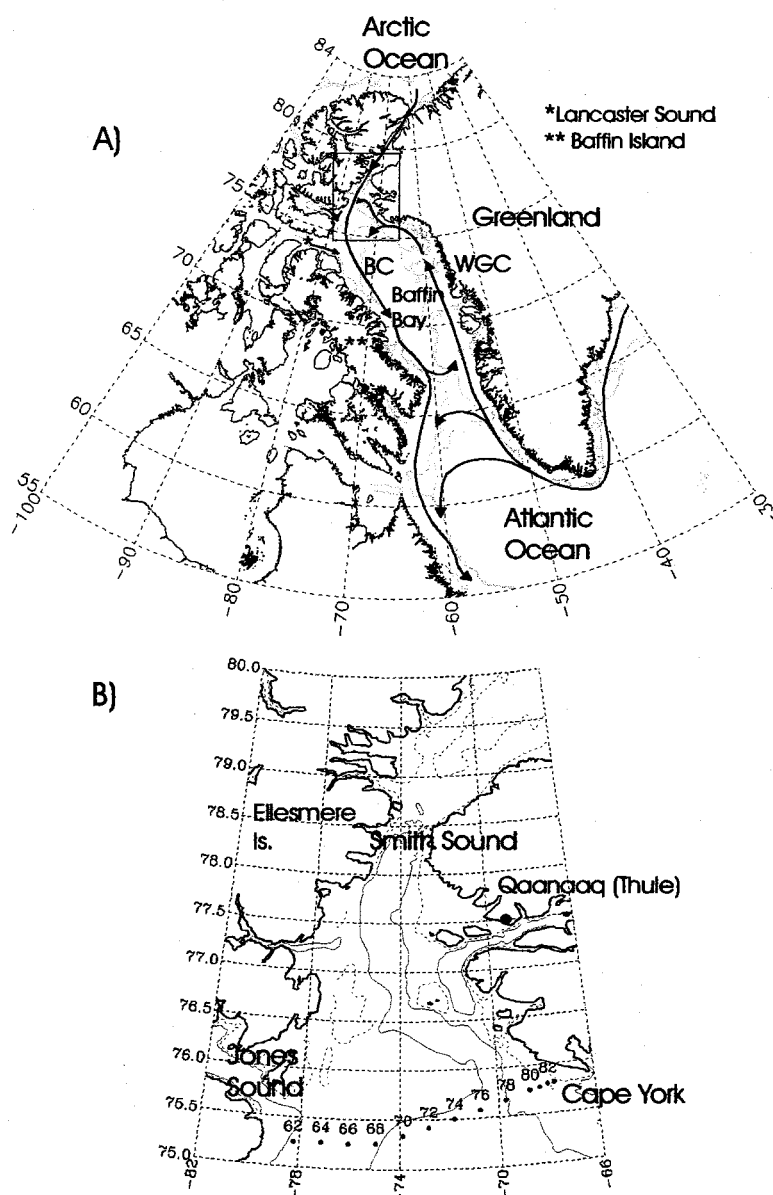


Fig. 4.15: A) Regional map of Baffin Bay. B) Close-up of northern Baffin Bay (aka North Water Polynya region) with stations sampled in June 1998 and September 1999. Five additional stations were sampled between Stn. 68 and Stn. 70 in September 1999 (not shown). 600 (solid) and 200m (dotted) isobaths are indicated.

(Fig. 4.15). It is formed by the convergence of waters of Atlantic and Arctic origin, the respective carriers of which are two currents: The northward-flowing West Greenland Current (WGC) along western Greenland, and the southern-flowing Baffin Current (BC) along the Canadian Coast. Waters carried by the WGC consist of an upper cold halocline (CH: depth < 100 m; S < 33.5) wherein temperature generally decreases with depth, and an underlying warm halocline (WH: depth > 100 m; S > 33.5) wherein temperature generally increases with depth to a maximum of 2.6 °C. Waters carried by the BC consist of similar CH characteristics (depth < 100 m; S < 33.5) but have a colder WH (depth > 100 m; S > 33.5) wherein temperature generally increases with depth to a maximum of 0.5 °C. A cold core near 33.5 separates the CH and WH layers. For both currents, the origin of the WH is ultimately traced to the Atlantic: directly via the Labrador Sea in the case of waters carried by the WGC, or via the Atlantic layer of the Arctic Ocean for waters carried by the BC.

The northward transport of Atlantic water in the WGC is strongly constrained by the 600m isobath which marks the southern boundary of northern Baffin Bay (cf. Melling et al., 2001; Ingram et al., 2002). This results in a cyclonic redirection of the WGC back into the main basin of Baffin Bay around 75 °N. A second branch of WGC waters, however, continues northward into northern Baffin Bay where confluence and mixing with Arctic outflows from Smith Sound and Jones Sound occurs (Bâcle et al., 2002). The resulting “North Water outflow”, distinctly characterised by thermohaline intrusions throughout

both the CH and WH, then joins outflow from Lancaster Sound to define the characteristics of the BC.

The frontal boundary described here is formed between cyclonically-redrafted WGC waters and southward North Water outflow at $\sim 75.25^\circ\text{N}$. The purpose of this paper is 1) to describe water structure across the front using profiled conductivity-temperature-depth (CTD) data, and 2) to evaluate mixing mechanisms at the frontal boundary, including double-diffusion and cabelling. We note that our data is not the first to recognize the convergence of Arctic and Atlantic-derived waters in northern Baffin Bay. For a summary of 1967-1970 surveys to the region, the reader is referred to Muench (1971). However, earlier data (e.g. section D in Muench, 1971, Fig. 5) depict much weaker frontal conditions than presented here. This is a reflection of the WGC's northerly limit due to topographical constraint by the 600 m isobath (Melling et al., 2001).

Materials and Methods

CTD data were obtained along a section crossing the front in June 1998 (early summer conditions), and in September 1999 (late summer conditions) (see Fig. 4.15 for station locations). Profile measurements were obtained on both occasions using a Falmouth Scientific Instruments Integrated CTD. In 1998, stations 62 to 80 were sampled at a collection rate of 4 Hz; in 1999, stations 62 to 80 were sampled at a collection rate of 13 Hz, with 5 extra stations between stations 68 and 70 to more accurately define the front. Temperature, pressure and conductivity sensors were calibrated prior to both expeditions.

In addition, post-cruise calibrations were performed on pressure (1998 cruise), temperature (1998 and 1999 cruise) and conductivity (1999 cruise). Water samples were collected during both cruises and analysed on a Guildline Auto-Sal salinometer to further calibrate salinity. The delays in temperature measurements that were found to be optimal for salinity calculations were 500 ms (1998) and 325ms (1999). Median box-car filtering was applied to salinity (1m averaged data) for all stations (in 1998 the filter width was 21; in 1999, three filter widths were used: 25 for 0-100 db; 40 for 100-300 db; 65 for >300 db). Accuracy in the data is estimated at temperature = ± 0.002 °C; salinity = ± 0.008 ; pressure = ± 1.5 db. Precision is estimated at temperature = ± 0.0005 °C; salinity = ± 0.03 ; pressure = ± 0.5 db. Because of the low precision (± 0.03) of salinity, minor inversions related to sensor response time mismatch (yielding 'loops' in temperature-salinity correlation plots) remained in the processed data. To correct this, salinity was edited assuming that profiles were monotonic in density. While real density inversions are known to occur in the ocean (Dunbar, 1958), the magnitude of corrections applied to salinity for a given profile as estimated from the Root Mean Square of the difference between edited and original salinities (0.004) was well within our stated precision for the instrument. All values of potential temperature (θ) and potential density (σ_θ) were computed from algorithms in UNESCO (1983).

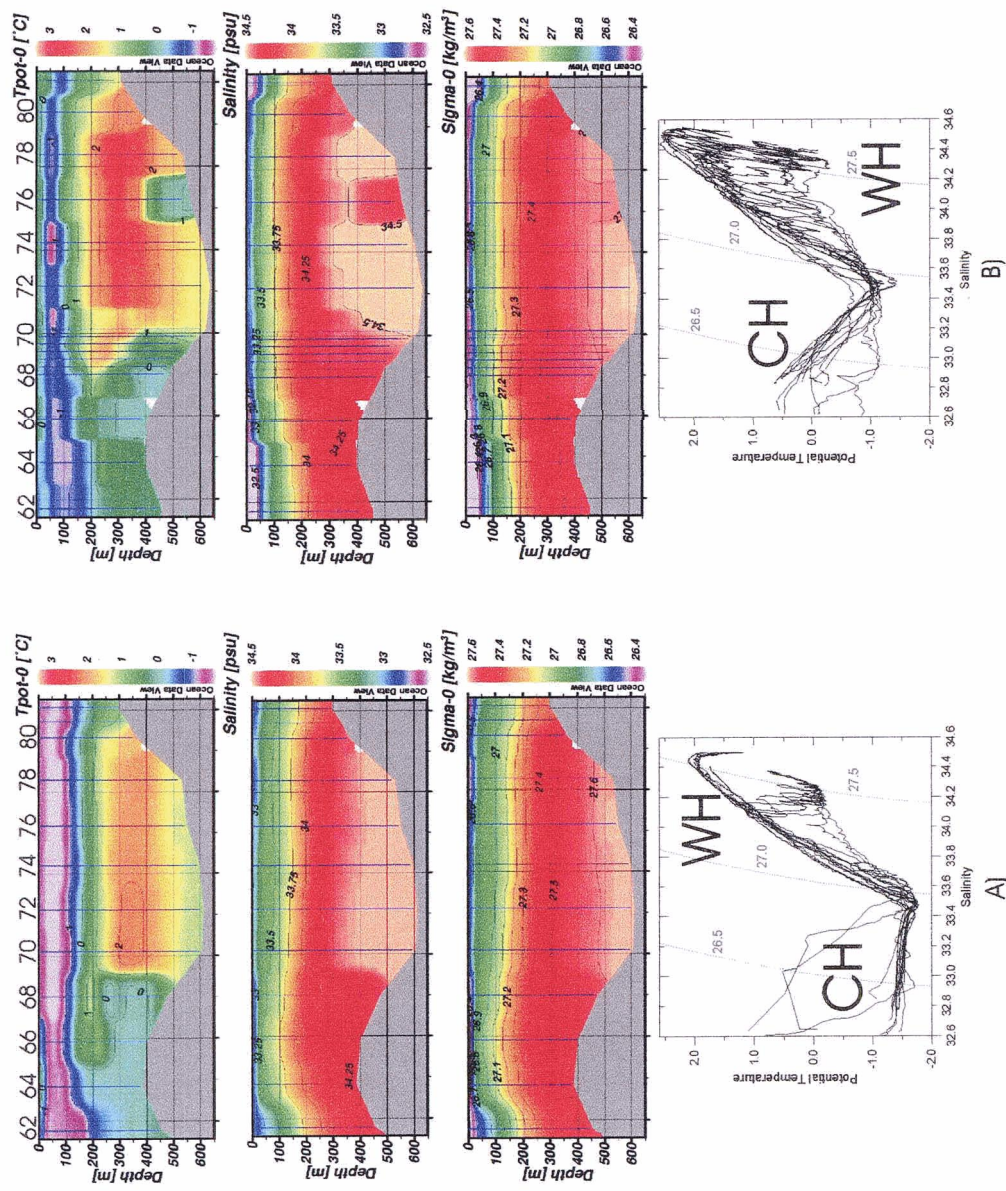


Fig. 4.16: Horizontal distribution of properties and potential temperature-salinity curves for a) June 1998 and b) September 1999.

Results

a) Frontal Structure

The front was bound to the west by North Water outflow and to the east by waters of the WGC (Fig. 4.16). For both June 1998 and September 1999 the frontal transition occurred over ~ 40 kms between stations 68 and 70, and roughly above the 600 m isobath. Maximum cross-frontal gradients for θ and salinity (between stations 68 and 70) were $0.067 \text{ }^\circ\text{C}\cdot\text{km}^{-1}$ and 0.0071 km^{-1} at 350m depth in 1998, and $0.058 \text{ }^\circ\text{C}\cdot\text{km}^{-1}$ and 0.0046 km^{-1} at 400 m depth in 1999). Lateral density gradients were weak (σ_θ between stations 68 and 70 were 0.0014 km^{-1} at 400 m in 1998 and 0.00075 km^{-1} in 1999), indicating that the front's dynamics were largely determined by density-compensation. This was also reflected in the high degree of isopycnal interleaving and intrusions between stations 68 and 70 noted in September 1999. These intrusions ranged in thickness from 5-55 m while associated θ and salinity differences along intrusions were $\Delta\theta < 0.82 \text{ }^\circ\text{C}$ and $\Delta S < 0.05$, respectively.

Several differences in the frontal transition and the characteristics of both North Water outflow and WGC waters were noted between June 1998 and September 1999. North Water outflow in September 1999 exhibited higher θ values throughout both the CH and WH than in June 1998. The difference in θ at the base of the CH ($\Delta\theta_{\text{CH}} = \theta_{\text{CH in 1999}} - \theta_{\text{CH in 1998}}$) was $0.5 \text{ }^\circ\text{C}$, while the difference in maximum θ value of the underlying WH ($\Delta\theta_{\text{WH}}$) was $0.3 \text{ }^\circ\text{C}$. Higher CH and WH temperatures in WGC waters were also observed

between June 1998 and September 1999. Here, $\Delta\theta_{CH}$ was 0.4 °C, while $\Delta\theta_{WH}$ was 0.5 °C (with 2.1 °C and 2.6 °C as maximum WH temperatures in 1998 and 1999, respectively). In September 1999, a near-bottom intrusion of relatively cold water ($\Delta\theta_{min} = -0.2$ °C; depth > 400 m) was observed within the WH of WGC waters between stations 74 and 78. The θ and salinity characteristics of this cold water correspond to North Water outflow of the same depth (Björle et al. 2002).

b) Mixing Considerations

Profiles collected between station 68 and 70 in September 1999 revealed thermohaline intrusions within the frontal transition, particularly between $27.0 < \sigma_\theta < 27.66$ (or 100-600 m; Fig. 4.16b). Spatial and temporal coherence of intrusions was smaller than sampling intervals (e.g. less than the ~ 5 km distance and 1-2 hour time intervals between stations), making them fundamentally different than those described for the Arctic Basin by Carmack et al. (1998). However, their presence in the frontal domain and their tendency to align with isopycnal surfaces warrants evaluation of cross-frontal mixing by double-diffusion and cabelling.

i) Double-diffusion

Convective motions can occur in an overall stably stratified ocean when a) either temperature or salinity are destabilising and b) temperature and salinity diffuse at different rates (Schmitt, 1994). As such, Ruddick (1983) developed a practical measure, the Turner Angle (Tu), for describing the nature and strength of double-diffusive activity within a

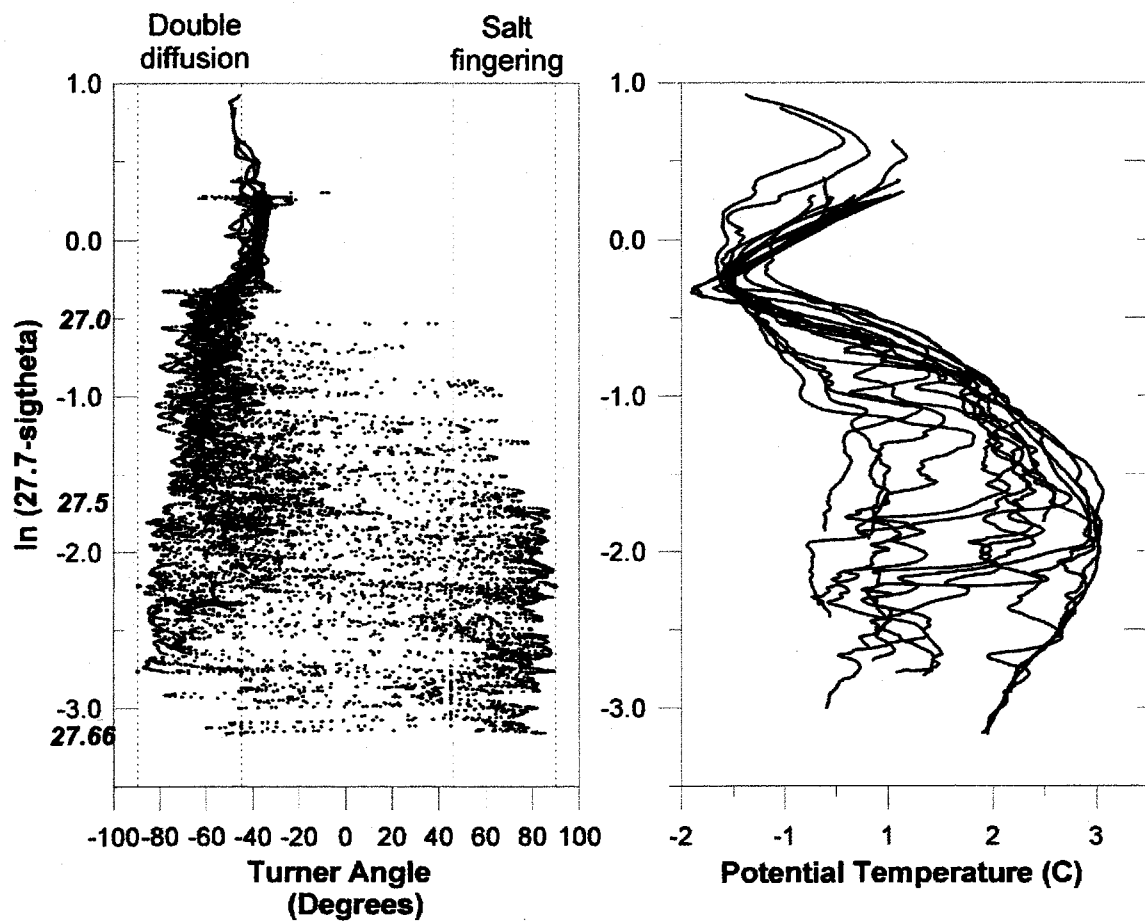


Fig. 4.17: a) θ and b) T_u across the frontal zone in September 1999. Both graphs are plotted on a logarithmic density scale relative to the maximum density in the water column, allowing better resolution of the intrusive features at depth. Density equivalencies are indicated in *italic*.

water column. It is based on the scaled contribution of vertical S and θ gradients to the vertical density gradient: $Tu = \arctan [(N_\theta^2 - N_S^2) / (N_\theta^2 + N_S^2)]$, where $N_\theta^2 = +/- g\beta\partial_z S$ and $N_S^2 = +/- g\alpha\partial_z\theta$ (positive N_θ^2 and N_S^2 correspond to stable S and θ stratification). With this definition, vertical gradients will be diffusively unstable for $-90^\circ < Tu < -45^\circ$, doubly stable for $|Tu| < 45^\circ$, salt finger unstable for $45^\circ < Tu < 90^\circ$, and gravitationally unstable when $|Tu| > 90^\circ$. Profiles of Tu and θ for stations 62 to 80 in September 1999 (Fig. 4.17) reveal a background affinity toward mixing via the diffusive instability from the surface to $\sigma_\theta \sim 27.0$ (-0.5 on the vertical scale of Fig. 4.17). Intrusive features whereby diffusive instability and salt fingering alternately affect buoyancy of the water column occurred at $27.0 < \sigma_\theta < 27.66$. Approximately 80 % of the water column within this range favoured mixing via diffusive instability while 15 % favoured mixing via salt fingering (particularly between $27.5 < \sigma_\theta < 26.66$ or depth > 320 m). Despite the fact that this system was poised for double-diffusion, the necessary requirement for differential diffusion of heat and salt may have been overwhelmed by tidally driven turbulence.

ii) Cabelling

Cabelling refers to an increase in density via mixing which is a consequence of the nonlinearity of the equation of state of seawater. Hence, the product of mixing between two water masses of equal density (σ_θ) but differing temperature and salinity will have a new density which is greater than either parent water type, and thus tend to sink in zones of convergence (Fedorov, 1983). To estimate the potential effect of cabelling at the frontal interface we first assumed that lateral mixing occurred strictly along straight lines in θ - S

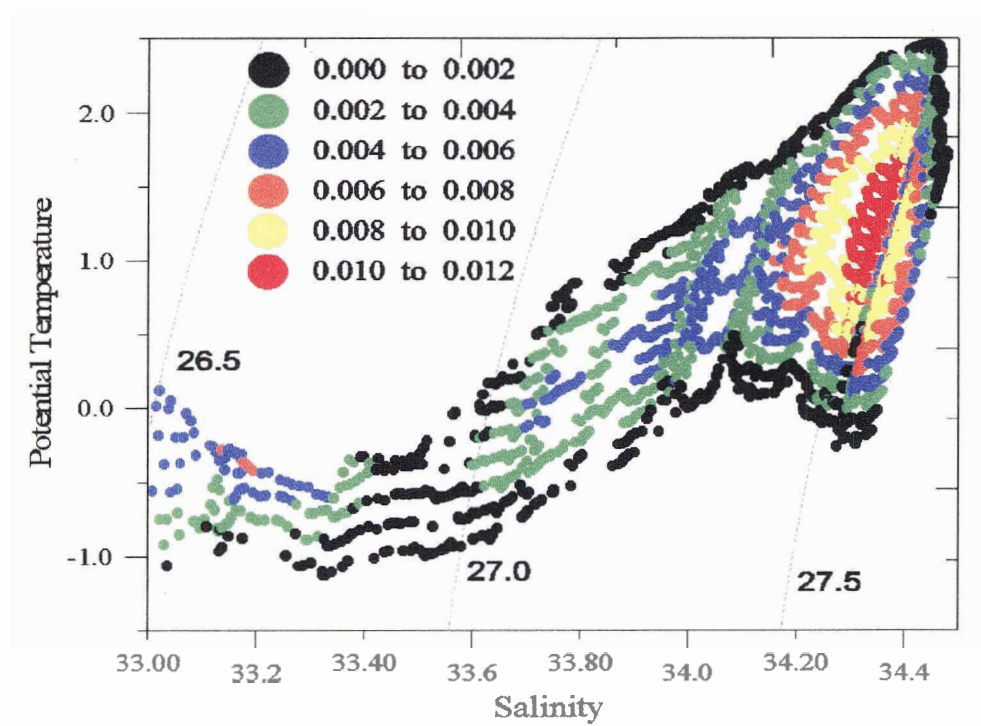


Fig. 4.18: Estimated changes in density across the frontal zone due to cabelling in September 1999.

space between end members of equal σ_θ . Assigning average θ -S curves for WGC waters and North Water outflow as the parent mixing members, we then calculated changes in density along successive isopycnals under all possible mixing proportions (Fig. 4.18). The largest calculated increase in σ_θ (~ 0.01) occurred approximately along the 27.5 isopycnal. This corresponded to the largest difference in θ ($\Delta\theta \sim 2.45$ °C) and S ($\Delta S \sim 0.21$) between WGC waters and North Water outflow.

Discussion

The front presented here displayed juxtaposition of differing water masses via the cyclonic WGC, which originates in the North Atlantic, and southern-flowing Arctic outflow, which is modified locally within the North Water region. The front was found to be density-compensated. This was evidenced in small lateral gradients of σ_θ and a high degree of isopycnal interleaving across the frontal transition. The background stratification in σ_θ was largely a function of salinity (as is typical in high latitudes), leaving evidence of the front mainly in the temperature field. In addition, active interleaving followed along isopycnal surfaces, as water parcels under these conditions require little work to travel from one side of the front to the other. Such interleaving establishes temperature and salinity structure which may be conducive to mixing via double-diffusion and cabelling. While the present data does not allow us to estimate the relative importance of these mechanisms in maintaining the frontal boundary, some speculation is possible. Owing to regional currents and tidal mixing (Fissel et al., 1981), background turbulence levels are likely to be large and act to inhibit double-diffusion fluxes. On the other hand, the largest estimated density

increase due to cabelling (~ 0.01) was roughly and order of magnitude greater than lateral density gradients across the front. This suggests that cabelling may play a dynamically significant role in maintaining convergent flow at the frontal boundary.

While density compensation significantly characterised the front's structure and its disposition to mixing, the extent of this compensation may change with variation in the transport (mass or property) of the WGC or North Water outflow. Such variation could be either seasonal (cf. Stein and Buch, 1986) or decadal (e.g. in the form of North Atlantic GSA signals or freshwater outflow pulses through Smith Sound; Belkin et al., 1998) in scale. Its resulting impact would depend on mixing processes within the mouth of Lancaster Sound (the imminent downstream destination of North Water outflow, WGC waters and their frontal transition; cf. Melling et al., 2001) and their role in forming and exporting water structures to the Labrador Sea via the BC.

4.4 Geochemical structure

Although θ and S properties are useful for identifying water structure components, they give little insight into the source waters (i.e. Arctic and Atlantic) or the time scale of ventilation events. Plots of CFC-11, CFC-12, CFC-113, CCL₄, and dissolved nutrient (nitrate, silicate, phosphate and dissolved oxygen) concentrations versus S from an August 1997 cruise were thus examined to complement observations made from the physical data set.

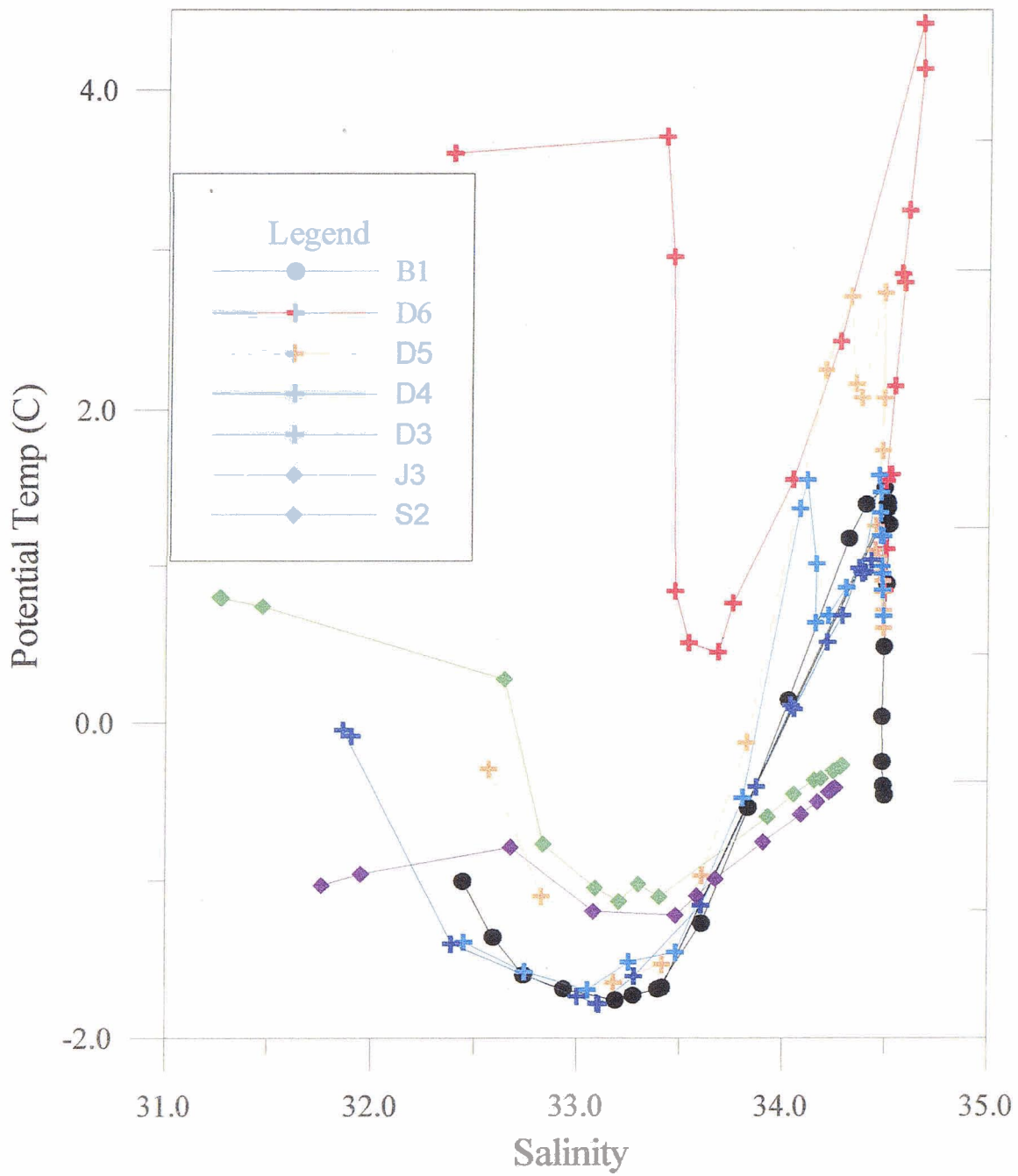


Fig. 4.19 a) θ versus S for geochemical stations sampled in August 1997.

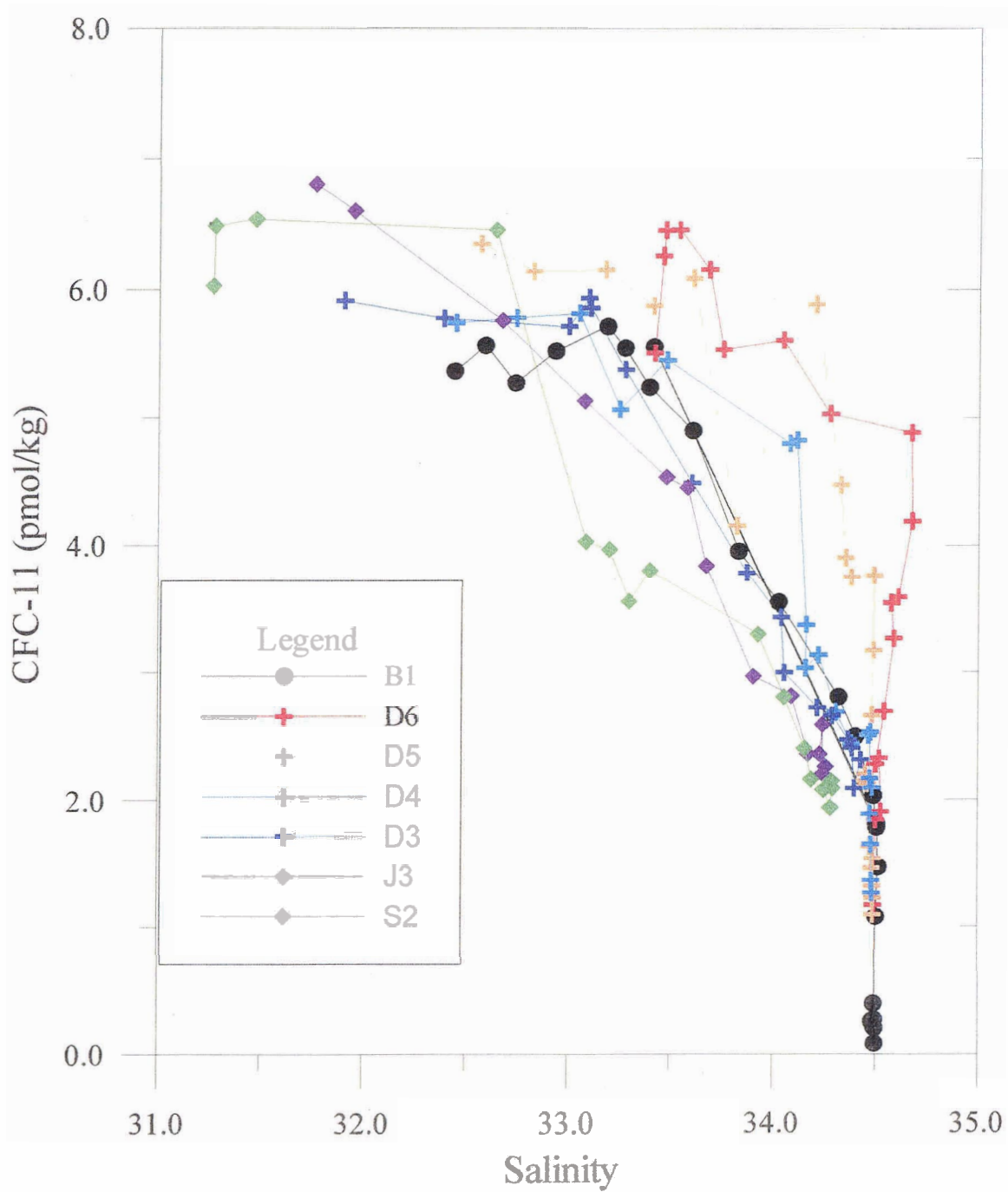


Fig. 4.19b) CFC-11 versus S for geochemical stations sampled in August 1997.

Variations in CFC-11 concentration immediately north of Davis Strait (cross symbols in Fig. 4.19) reflected differing ventilation histories for WGC (Station D5) and BC (Stations D4 and D3) waters. Both currents exhibited high concentrations within the CH core ($33.0 < S_{\text{core}} < 33.5$ for WGC and BC waters) associated with direct surface exchange during wintertime convection. However CFC-11 concentrations within the WH core ($S > 34.0$) were much higher in WGC waters than BC waters (~ 5 pmol/kg versus ~ 2 pmol/kg). Because concentrations in the WH core were associated with corresponding large temperature differences ($\theta_{\text{core}} \sim 4.3$ °C at D6 versus $\theta_{\text{core}} \sim 1.7$ °C at D4, or $\Delta\theta = 2.6$ °C), their interpretation had to be carefully considered. That is, differences in concentration could simply have reflected the effect of temperature on the solubility of CFC-11 at the time when the WH core had initially been in contact with the atmosphere (e.g. a difference of 2.6 °C causes a concentration difference of 0.9 pmol/kg; Warner and Weiss, 1985). Considering, however, that the WH core for both the WGC and the BC originated in the same region (i.e. the North Atlantic), differences in concentration for these two currents were instead an indication of their different ventilation times. In other words, concentration differences were set by differences in atmospheric concentration at their times of subduction, not differences in temperature. Ages for the WH core of the WGC (Station D5) and the BC (Station D3) were estimated at 10 years and 25 years, respectively, based on CFC-11 concentrations, CFC-11 atmospheric source history (Walker et al., 2000), and an assumption of 85% saturation (Frank et al., 1998). Hence, lower concentrations in the WH core of the BC reflected a long flow path via the Arctic

Ocean, which subducted earlier in the North Atlantic under lower atmospheric concentration than for the WGC. Intrusive features within the WH along Davis Strait (eg. Station D5 at $S = 33.8$) maintain these concentration differences between WGC and BC waters.

Despite similarity in θ - S signature, CFC concentrations indicated differing local processes for the waters of Smith Sound (Station S2) and Jones Sound (J3). CFC-11 concentrations in Smith Sound were highest at the surface and linearly stratified with S to the bottom of the CH ($S \sim 33.5$). In contrast, waters in Jones Sound (J3) exhibited a relative CFC-11 maximum (and associated dissolved oxygen maximum; Fig. 4.20c) immediately above the CH core ($32.6 < S < 32.8$), suggesting the likely occurrence of recent local ventilation. Near-surface nutrient depletion was noted for both Smith Sound and Jones Sound (particularly in the case of Nitrate; Fig. 4.20a). Whether this depletion signified a local (i.e. biological consumption) or advected (i.e. low nutrient Pacific-origin water which had undergone summer modification over the Chukchi Shelf; Fig. 2.3a) signal could not be distinguished. A relative maximum in Silicate and Phosphate concentrations was also noted for $33.0 < S < 33.5$ in Jones Sound, likely corresponding to Pacific-origin winter water from the Chukchi Shelf (Fig. 2.3a). Finally, high nutrient (particularly phosphate and silicate) and corresponding low dissolved oxygen concentrations were observed in Jones Sound at $S > 34.0$, indicating significant nutrient regeneration below 600 m within its deep (700 m) sill-bound waters.

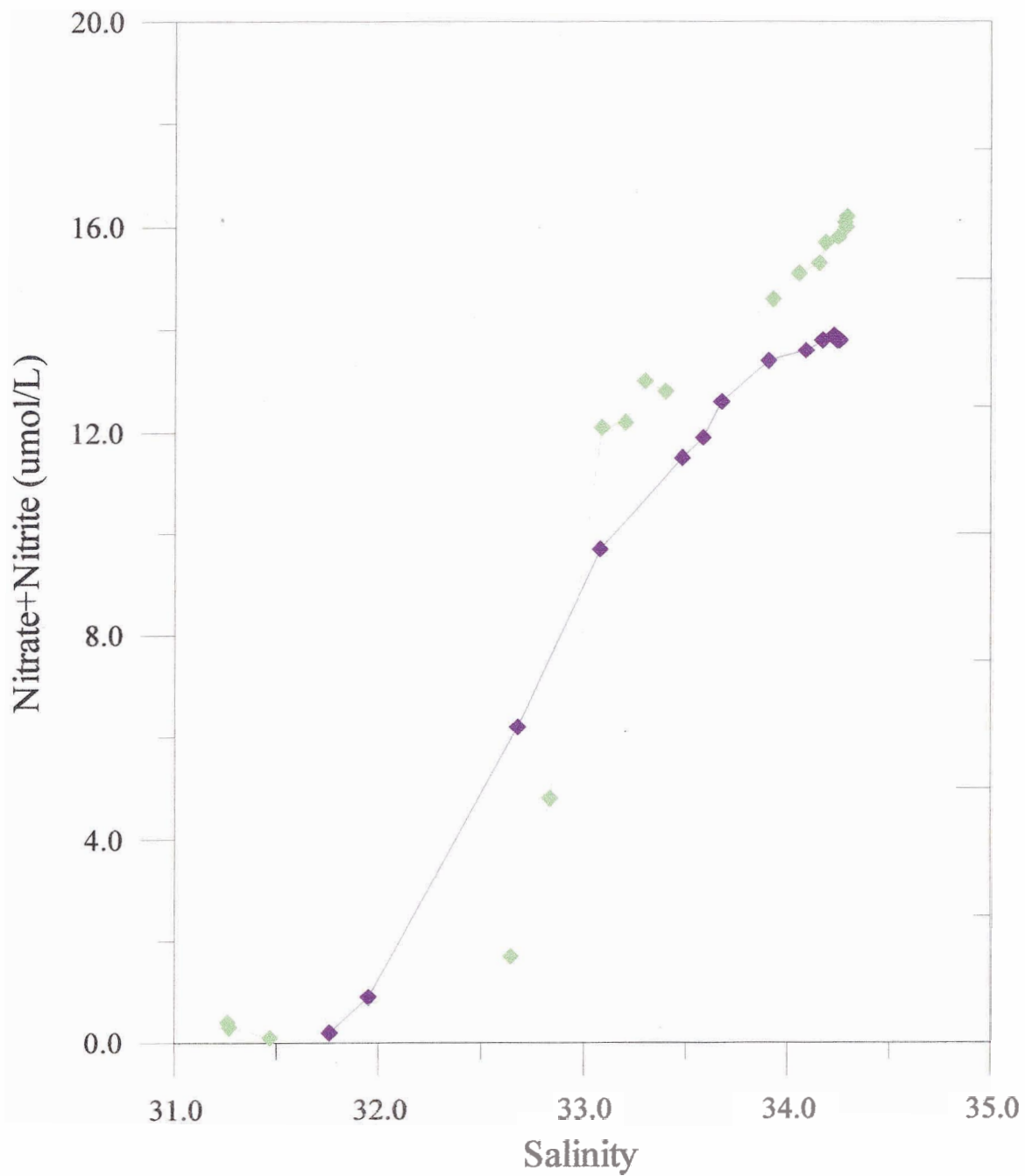


Fig.4.20 a) Nitrate versus S for Jones Sound (J3, green) and Smith Sound (S2, purple) in August 1997.

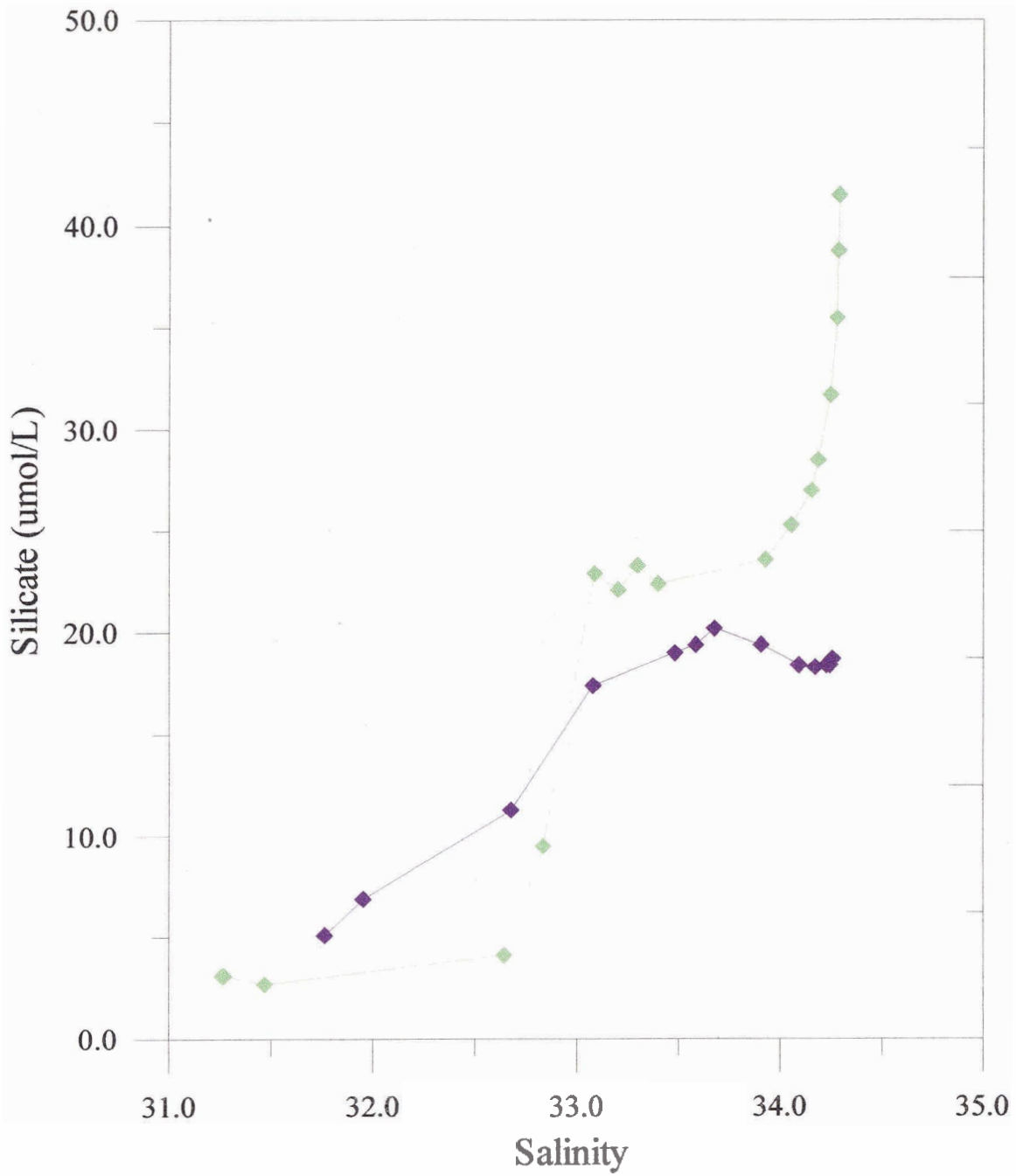


Fig.4.20b) Silicate versus S for Jones Sound (J3, green) and Smith Sound (S2, purple) in August 1997.

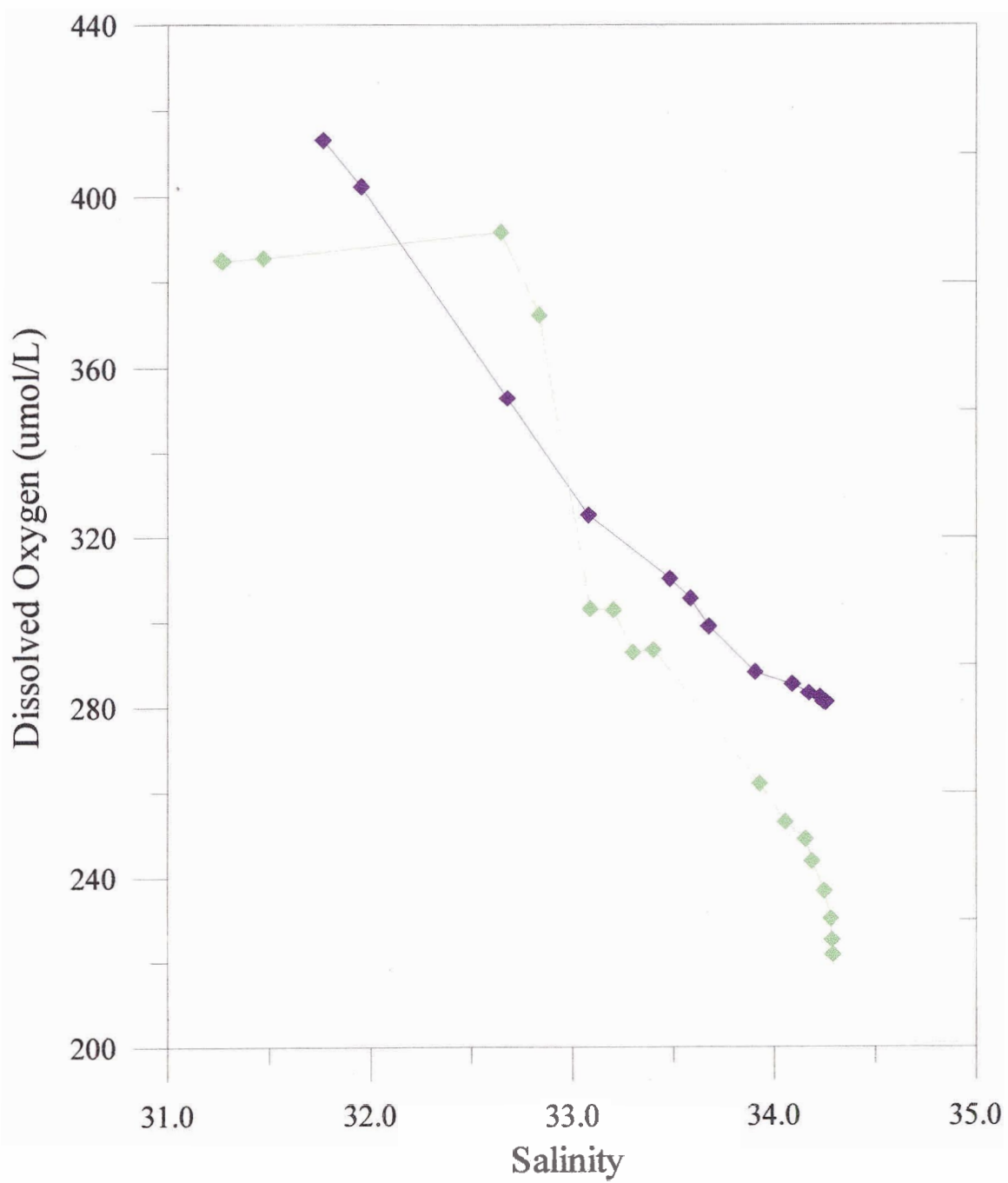


Fig.4.20 c) Dissolved Oxygen versus S for Jones Sound (J3, green) and Smith Sound (S2, purple) in August 1997.

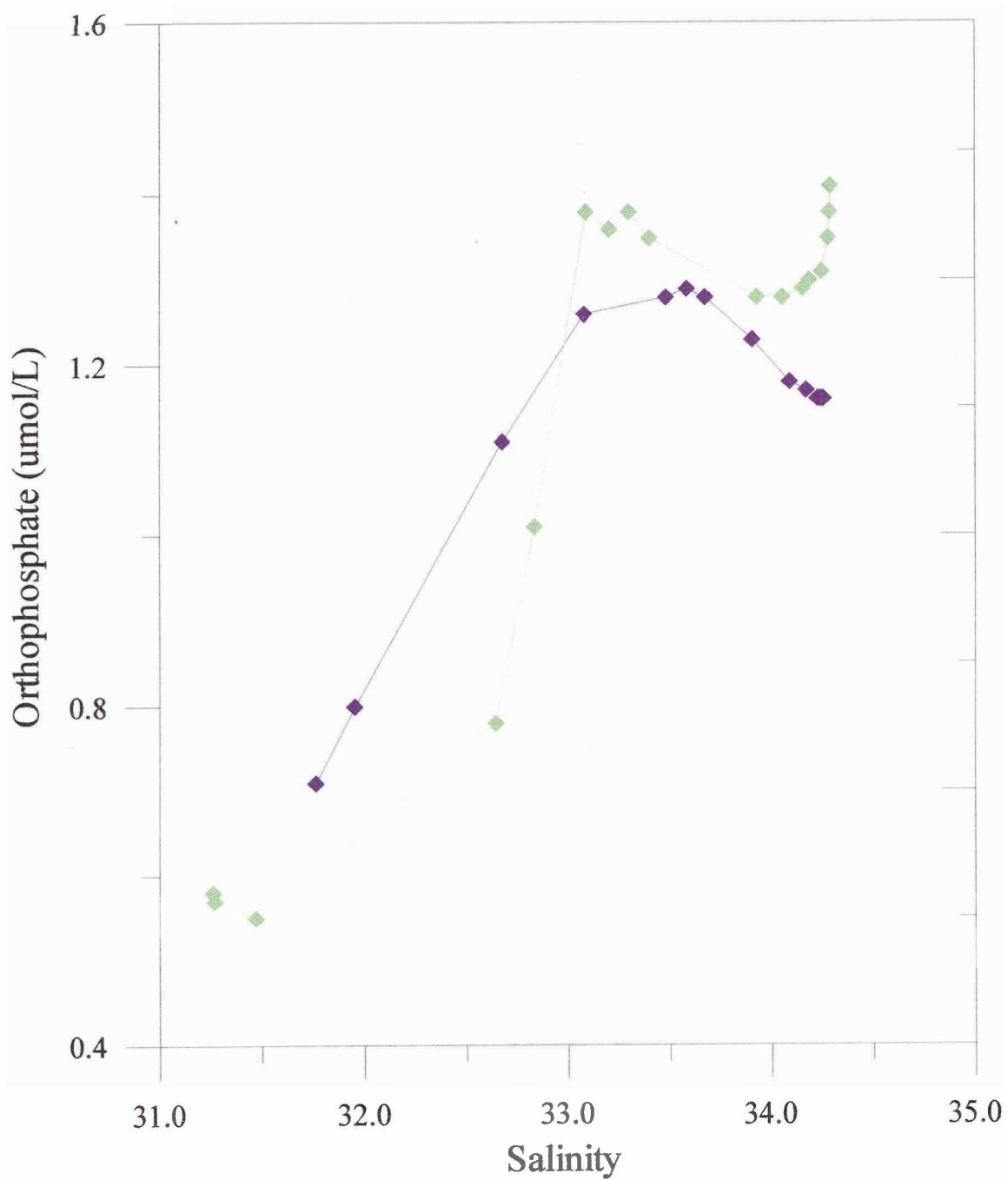


Fig.4.20 d) Phosphate versus S for Jones Sound (J3, green) and Smith Sound (S2, purple) in August 1997.

CFC-11 signatures for the BC (eg. Station D3) and central Baffin Bay (B1) roughly resembled that of Smith Sound (S2). Waters at D3 and B1 however exhibited higher concentrations within the CH core ($33.0 < S < 33.5$), reflecting recent ventilation within the mouth of Lancaster Sound. Concentrations within the WH of D3 and B1 ($33.5 < S < 34.5$) were also slightly higher with S compared to Smith Sound. This was likely a reflection of CFC concentrations from the WGC, which were contributed to the central basin and the BC after travelling cyclonically around Baffin Bay.

Finally, CFC-11, CFC-12, CFC-113 and CCL4 concentrations were examined for waters in central Baffin Bay (Station B1) below the WH core (i.e. > 1000 m)(Fig. 4.21). CFC-113 concentrations for these depths were below detection (~ 0), indicating that the ventilation of the Baffin Bay's deep waters was either intermittent (that is, it hadn't occurred in ~ 35 years, given the time period between the introduction of CFC-113 to the atmosphere and 1997) or continuous but in very low amounts. Increases in CFC-11 and CFC-12 measurements between 1983 (Wallace, 1985) and 1997 at the same location favored the latter preposition (Table 4.4).

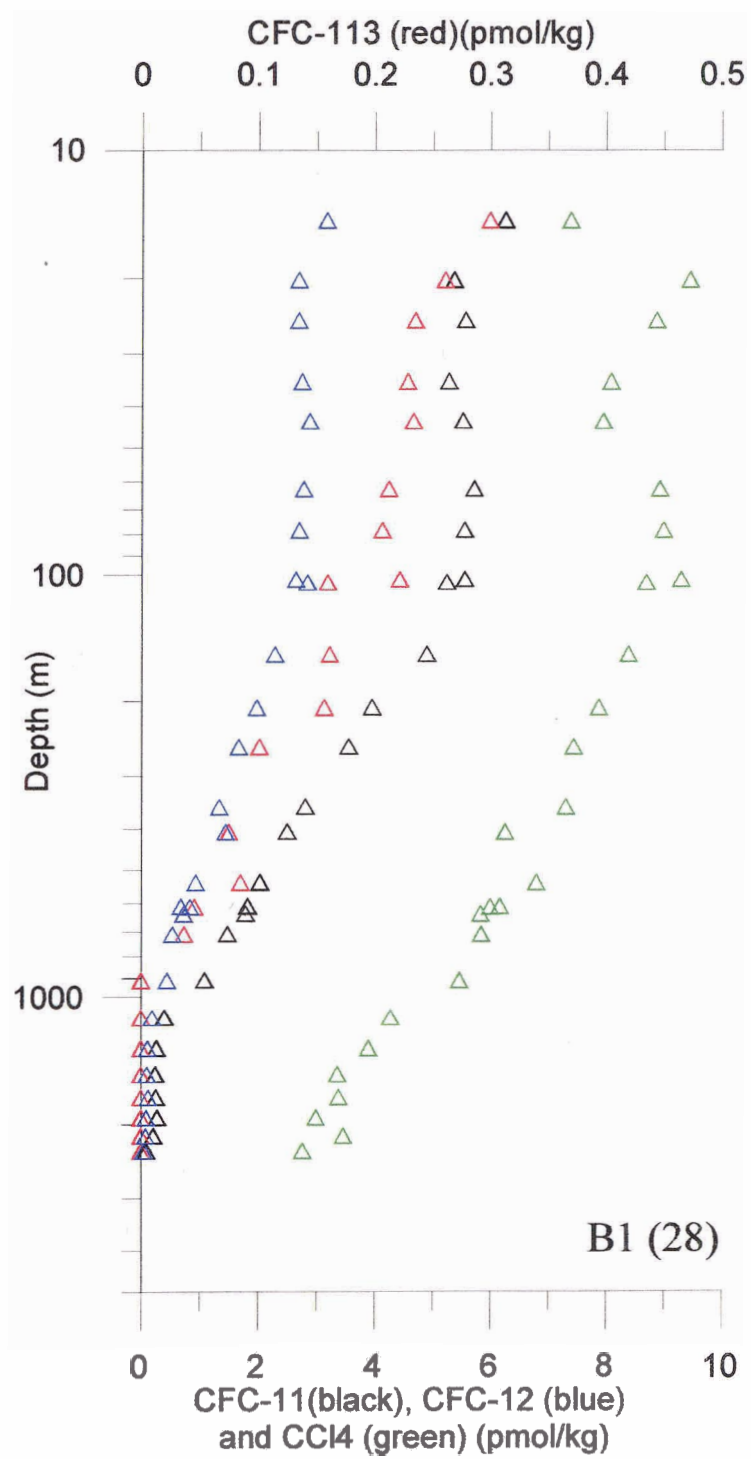


Fig. 4.21: Tracer concentrations at station B1 in central Baffin Bay

Depth (m)	CFC concentration in 1983 pmol/kg	CFC concentration in 1997 pmol/kg
1000	CFC-11: 0.120 CFC-12: 0.085	CFC-11: 0.741 CFC-12: 0.314
1500	CFC-11: 0.060 CFC-12: 0.050	CFC-11: 0.246 CFC-12: 0.097
2000	CFC-11: 0.040 CFC-12: 0.020	CFC-11: 0.250 CFC-12: 0.082
2300	CFC-11: 0.010 CFC-12: not reported	CFC-11: 0.086 CFC-12: 0.036

Table 4.4: Comparison of CFC concentrations between 1983 (Wallace, 1985) and 1997 for Station B1.

4.5 Temporal patterns in halocline structure: Eastern Davis Strait

The spatial/temporal distribution of the data used in this dissertation made it impossible to attempt time series investigations over Baffin Bay as a whole. However, an inter-annual comparison of data was possible for a small area (66.5 - 66.7 ° N and 56 ° W) located approximately over the 500 m isobath in eastern Davis Strait. CTD and bottle data available for this exercise spanned between 1966 and 2000, but no data were available for 1970, 1979 and 1994. Features that emerged from this investigation laid the basis for discussing the impact of advected climatological signals like 'great salinity anomalies' on local Baffin Bay oceanography.

Great Salinity Anomaly (GSA) refers to the decadal scale propagation of an anomaly in S (and to a lesser extent θ and sea ice concentration) around the northern North Atlantic (Dickson et al., 1988). The documentation of three such features in the 1970s, 1980s and 1990s (labelled GSA70s, GSA80s and GSA90s; Dickson et al., 1988; Belkin et al., 1998; Häkkinen, 2002; Belkin, in press) has demonstrated both commonalities and differences in mode of formation and advection path. Commonly, all three events have been associated with extremes in the *North Atlantic Oscillation* (NAO) index (Dickson et al., 2000). The NAO is one of the most prominent patterns of atmospheric variability in the Northern Hemisphere (Hurrell et al., 2003) and consists of a recurring redistribution of atmospheric mass between two nodes: the Arctic and the subtropical Atlantic. As the NAO shifts intensity from one node to the other, large changes in mean wind patterns occur over the Atlantic, creating local and downstream impacts on ocean weather, circulation, hydrography and ecology that are currently the subject of much investigation. GSA70s has been associated with a negative NAO index (Fig 4.22) and appears to have originated via large freshwater/sea-ice export through Fram Strait in the mid-60s. In contrast, GSA80s and GSA90s have been associated shifts toward positive NAO indices and are thought to have originated within Baffin Bay and the Labrador Sea due to harsh winter conditions which led to increased sea ice export to the North Atlantic (Belkin et al., 1998). This 'local' formation (as opposed to 'remote', i.e. via Fram Strait) may have also been facilitated by increased Arctic Ocean freshwater export through the Canadian Archipelago (Belkin et al., 1998; Belkin, in press).

SLP-based Indices (Dec-Mar)

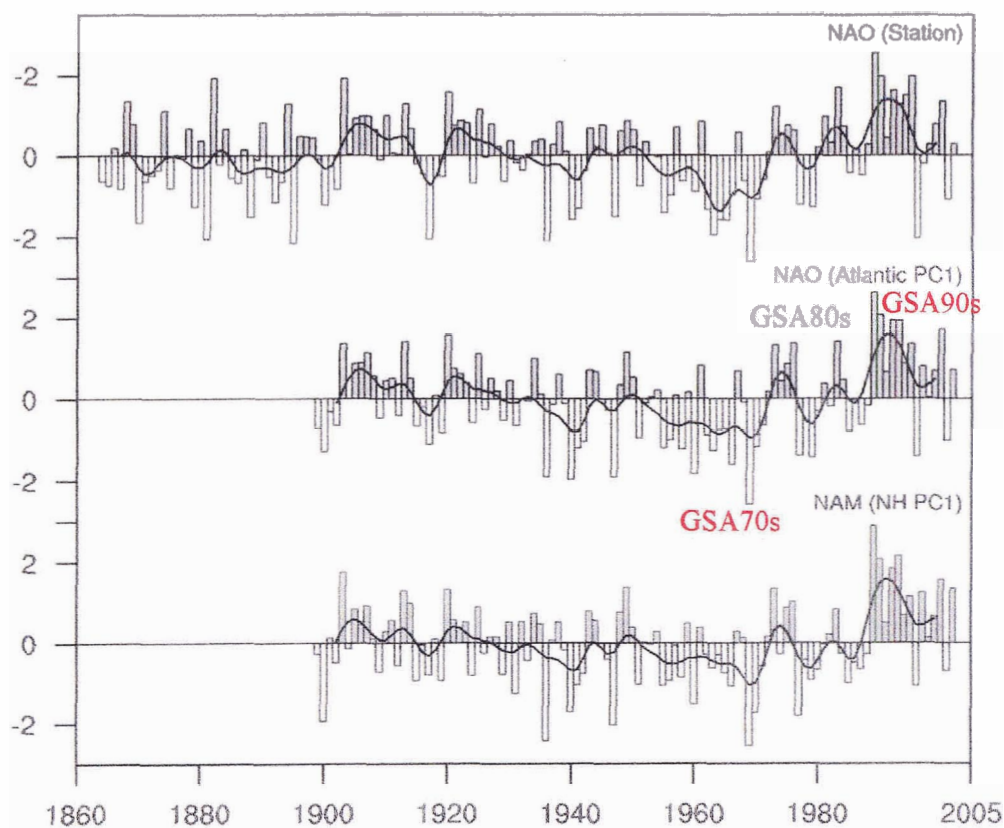


Fig. 4.22: Normalized mean winter NAO indices. The top panel indices are based on the difference in normalized sea level pressure between Lisbon, Portugal and Iceland. Indices in the middle panel derive from the principal component of the leading empirical orthogonal function (EOF) of Atlantic sea-level pressure. Indices in the lower panel derive from the principal component of the leading EOF of Northern Hemisphere sea level pressure. Heavy solid lines represent the indices smoothed to remove fluctuations with periods less than 4 years. Modified from Hurrell et al., 2003.

Although Baffin Bay appears to play a significant role in propagating upstream conditions favourable to the development of GSAs (particularly in the case of GSA80s and GSA90s), how these signals feed back into the region along the WGC is not documented. Previous authors have presented GSA signals along the WGC at Fylla Bank (~64°N; Buch and Stein, 1987; Myers et al., 1989; Myers et al., 1990; Hovgård and Buch, 1990; Drinkwater, 1994; Stein, 1995); a location that is south of the WGC's westward bifurcation toward the Labrador Coast. However, this investigation allowed the examination of GSA propagation within the Baffin Bay region north of Davis Strait.

Several patterns were noted (Fig. 4.23) in the θ and S versus time plots, including recurrent periods of relative minima in surface S (< 50 m), relative minima in subsurface S (> 50m), and relative minima in subsurface θ . In the upper 50 m, periods of relative surface freshness were observed in 1966-1970, 1978-1982, 1990-1992, and 1995-1999. The first three appeared to be correlated with GSA70s, GSA80s and GSA90s, whose peak signals were reported at Fylla Bank in 1969, 1982 and 1989 (cf. Belkin et al., 1998; Deser et al., 2002). The freshness observed the 1966-1970 signal was accompanied by relatively warm near-surface (< 50 m) conditions that were not observed in 1978-1982 or 1990-1992. This could have been due to different formation mechanisms for the three signals. That is, remote initiation (as postulated for GSA70s) would have allowed the 1966-1970 signal to establish a sharp near-surface thermocline along its advection route; whereas near-surface conditions for the 1978-1982 and 1990-1992 signal may have been entirely

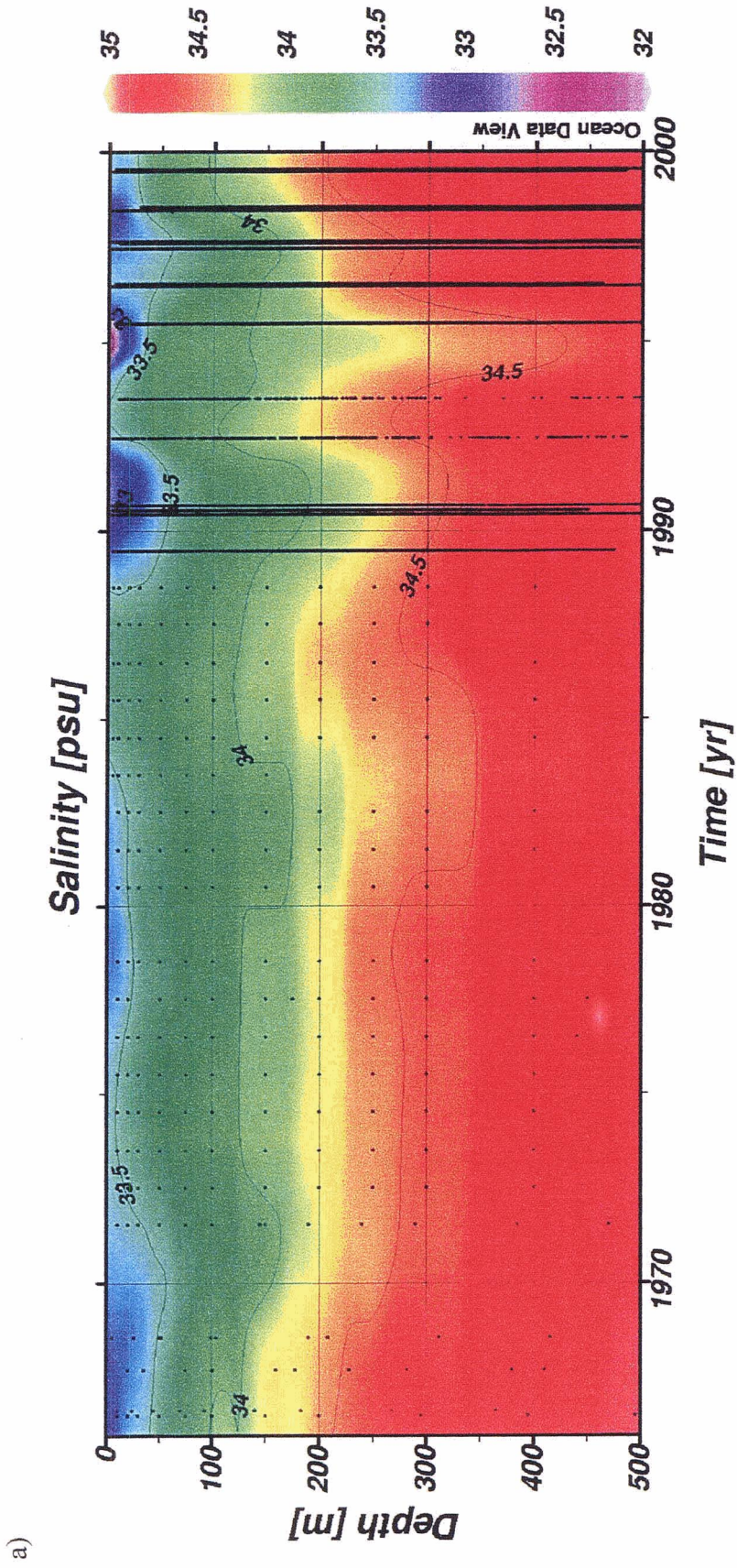
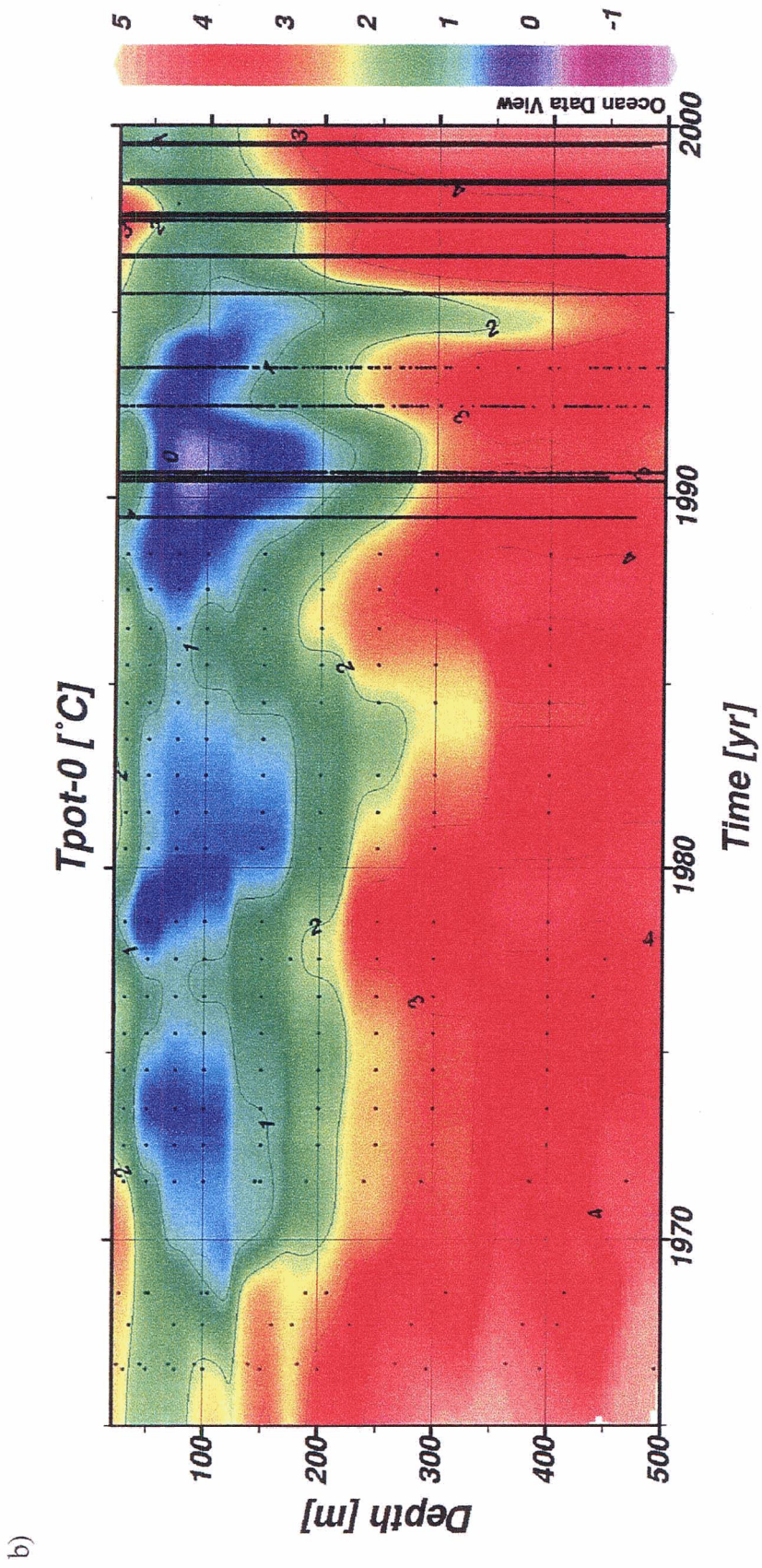


Fig. 4.23: Contoured a) S and b) θ (Tpot-0) time series for Eastern Davis Strait (1966-2000) based on available CTD and bottle data. No data was available for 1970, 1979 and 1994. Data points are indicated with black dots.



driven by severe local winter conditions within the Labrador Sea (as postulated for GSA80s and GSA90s).

Subsurface (> 50 m) cooling and freshening were noted for the periods 1971-1975, 1979-1984 and 1988-1993. The latter two (1979-1984, 1988-1993) were approximately synchronous with the near-surface salinity signals of GSA80s and GSA90s whereas the former (1971-1975) lagged the GSA70s signal. Again, there was consistency with proposed differences in GSA formation: For GSA80s and GSA90s, severe winter conditions in the Labrador Sea led to positive local sea-ice anomalies, evidenced by immediate changes in subsurface characteristics brought on by brine-driven convection (Belkin et al., 1998). In contrast, warm and fresh near-surface conditions associated with the GSA70s signal in 1968-1969 inhibited sea ice formation during these years. The subsurface cooling/freshening signal observed in 1971-1975 may instead have been associated with a large sea ice anomaly reported in the Labrador Sea which was brought on by severe local atmospheric and oceanic conditions (Mysak and Manak, 1989).

Overall, θ -S structure between 1966 and 2000 at 66.5 - 66.7 ° N / 56 ° W followed that outlined in Chapter 4.1 for eastern Davis Strait (CH: $-1.0 < \theta_{\text{core}} < 1.5$ °C; $33.4 < S_{\text{core}} < 33.8$; core thickness: 60-100 m ; core depth: 50-150 m; WH: $3.0 < \theta_{\text{core}} < 4.5$ °C ; $34.5 < S_{\text{core}} < 34.66$; core thickness: ~100 m; core depth: 250-500 m; Fig. 4.1). Data from 1989 and 1990 were anomalous, however, with properties analogous to those advected along the Baffin Island coast with the BC (CH: $-1.65 < \theta_{\text{core}} < -1.55$ °C, $32.5 < S_{\text{core}} < 33.7$, core

thickness: 200-250 m, core depth: 35-300 m; WH: $0.9 < \theta_{\text{core}} < 1.8$ °C, $34.42 < S_{\text{core}} < 34.5$, core thickness: 200-300 m, core depth: 400-900 m; Fig. 4.5). This presence of BC characteristics in eastern Davis Strait is considered below:

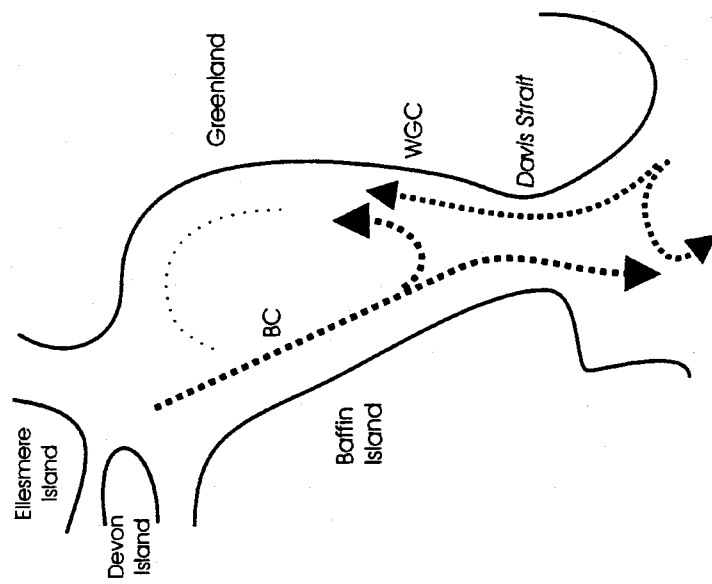
In 1989, the NAO index shifted toward its highest value on record since 1964 (Hurrell et al., 2003). This dramatic change in atmospheric pattern has been associated with several events within the Arctic Ocean. Specifically: 1) an increased northward delivery of Atlantic-origin water through the Barents Sea; 2) an eastward shift in the boundary between Pacific-origin and Atlantic-origin waters within the Arctic Ocean; and 3) a shrinking of the Beaufort Gyre (McLaughlin et al., 1996 & 2002; Morison et al., 1998; Proshutinsky and Johnson, 1997; Steele et al., 2004). The downstream impact of these changes on Arctic export to the North Atlantic has not been documented. However, there is speculation that events in the Arctic Ocean associated with shifts in NAO index may lead to the preferential export of Arctic waters through either Fram Strait or the Canadian Archipelago (McLaughlin et al., 2002; Steele et al., 2004). That is, atmospheric shift toward a weaker NAO index could result in higher Arctic export through Fram Strait, whereas a shift toward a stronger NAO index could result in higher export through the Canadian Archipelago.

Shift toward weaker NAO index

Preferred route for Arctic export: Fram Strait

Impacts:

- 1) Weakens BC flow
- 2) Shifts BC/WGC boundary westward along Davis Strait
- 3) Weakens topographic recirculation of BC waters at Davis Strait



Shift toward stronger NAO index

Preferred route for Arctic export: Canadian Archipelago

Impacts:

- 1) Augments BC flow
- 2) Shifts BC/WGC boundary eastward along Davis Strait
- 3) Augments topographic recirculation of BC waters at Davis Strait

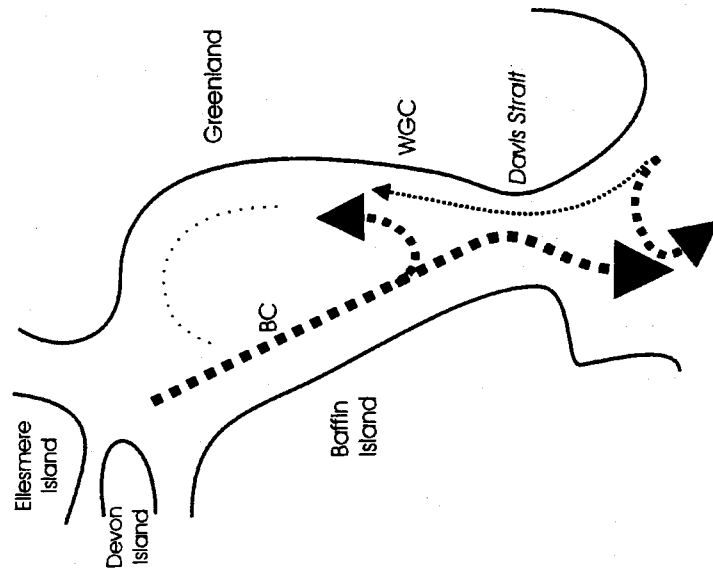


Fig. 4.24: Schematized impacts to Baffin Bay of the preferential export hypothesis for Arctic outflow in response to NAO change.

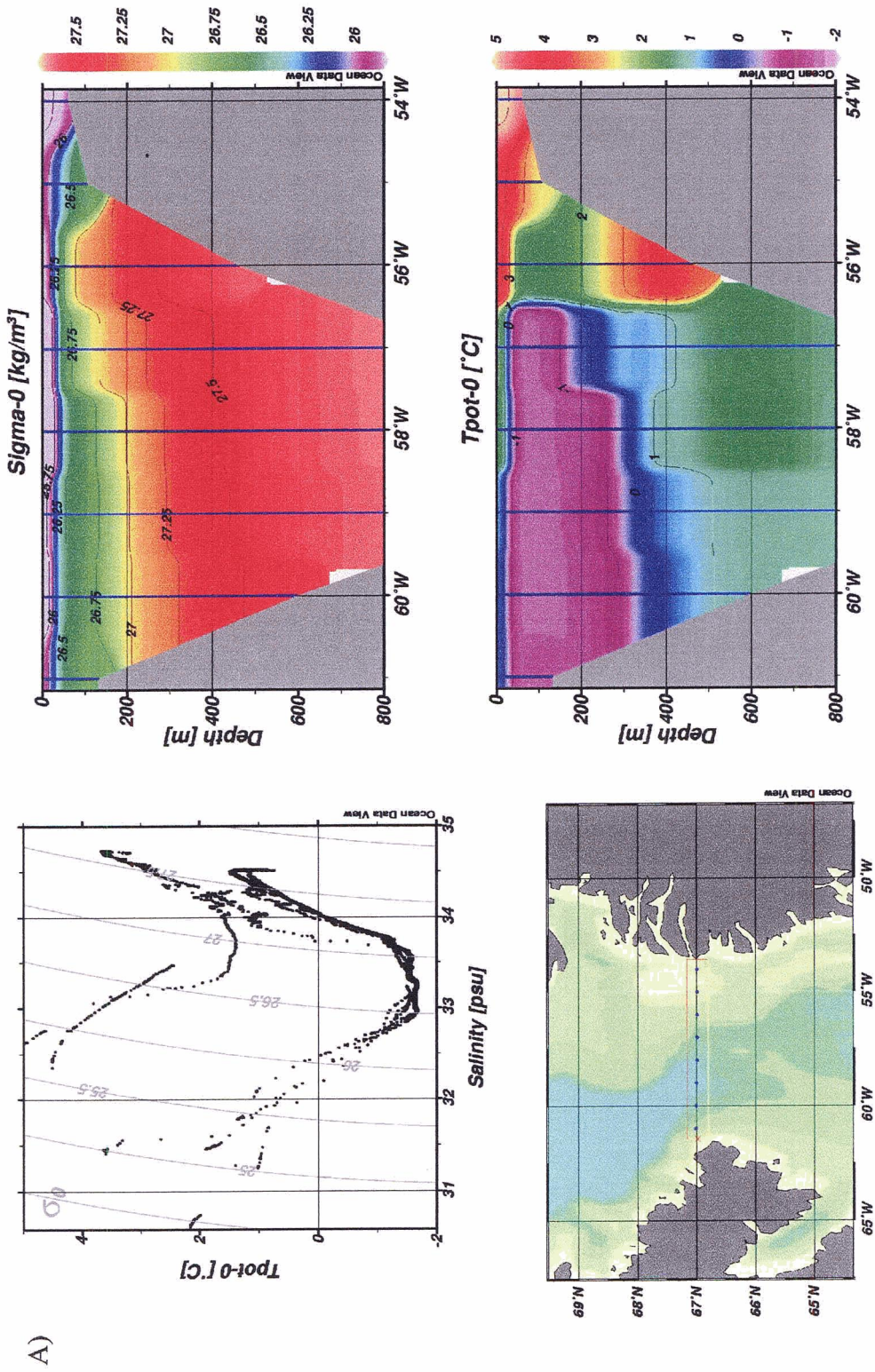
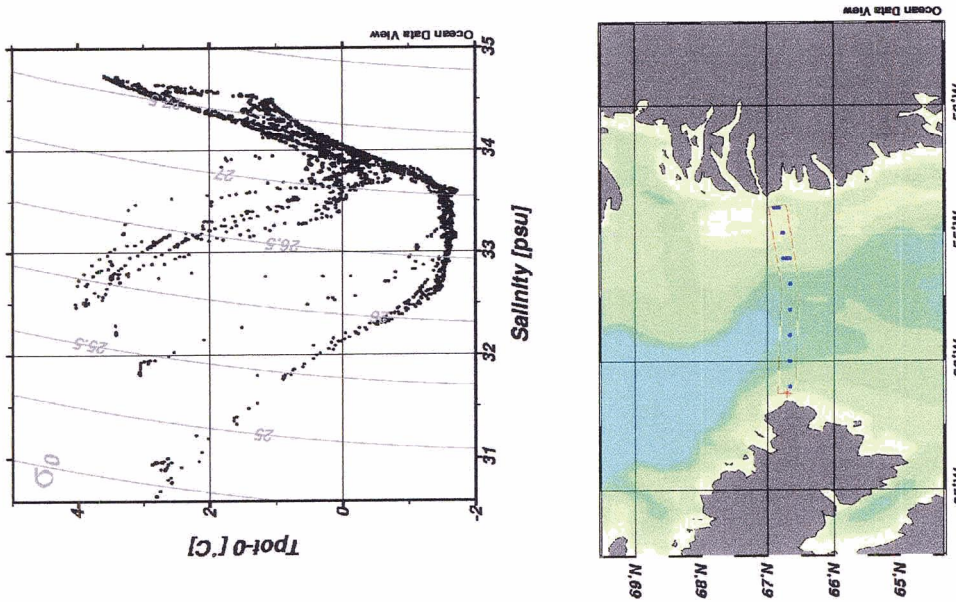
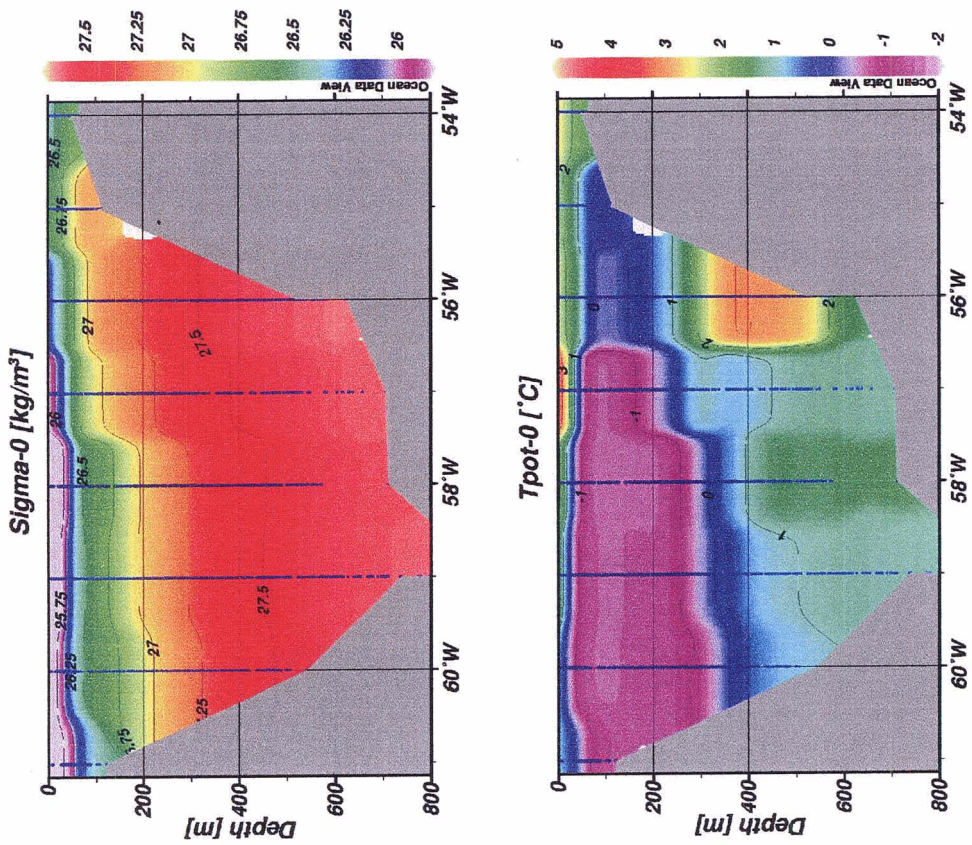
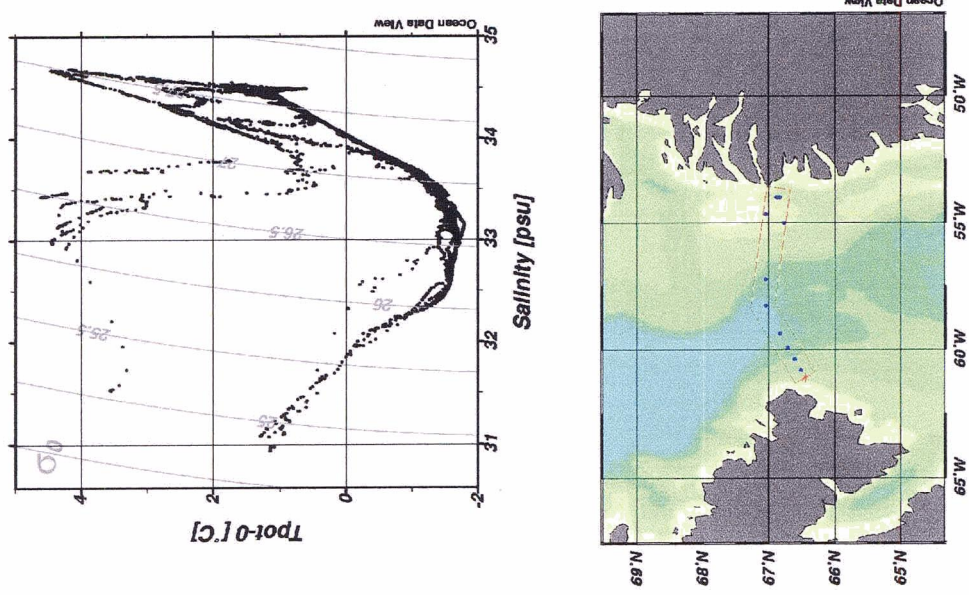
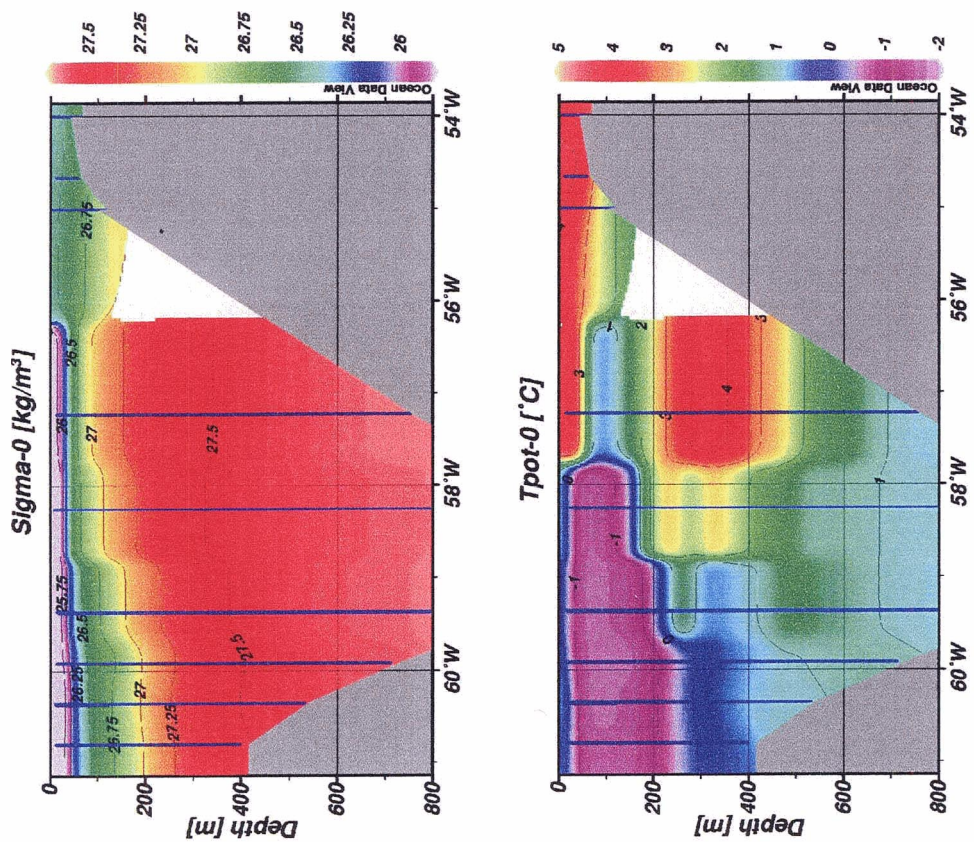


Fig. 4.25: Properties along Davis Strait at ~67°N in a) 1987, b) 1988, c) 1990 and d) 1997.



C)



D)

Following these speculations, in combination with the time-series observations, leads to a hypothesis about the impact of NAO changes on circulation within the Baffin Bay region. This hypothesis is shown in Fig. 4.24. It predicts that for the years associated with a strengthening of the NAO index the following occurs: 1) an augmentation/broadening of the BC; 2) a corresponding eastward shift of the BC/WGC boundary at Davis Strait; and 3) an increase in BC recirculation below the Davis Strait sill depth. To test this hypothesis, available data from four years were examined (corresponding to 1987, 1988, 1990 and 1997, respectively; see Table 4.3). 1987, 1988, and 1990 were years associated with a progressive strengthening of the NAO index and increased export through the Canadian Archipelago. In contrast, 1997 was associated with a weakening of the NAO index and increased export through Fram Strait. Data showed that the boundary between BC properties and WGC properties was located at $\sim 56.5^\circ\text{W}$ in 1987, 1988 and 1990 but at $\sim 58^\circ\text{W}$ in 1997 (Fig. 4.25). In other words, BC properties occupied relatively more of Davis Strait during years of strengthening NAO index, in agreement with the hypothesis stated above.

In addition, an eastward shift of the BC/WGC boundary in years associated with a strengthening of the NAO index would affect the characteristics of inflowing WGC waters, making its WH deeper, cooler and fresher. This would result from 1) the eastward restriction of flow onto shallower topography and 2) enhanced presence of the BC's thick CH ($-1.65 < \theta_{\text{core}} < -1.55^\circ\text{C}$, $32.5 < S_{\text{core}} < 33.7$, core thickness: 200-250 m, core depth:

35-250 m), which would 'push' the WGC's WH deeper into the water column. θ , S and depth data, reported in Table 4.5, shows that the WGC's WH core was found deeper in the water column in 1987, 1988 and 1990 compared to 1997 (an average value of 473 m versus 303 m). Also, the temperature of the WH core (i.e. θ maximum) was cooler in 1987, 1988 and 1990 than in 1997 (an average value of 3.60 °C versus 4.48 °C). Values of S and σ_θ in the WH core were higher, however, in 1987, 1988 and 1990 than in 1997. This could have been due to poor station spacing between 55 and 57 ° W in 1997, which did not allow the proper sampling of the WGC's WH core.

Year	θ_{\max} (° C)	D at θ_{\max} (m)	S at θ_{\max}	σ_θ at θ_{\max}
1987	3.68	425	34.73	27.604
1988	4.11	460	34.77	27.558
1990	3.63	534	34.73	27.613
1997	4.48	303	34.67	27.475

Table 4.5: Comparison of WH properties for WGC waters along Davis Strait in 1987, 1988, 1990 and 1997.

5 Discussion

This chapter discusses how changes in the relative proportion or characteristics of North Atlantic and Canadian Archipelago inputs might regulate water properties in the Baffin Bay region. It begins with a summary of the observed local mechanisms responsible for spreading/mixing water structures within the study region from Chapter 4. It then develops an advective-diffusive model in order to discuss the sensitivity of central Baffin Bay to variations in WGC and Canadian Archipelago input characteristics. Finally, it speculates on the role of recirculation near Davis Strait in maintaining the deep structure of central Baffin Bay.

5.1 Summary of mixing transformations

The data examined thus far have shown significant spatial and temporal variability in the water properties of the Baffin Bay region. Such variability was a function of differing inflows from the Arctic Ocean and the North Atlantic and their subsequent mixing and interaction. A descriptive summary of the origin and structure of Baffin Bay's inflows, via eastern Davis Strait and the Canadian Archipelago, is presented in Table 5.1.

	<i>Davis Strait Inflow (East)</i>	<i>Canadian Archipelago Inflow (Smith, Jones, Lancaster Sounds)</i>	<i>Davis Strait Outflow (West)</i>
<i>Seasonal Halocline</i>	Properties reflect local surface conditions in the Labrador Sea and Davis Strait	Properties reflect local surface conditions in the Canadian Archipelago	Properties reflect local surface conditions in western Baffin Bay
<i>Permanent Halocline</i>	<p>Water origin: Arctic via the EGC/WGC</p> <p>⊕ and S properties reflect wintertime convection events in the Labrador Sea and Davis Strait</p>	<p>Water origin: Arctic (Pacific Ocean) via the Canada and Makarov basins, and the Canadian Archipelago</p> <p>⊕ and S properties reflect wintertime convection events in the Canadian Archipelago</p>	<p>Water origin: Arctic via mixing between Lancaster Sound outflow (<100 m), the CH of Smith Sound and Jones Sound waters, and the CH of the WGC.</p> <p>⊕ and S properties reflect wintertime convection events in western Baffin Bay</p>
	<p>Water origin: North Atlantic via the Irminger Current/WGC</p> <p>⊕ and S properties differ from those further upstream in the Labrador Sea through diffusion and topographic constraints near Davis Strait.</p>	<p>Water origin: North Atlantic via the Arctic Ocean (Fram Strait/Barents Sea)</p> <p>⊕ and S properties result from 1) mixing between inflowing Atlantic-origin and ambient Arctic Ocean waters, and 2) diffusion and turbulent mixing within the Canadian Archipelago.</p>	<p>Water origin: North Atlantic via the WGC and the Canadian Archipelago</p> <p>⊕ and S properties result from intrusive mixing between WGC waters and North Water Outflow, and diffusion</p>

Table 5.1: Summary of the halocline anatomy of Baffin Bay inflows (via eastern Davis Strait, and the Canadian Archipelago) and outflow (via western Davis Strait).

Local mixing/interaction pathways for these inflows, which accounted for the region's structural diversity and the outflowing structure of the BC via western Davis Strait, included:

1. Regional variations in the relative stability of surface layers: This refers to differing depths for wintertime convection as reflected by the structure of the CH. The CH of WGC waters near Davis Strait, for example, was relatively shallow, thin, warm and salty, reflecting temperate upstream conditions. In contrast, the CH of BC waters was relatively thick, highly stratified and close to freezing temperature, reflecting the impact of ice formation near Lancaster Sound and along the Baffin Island coast.
2. The dispersion (horizontal and vertical) of properties along current paths: This was observed, for example, in the WH of WGC waters, which cooled, freshened and thickened as it travelled cyclonically around the region.
3. The convergence of waters leading to changes in halocline depth: This resulted from the east-west convergence of CH waters from the WGC and the BC. Because the CH of the BC was relatively thick and fresh (i.e. less dense) than that of the WGC, it tended to displace WH waters of the WGC deeper into the water column as they flowed around the region toward Lancaster Sound (from 250-500 m in Davis Strait, to 275-650 m in Melville Bay; see Table 4.2).

4. The thickening of CH waters leading to changes in halocline depth: This was seen primarily along the Baffin Island coast. As the CH of the BC thickened between Lancaster Sound and western Davis Strait (from ~150 m to 200-250 m, likely reflecting spatial variation in ice formation between Lancaster Sound and the Baffin Island coast), the WH was displaced slightly deeper into the water column (from 400-800 m in Lancaster Sound to 400-900 m along the Baffin Island coast; Table 4.2).

5. The convergence of waters leading to small-scale halocline transformations. This refers to mixing instabilities in the form of thermohaline intrusions. These were observed particularly in the North Water region, Lancaster Sound, southern Baffin Bay and around the eastern and western sides of the central basin over the 500-1000 m isobaths. Existing data did not allow an estimate of the overall importance of intrusions in the mixing of Baffin Bay waters. However, some speculation was possible: Although intrusions create conditions favourable for double-diffusion fluxes, background turbulence levels, where they were observed, may inhibit this type of mixing (i.e. maintain the intrusions rather than dissipate them). For example, M2 tidal heights in the North Water region, Lancaster Sound and Davis Strait exhibit strong amplitudes of 80 cm, 60 cm and 60 cm, respectively (Godin, 1966). However, density increases due to cabelling (~ 0.01) where intrusions were observed in the North Water region (Chapter 4.3) were found to be roughly an order of magnitude greater than local lateral density gradients. This suggests that cabelling might be the more dominant mechanism for mixing convergent flows within Baffin Bay.

5.2 Advective-diffusive model

In this section, the impact of North Atlantic and Arctic inputs on the structure of central Baffin Bay is examined. Specifically, the question was asked: What is the relative role of WGC and Canadian Archipelago inputs in maintaining θ and S properties in central Baffin Bay within and below the WH core (i.e. the portion of the halocline not directly impacted by winter convection, or > 300 m)? To answer this, an advective-diffusive model was developed, wherein the structure of the deep basin was assumed to result from the mixing of three water types (Fig 5.1). These included:

- 1) WH core properties entering Baffin Bay with the WGC (referred to as AT);
- 2) Relatively cold/fresh WH properties characteristic of outflow from the North Water/Lancaster Sound regions (AR);
- 3) Bottom properties observed in Baffin Bay's central basin (Bottom Water, BW).

The advective-diffusive model consisted of 3-boxes (Fig. 5.2). Properties within the upper box (300-500 m) were governed by the horizontal input and subsequent vertical mixing of AT and AR. Properties within the middle box (500-1000 m) were governed by AR input and vertical mixing. Finally, properties below 1000 m were maintained by vertical mixing alone. The associated equations for the three boxes were as follows:

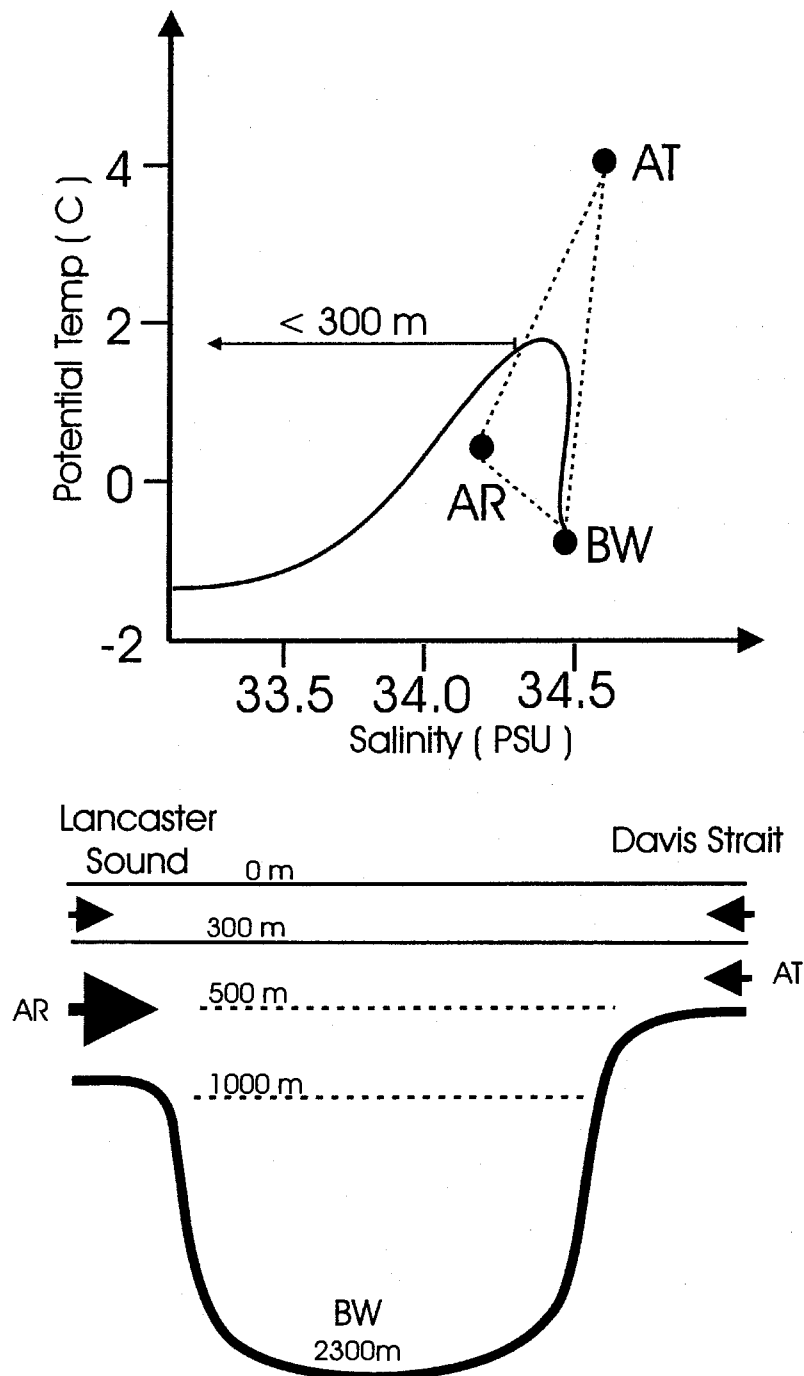


Fig. 5.1: Waters within and below the WH core of central Baffin Bay lie within a mixing triangle between the WH core of WGC waters (AT), WH waters from the North Water/Lancaster Sound region (AR) and pre-existing Bottom Water (BW)

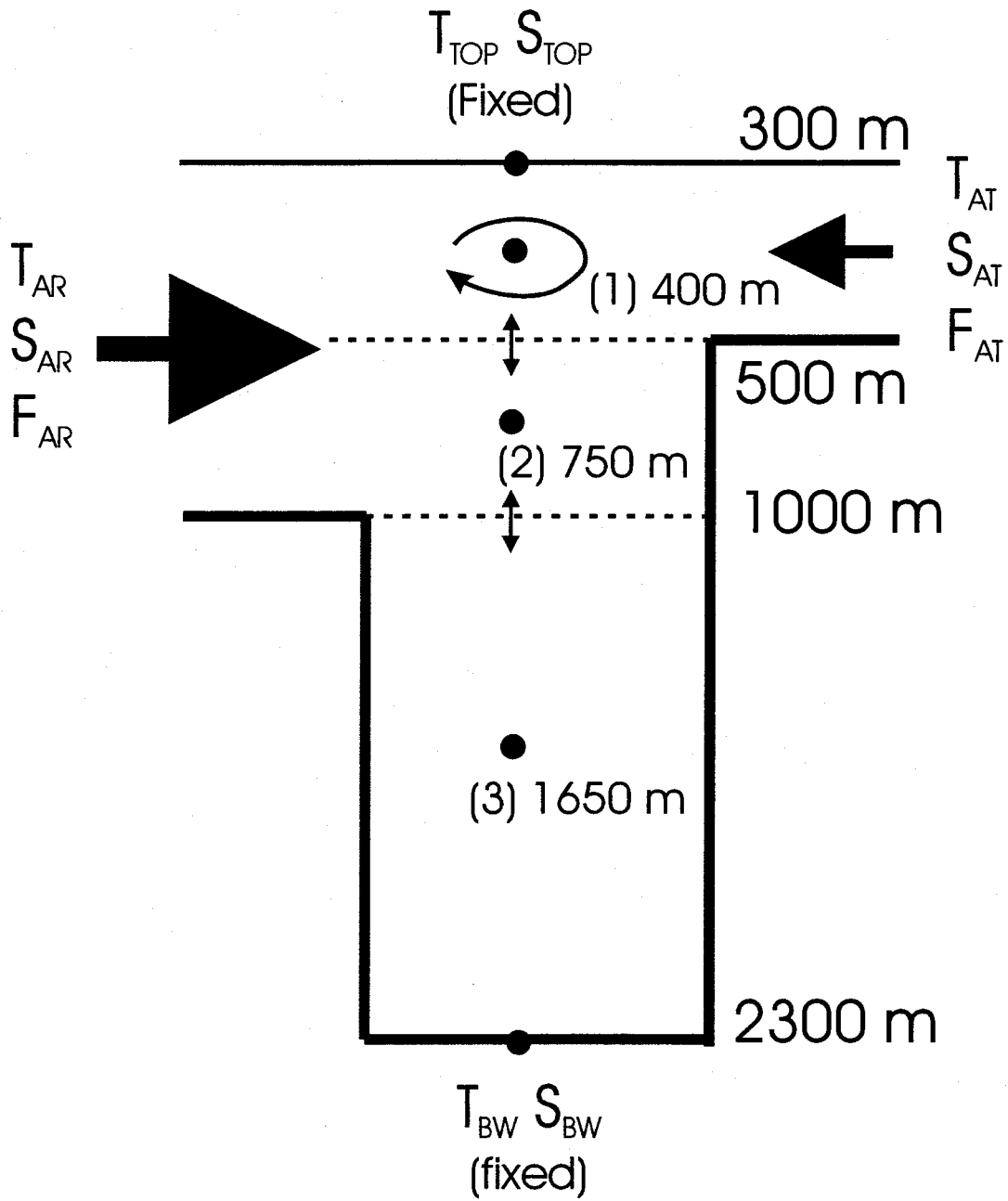


Fig. 5.2: Schematic of 3-box model

Upper Box:	$\partial\theta/\partial t = K\partial^2\theta/\partial z^2 + (M\theta_{AT} + (1-M)\theta_{AR} - \theta)/\tau_1$
	$\partial S/\partial t = K\partial^2 S/\partial z^2 + (MS_{AT} + (1-M)S_{AR} - S)/\tau_1$

Middle Box:	$\partial\theta/\partial t = K\partial^2\theta/\partial z^2 + (\theta_{AR} - \theta)/\tau_2$
	$\partial S/\partial t = K\partial^2 S/\partial z^2 + (S_{AR} - S)/\tau_2$

Lower Box:	$\partial\theta/\partial t = K\partial^2\theta/\partial z^2$
	$\partial S/\partial t = K\partial^2 S/\partial z^2$

Where:

- K ...** Diffusivity coefficient (m^2/s). This term parameterised all vertical transfer via double-diffusion, cabelling, and eddy diffusion.
- θ, S ...** Potential temperature and Salinity of the water column at time (t) and depth (z)
- θ_{AT}, S_{AT} ...** Potential temperature and Salinity of AT
- θ_{AR}, S_{AR} ...** Potential temperature and Salinity of AR
- M ...** Mixing fraction as determined by the relative flow rates of the WGC and Canadian Archipelago waters: $(F_{AT})/(F_{AR} + F_{AT})$
- F_{AT} ...** Volume flow rate of the WGC (m^3/s)
- F_{AR} ...** Volume flow rate of Canadian Archipelago waters (m^3/s)

- τ_1 ... Renewal time of top box (i.e. time it took for complete isopycnal mixing to occur within top box): $(\text{volume top box}) / (F_{AR} + F_{AT})$
- τ_2 ... Renewal time of middle box (i.e. time it took for complete isopycnal mixing to occur within middle box): $(\text{volume middle box}) / (F_{AR})$
- θ_{top}, S_{top} ... Potential temperature and Salinity at the top of the model ($z = 300$ m). These values were assumed constant. This was justified by the strong stratification (i.e. salinity gradient) observed for waters in central Baffin Bay < 300 m which isolated the CH from the WH.
- θ_{BW}, S_{BW} ... Potential temperature and Salinity at the bottom of the model ($z = 2300$ m). These values were assumed constant. This was equivalent to assuming diffusion at 2300 m with an endless reservoir of BW properties.

Parameters	Values
θ_{top}, S_{top}	0.81 °C, 34.226
θ_{BW}, S_{BW}	-0.46 °C, 34.493
θ_{AT}, S_{AT}	4.46 °C, 34.668
θ_{AR}, S_{AR}	0.40 °C, 34.310
F_{AR}, F_{AT}	$2.28 \times 10^6 \text{ m}^3/\text{s}$, $1.13 \times 10^6 \text{ m}^3/\text{s}$ (Muench, 1971; Smith et al., 1937)

Table 5.2: Input parameters used in finite-difference approximation of advective-diffusive model. θ and S values were obtained from August 1997 CTD data.

To solve this system, the properties of the central basin were assumed in steady-state (i.e. non-changing with time, or $\partial\theta/\partial t=0$ and $\partial S/\partial t=0$) and a finite difference approximation⁷ was used. The system was solved for three locations in the water column: 400 m, 750 m and 1650 m (corresponding to the mid-depth of each box). Modelled values for these depths were compared to CTD values observed in the central basin (72 °N, 64.7 °W) in August 1997 (see Table 5.3). A first objective was to find a value for K which would give the overall least combined absolute error for all three nodes (absolute error at each node was defined as |(modelled θ or S value)-(observed θ or S value)|). Next, θ and S values for AT and AR were varied in order to observe the relative sensitivity of the central basin to WGC and Canadian Archipelago input parameters. Finally, τ_1 and τ_2 were varied in order to observe the model's sensitivity to mixing time scale.

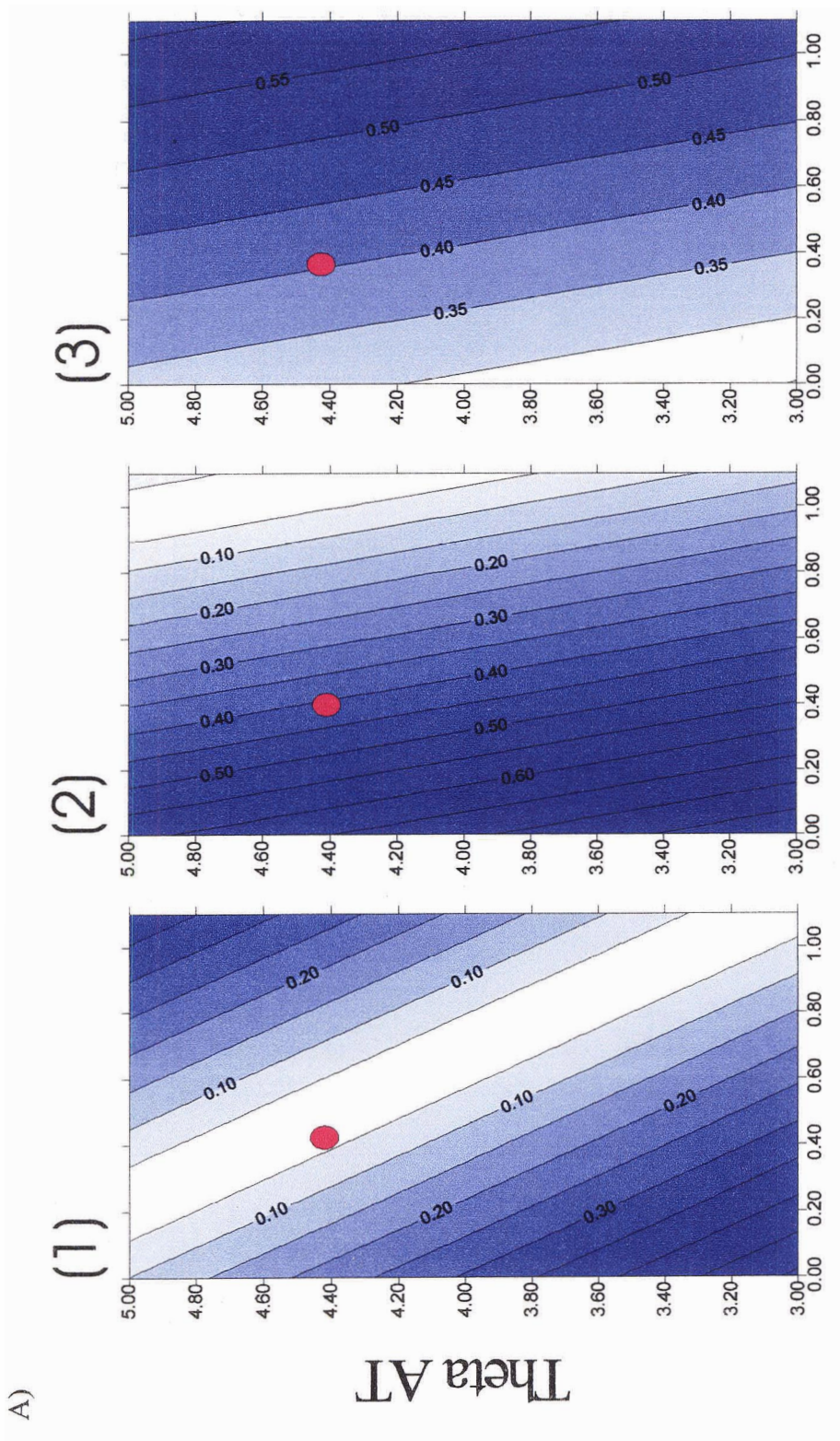
Table 5.3 shows the best-modelled values for θ and S at the three nodes. The corresponding K used to obtain these values was 7.5×10^{-9} m²/s. It should be noted that there were several limits in prescribing a single value of K for the model domain. First, it did not take into account spatial variations in vertical mixing processes (e.g. diffusion, or cabelling) throughout the Baffin Bay region. Second, it assumed that vertical mixing occurred uniformly with depth. In reality, K was likely much larger in the upper two boxes of the model (where horizontal input of AR and AT helped enhance diffusion by maintaining vertical θ and S gradients) than in the lower box.

⁷ Numerical method used to solve a set of differential equations. It involves 1) designating a finite number of points (nodes) over the domain where the approximation of the true solution will be computed, 2) replacing derivatives by discrete difference approximations written in terms of nodal characteristics and boundary conditions, and 3) solving the resulting system of algebraic equations.

Node	Parameter	Depth	Value from observed CTD data (August 1997)	Modelled Value	Absolute error
1	Θ (1)	400	1.39 °C	1.39 °C	0 °C
1	S (1)	400	34.403	34.383	0.02
2	Θ (2)	750	1.19 °C	0.87 °C	0.32 °C
2	S (2)	750	34.512	34.366	0.146
3	Θ (3)	1650	-0.35 °C	0.099 °C	0.449 °C
3	S(3)	1650	34.448	34.440	0.008

Table 5.3: Modelled θ and S values corresponding to the least combined absolute error with respect to observed θ and S values in 1997. The K value used was $7.5 \times 10^{-9} \text{ m}^2/\text{s}$

Fig. 5.3 shows how absolute error at the three nodes varied with changes in θ and S properties for AT and AR. Two things were noted from this figure. First, absolute error was a stronger function of AR (θ_{AR} , S_{AR}) than AT (θ_{AT} , S_{AT}) at all three nodes. This suggested that properties of the central basin were more sensitive to the characteristics of Canadian Archipelago waters than those of the WGC. Second, absolute error tended to vary most strongly at nodes (2) and (3), corresponding to the model's middle and lower boxes. This would further indicate that a more accurate model description for Baffin Bay would consider different K values for the upper, middle and lower boxes.

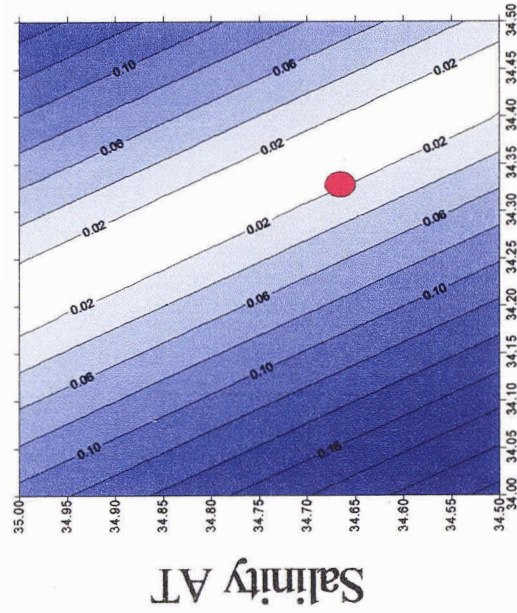


Theta AR

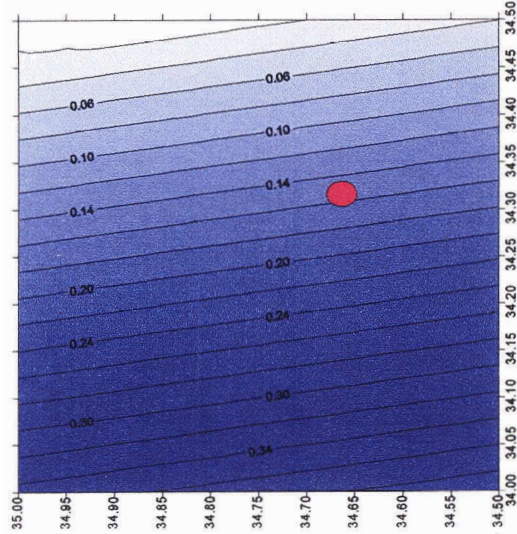
Fig. 5.3: Absolute error at nodes (1), (2), and (3) as a function of a) theta and b) S values for AT and AR. K was kept constant at $7.5 \times 10^{-9} \text{ m}^2/\text{s}$. Red dots indicate the original input values for AT and AR listed in Table 5.2.

B)

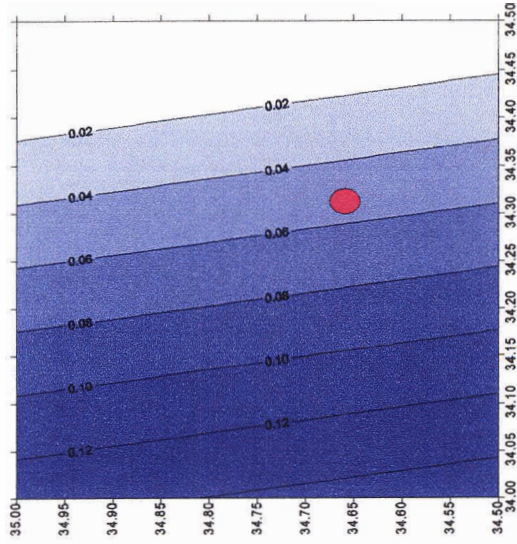
(1)



(2)



(3)



Salinity AR

Salinity AT

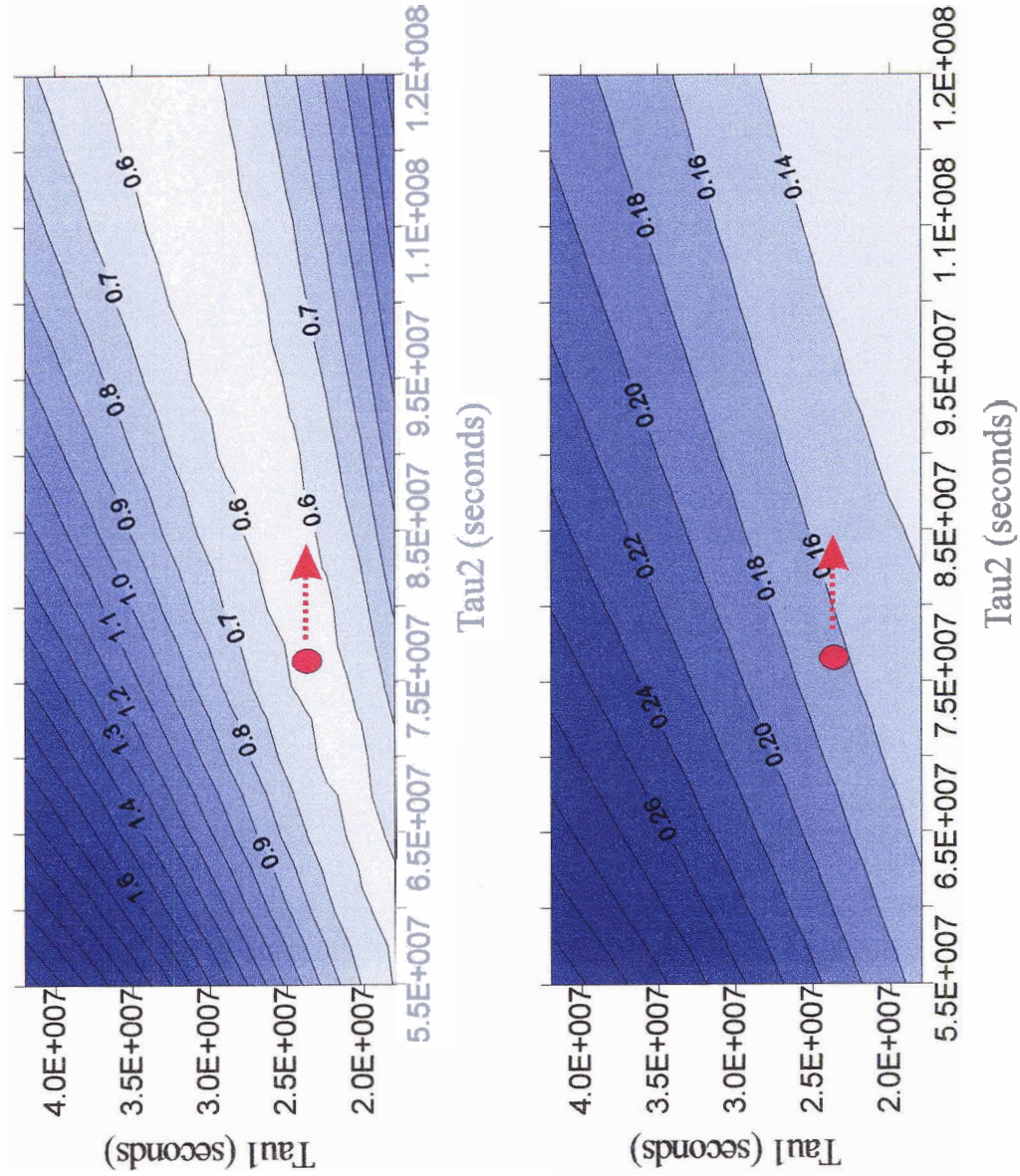


Fig. 5.4: Combined absolute error for nodes (1), (2), and (3) as a function of Tau 1 and Tau2. Above Panel indicates absolute error values for theta, below for S. K was kept constant at $7.5 \times 10^{-9} \text{ m}^2/\text{s}$. Red dots indicate the original input values for Tau1 and Tau2 listed in Table 5.2. Red arrows show how increasing Tau2 (via the recirculation of water in the model's middle box) would reduce absolute error.

Finally, Fig. 5.4 presents combined absolute error for the three nodes as a function of τ_1 (replenishment time of the model's upper box) and τ_2 (replenishment time of the model's middle box). Expectedly, the combined absolute error for the three nodes was more sensitive to τ_1 (which is a function of both the flow rate of WGC input and Canadian Archipelago input) than τ_2 (only a function of Canadian Archipelago input). To understand the implications of this figure, let us consider the example of an increase in Arctic flow (F_{AR}) and an equal decrease in Atlantic flow (F_{AT}) compared to the input values of Table 5.2. Under these conditions, the time scale over which mixing takes place in the upper box (τ_1) would remain the same, but that of the intermediate box (τ_2) would decrease. This would ultimately increase the combined absolute error of the model's output for the three nodes unless a secondary mechanism was in place to increase τ_2 , such as a recirculation of waters within the middle box (i.e. below the Davis Strait sill depth). Such recirculation was referred to in Chapter 4.5 (Fig. 4.23) in response to increased Canadian Archipelago outflow and subsequent augmentation/broadening of the BC near Davis Strait. Further discussion of the potential significance of this recirculation in determining and maintaining the deep properties of central Baffin Bay is presented in the following section.

5.3. Recirculation and the deep halocline of the central basin: A hypothesis

The narrow (300 km) region of Davis Strait regulates exchange between Baffin Bay and the North Atlantic both by constricting flow and prohibiting waters deeper than ~ 640 m

from traversing from one basin to the other. To the south of Davis Strait, this regulation reflects itself in the veering of WGC waters toward the Labrador Current with subsequent impact on the maintenance of the deep Labrador Sea halocline (Lazier, 1973). To the north of Davis Strait, the result is a recirculation of BC waters back into the Baffin Bay region. The extent and local mixing impact of this recirculation is not documented.

This section speculates on the potential role of BC recirculation at Davis Strait in maintaining the deep properties of central Baffin Bay. The discussion is placed in the context of events within the Arctic Ocean associated with large-scale shifts in atmospheric patterns (namely the NAO index) as mentioned in Chapter 4.5 and reported by McLaughlin et al. (1996 & 2002), Morison et al. (1998), Proshutinsky and Johnson (1997), and Steele et al. (2004). That is, changes in: 1) the northward delivery of Atlantic-origin water through the Barents Sea; 2) the position of the Arctic Ocean's Pacific/Atlantic boundary; and 3) the size the Beaufort Gyre. These changes are assumed to have a bimodal effect on Arctic export to the North Atlantic (whereby export occurs primarily via Fram Strait some years and the Canadian Archipelago other years).

Following the assumption of bimodal Arctic export in response to major atmospheric change, circulation within the Baffin Bay region can also be inferred bimodal. In years favouring Canadian Archipelago export, for example, the volume flow of the BC would increase and the boundary between the WGC and BC at Davis Strait would shift eastward. The latter would have two impacts (Fig. 5.5). First, it would promote greater recirculation

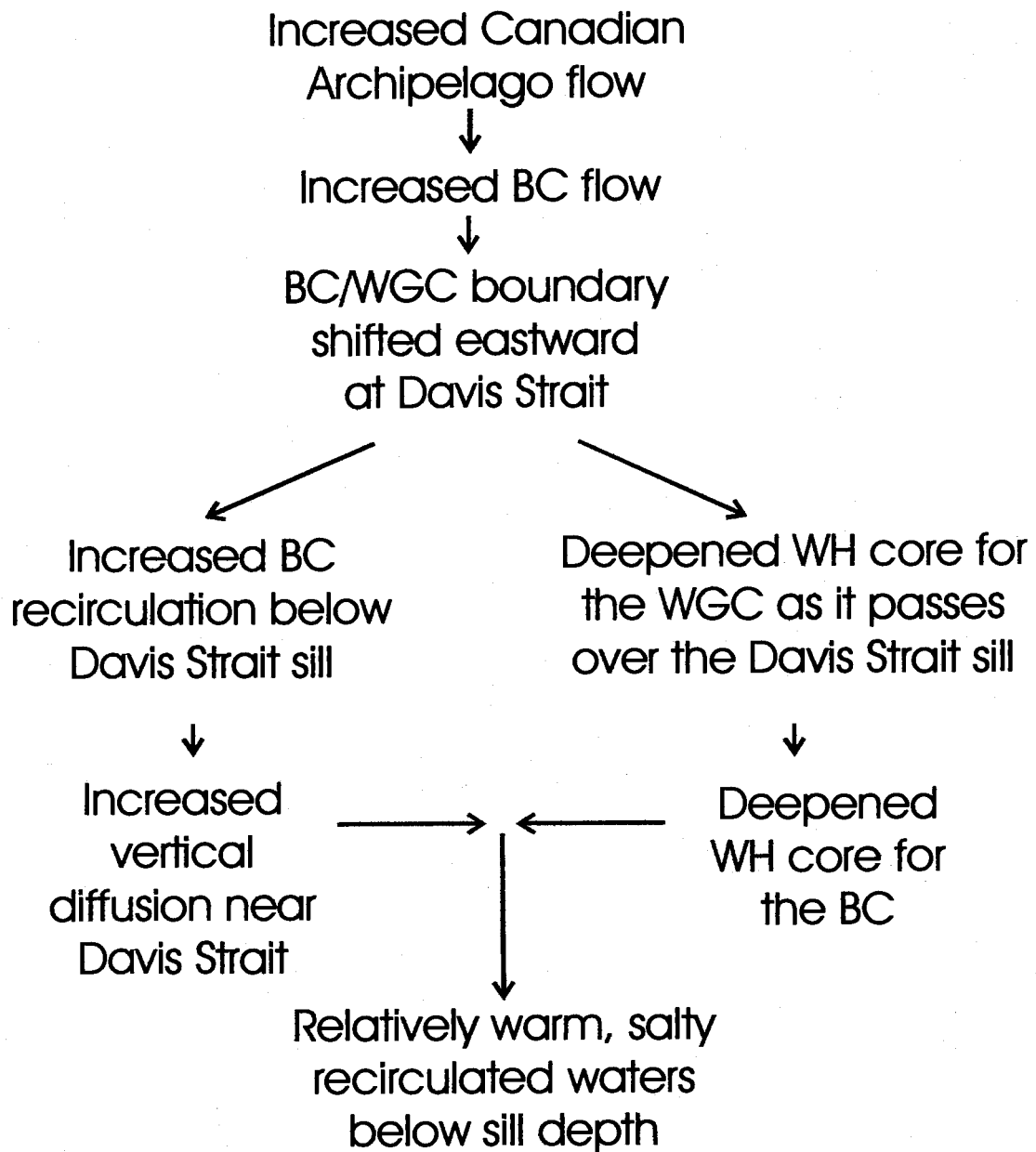


Fig. 5.5: Summary of the impacts of increased Canadian Archipelago outflow on the Baffin Bay region.

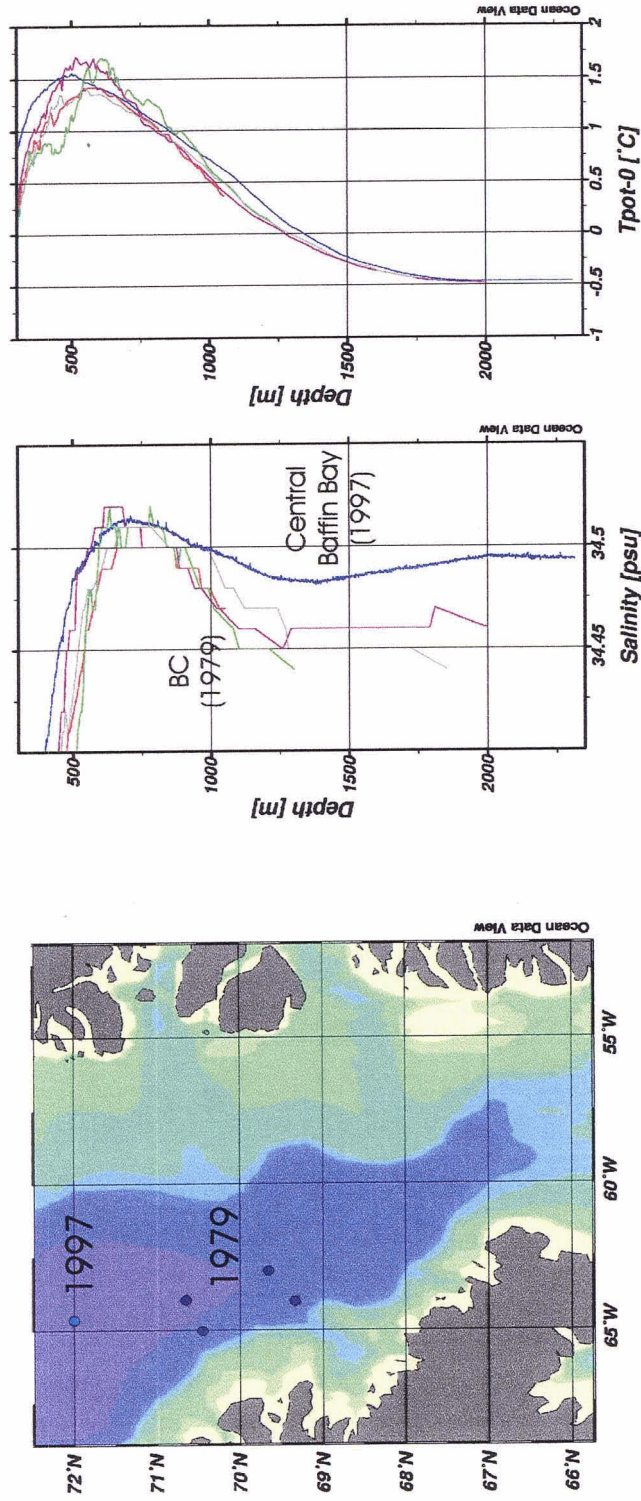


Fig. 5.6: a) Potential Temperature and Salinity profiles for BC waters in 1979 (weakening NAO index/relatively unfavored Canadian Archipelago export). The blue curves correspond to central Baffin Bay (August 1997).

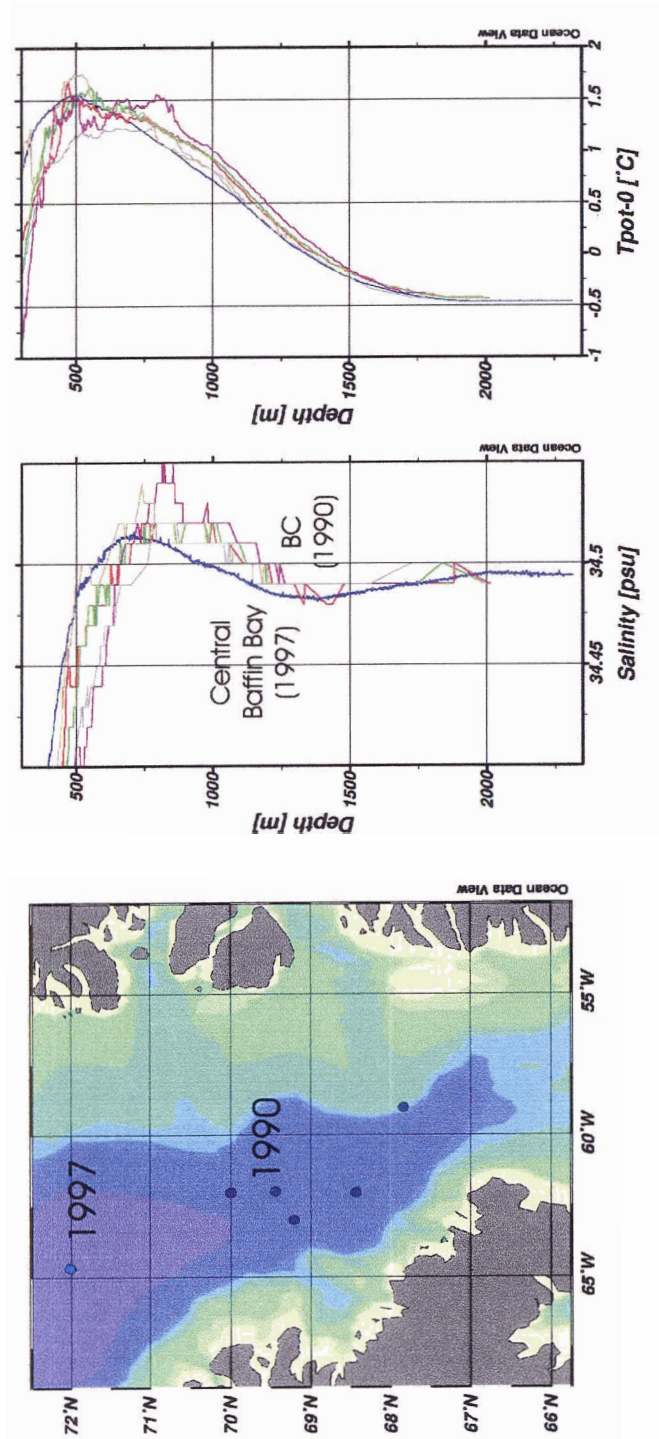


Fig. 5.6: b) Potential Temperature and Salinity profiles for BC waters in 1990 (strengthening NAO index/relatively favored Canadian Archipelago export). The blue curves correspond to central Baffin Bay (August 1997).

of BC waters below the Davis Strait sill depth and increase vertical diffusion to the deep via turbulent mixing. Second, it would modify WGC inflow to the region by deepening its WH. This relatively deep WH for the WGC would eventually contribute to a correspondingly deeper WH signature for the BC (via mixing with Canadian Archipelago outflow in the North Water/ Lancaster Sound regions). The resulting properties of BC waters > 640 m that would be recirculated into Baffin Bay at Davis Strait would then be relatively warm and salty. In contrast, years of relatively lessened Canadian Archipelago outflow would allow the entry of a shallower WH core for the WGC. This would result in a recirculation signature for BC waters > 640 m that was relatively cool and fresh.

To illustrate this hypothesis, BC signatures from 1990 (a year associated with a strengthening NAO index) and 1979 (a year associated with a weakening NAO index) were compared. The bimodal Arctic export theory of McLaughlin et al. (2002) and Steele et al. (2004) would predict export through the Canadian Archipelago to be more strongly favoured in 1990 than 1979. In accordance with this, relatively warm and salty BC conditions were noted below 640 m in 1990 compared to 1979.

How bimodal signatures for BC waters > 640 m recirculated near Davis Strait might impact the deep properties of Baffin Bay is uncertain. However, it is possible that they play a role in maintaining the salinity minimum reported in central Baffin Bay near 1400m (Fig. 4.7; Wallace, 1985). Earlier speculation on the origin of this minimum proposed the addition of a distinct water type through deep convection (e.g. Muench, 1971, suggested

that it was formed by a mixture of Lincoln Sea Water and 'Baffin Bay Intermediate Water'). However, given the low CFC concentrations observed around 1400 m (Fig. 4.21), the convective origin appears less likely than one of diffusion.

6 Conclusions

A historical compilation of hydrographic data from the Baffin Bay region was examined with the objective of synthesising local halocline structures, their primary mixing pathways, and their relationship to upstream Arctic and Atlantic basins. The data indicated that Baffin Bay is a region of significant transformation for Arctic and North Atlantic waters via variations in the relative stability of surface layers, the dispersion of properties along current paths (WGC and BC), and frontal convergence. The Lancaster Sound/North Water region and Davis Strait were found to be particularly significant for water interaction and mixing. The former appeared to play a primary role in establishing the structure of the BC, whereas the latter regulated exchange with the North Atlantic and the recirculation of BC waters back into Baffin Bay.

The relationship between the water structure of central Baffin Bay and the relative proportion/properties of Canadian Archipelago and North Atlantic inputs to the region is largely speculative. However, results from an advective-diffusive model suggest that the properties of the Canadian Archipelago might play a dominant role in maintaining the central basin structure. As a result, the discussion in Chapter 5.3 focused on the possible impacts of variations in Canadian Archipelago outflow on Baffin Bay circulation and mixing.

Over the past three decades, several changes in the circulation and hydrography of the Arctic Ocean have been linked to large-scale shifts in atmospheric (NAO) patterns (see Chapter 4.5). These changes have fostered the idea of corresponding shifts in the export path of Arctic waters to the North Atlantic. That is, in some years they would favour an export path through the Canadian Archipelago (thereby relatively enhancing BC flow), while in other years they would favour export through Fram Strait (thereby relatively diminishing BC flow). If this were the case, downstream variations in the circulation and hydrography of Baffin Bay could resemble the following: In years favouring Canadian Archipelago outflow, increased BC flow at Davis Strait would lead to WGC input with a deeper, cooler and fresher WH core. Recirculation of BC waters below the Davis Strait sill depth would be enhanced, as would vertical diffusion in response to enhanced turbulent mixing. The result would be a relatively warm and salty signature for > 640 m waters recirculated toward the central basin. In contrast, years of relatively diminished Canadian Archipelago outflow would be associated with the entry of WGC waters with a warmer, saltier and shallower WH core, and weaker recirculation/vertical diffusion near Davis Strait. This would result in a recirculation signature for the BC that is relatively cool and fresh below 640 m. Together in alternation, these two signatures might then maintain the current documented structure of the deep central basin.

While variations in Canadian Archipelago outflow build a plausible theory for the observed temporal variations in Baffin Bay's θ and S properties, as well as properties within the deep central basin, such variations also raise important questions. For example: how

would ventilation and sedimentation in the central basin respond to such variations? How would enhanced Canadian Archipelago outflow and subsequent BC recirculation near Davis Strait impact fish populations and species segregation along the Greenland, Baffin and Labrador coasts? Or, with respect to current and impending climate-related changes in Arctic sea-ice cycles and export: Under what variations in Canadian Archipelago outflow would the current structure of Baffin Bay's central basin fail to maintain itself? This, and its downstream impact on North Atlantic mixing transformations, becomes the most interesting question of all.

Bibliography

- Aagaard, K., Swift, J.H., Carmack, E.C., 1985. Thermohaline circulation in the Arctic mediterranean seas. *Journal of Geophysical Research*, 90, 4833-4846.
- Aagaard, K., Coachmen, L.K. Carmack, E.C., 1985. On the halocline of the Arctic Ocean. *Deep-Sea Research*, 28,529-545.
- Addison, V.G. Jr., 1987. The Physical Oceanography of the Northern Baffin Bay-Nares Strait Region. M.Sc. Thesis, Naval Post-Graduate School, Monterey, California, 108pp.
- Bâcle, J, Carmack, E.C, Ingram, R.G., 2002. Water column structure and circulation in the North Water during spring transition: April-July 1998. *Deep-Sea Res. II*, 49 (22-23),4907-4927.
- Bailey, W.B., 1956. On the Origin of Deep Baffin Bay Water, *J. Fish. Res. Bd. Canada* 13 (3), 303-308.
- Barwell-Clarke, J., Whitney, F.,1996. Institute of Ocean Sciences Nutrient Methods and Analysis. *Can. Tech. Rep. Hydrogr. Ocean Sci.* 182: vi +43p.
- Belkin, I.M., in press. Propagation of the "Great Salinity Anomaly" of the 1990s around the North Atlantic. *Geophysical Research Letters*.
- Belkin, I.M., Levitus, S., Anotonov, J., Malmberg, S.-A., 2000. Corrigendum to "Great Salinity Anomalies" in the North Atlantic'. *Progress in Oceanography*, 45, 107-108.
- Belkin, I.M., Levitus, S., Anotonov, J., Malmberg, S.-A., 1998. "Great Salinity Anomalies" in the North Atlantic. *Progress in Oceanography*, 41, 1-68.
- Bourke, R.H. Paquette, R.G., 1991. Formation of Baffin Bay bottom and deep waters. In *Deep Convection and Deep Water Formation in the Oceans*, Chu, P., Gascard, J.G. editors. Elsevier, pp 135-155.
- Bourke, R.H., Addison, V.G., Paquette, R.G., 1989. *Oceanography of Nares*

- Strait and northern Baffin Bay in 1986 with emphasis on deep and bottom water formation. *Journal of Geophysical Research* 94 (C6), 8289-8302.
- Buch, E., 1990. A monograph on the physical environment of Greenland waters. Greenland Fisheries Research Institute Report, 405pp. Re-issued in 2000 as Danish Meteorological Institute Scientific Report 00-12.
- Buch, E., 1993. The North Atlantic watercomponent of the West Greenland Current. ICES, C.M. 1993/C:20.
- Buch, E., Hansen, H.H., 1988. Climate and cod fishery at West Greenland. In: Long-term changes in marine fish polulations, T. Wyatt, Larrañeta, editors. Proc. Vigo Symposium, Nov. 1986, 345-364.
- Buch, E., Horsted, Hovgard, S.A., 1994. Fluctuation in the occurrence of cod in Greenland waters and their possible cuases. ICES Mar. SCI. Symposium, 198, 158-174.
- Buch, E., Stein, M., 1987. Time series of temperature and salinity at the Fylla Bank Section, West Greenland. ICES C.M. 1987/C:4, 22pp.
- Campbell, J.A., Yeats, P.A., 1982. The distribution of manganese, iron, nickel, copper and cadmium in the waters of Baffin Bay and the Canadian Arctic Archipelago. *Oceanol. Acta*, 5 (2), 161-168.
- Carmack, E.C., 2000. The Arctic Ocean's freshwater budget: sources, storage and export. In *The freshwater budget of the Arctic Ocean*, Lewis, E.L., Jones, E.P., Lemke, P., Prowse, T.D., Wadhams, P., editors. Kluwer Academic Publishers, pp 91-126.
- Carmack, E.C., Aagaard, K., Swift, J.H., Perkin, R.G., McLaughlin, F. A., Macdonald, R.W., Jones, E.P., 1998. Thermohaline Transitions. *Physical Processes in Lakes and Oceans, Coastal and Estuarine Studies* 54, 179-186.
- Carpenter, J.H., 1965. The Chesapeake Bay Institute technique for the Winkler dissolved oxygen method. *Limnol. Oceanogr.*, 10, 141-143.
- Clarke, R.A., 1984. Transport through the Cape Farewell-Flemish Cap section. ICES Rapp. Proc.-Verb, 185, 120-130.
- Coachman, L.K., Barnes, C.A., 1961. The contribution of Bering Sea water to the Arctic

- Ocean. Arctic, 14, 146-161.
- Codospoti, L.A., Owens, T.G., 1975. Nutrient transports through Lancaster Sound in relation to the Arctic Ocean's reactive silicate budget and the outflow of Bering Strait waters. *Limnology and Oceanography*, 20, 115-119.
- Collin, A.E., 1965. Oceanographic observations in Nares Strait, northern Baffin Bay, 1963 and 1964. Bedford Institute of Oceanography Report 65 (5), 9pp.
- Coote, A.r., Jones, E.P., 1982. Nutrient distributions and their relationships to water masses in Baffin Bay. *Canadian J. Fish. Aquat. Sci.*, 39, 1210-1214.
- Crawford, R.E., 1992. Life history of the Davis Strait Greenland Halibut, with reference to the Cumberland Sound fishery. *Can. Man. Rep. Fish. Aquat. Sci.* 2130, 19pp.
- Crawford, R.E., 1992. Life history of the Davis Strait Greenland Halibut, with reference to the Cumberland Sound fishery. *Can. Man. Rep. Fish. Aquat. Sci.* 2130, 19pp.
- Deser, C., Holland, M., Reverdin, G., Timlin, M., 2002. Decadal variations in Labrador Sea ice cover and North Atlantic sea surface temperatures. *Journal of Geophysical Research*, 107(C5), 10.1029/2000JC000683.
- Dickson, R.R., Brown, J, 1994. The production of North Atlantic Deep Water: sources, rates and pathways. *J. Geophys. Res.*, 99:,319-12,341, 1994
- Dickson, R.R., Meincke, J., Malmberg, S.-A., Lee, A.J. , 1988. The "Great Salinity Anomaly" in the North Atlantic 1968-1982. *Progress in Oceanography*, 15, 103-151.
- Dickson, R.R., Osborn, T.J., Hurrell, J.W., Meincke, J., Blindheim, J., Adlandsvik, B., Vinje, T., Alekseev, G., Maslowski, W., 2000. The Arctic Ocean Response to the North Atlantic Oscillation.
- Drinkwater, K.F., 1994. Climate and oceanographic variability in the Northwest Atlantic during the 1980s and early 1990s. NAFO SCR Doc. 94/71, 39pp.
- Dunbar, M.J., 1958. Physical oceanographic results of the "Calanus" expeditions in Ungava Bay, Frobisher Bay, Cumberland Sound, Husdon Strait, and Northern Hudson Bay, 1949-1955. *J. Fish. Res. Bd. Canada*, 15(2), 155-201.

- Fedorov, K.N., 1983. The physical nature and structure of oceanic fronts, Lecture Notes on Coastal and Estuarine Studies, 19, New York, Springer-Verlag, 290-295.
- Fissel, D.B., 1982. Tidal currents and inertial oscillations in Northwestern Baffin Bay. *Arctic*, 35(1), 201-210.
- Fissel, D.B., Lemon, D.D., Birch, J.R., 1981. The Physical Oceanography of Western Baffin Bay and Lancaster Sound. Environmental Studies No.25, Northern Affairs Program.
- Fissel, D.B., Lemon, D.D., Birch, J.R., 1982. Major features of the summer near-surface circulation of western Baffin Bay, 1978 and 1979. *Arctic*, 39(1), 180-200.
- Frank, M., Smethie, W.M., Bayer, R., 1998. Investigation of subsurface water flow along the continental margin of the Eurasian Basin using the transient tracers tritium, ^3He and CFCs. *Journal of Geophysical Research*, 103, 30773-30792.
- Fraser, D.B., 1983. Climate of northwestern Baffin Bay and Lancaster Sound. Environmental Study No. 29, Northern Affairs Program.
- Gascard, J.C., Clarke, R.A., 1983. The formation of Labrador Sea Water. Part II: Mesoscale and smaller-scale processes, *Journal of Physical Oceanography*, 13, 1779-1797.
- Godin, G., 1966. The tides in the Labrador Sea, Davis Strait and Baffin Bay. Manuscript Report Series No. 2. Marine Science Directorate, Ottawa.
- Griffies, S.M., Böning, C., Bryan, F.O., Chassignet, E.P., Gerdes, R., Hasumi, H., Hirst, A., Treguier, A.-M., Webb, D., 2000. Developments in ocean climate modelling. *Ocean Modelling*, 2, 123-192.
- Häkkinen, S., 2002. Freshening of the Labrador Sea surface waters in the 1990s: Another great salinity anomaly? *Geophysical Research Letters*, 29(24) 2232-2235.
- Hansen, P.M., 1949. Studies on the biology of cod in Greenland waters, ICES Rapp. Proc.-Verb, 123, 1-77.
- Hansen, H., Buch, E., 1986. Prediction of year-class strength of Atlantic cod (*gadus morhua*) of West Greenland. NAFO Sci. Coun. Studies, 10, 7-11.
- Hansen, H., Hermann, F., 1965. Effect of long-term temperature trends on occurrence of

- cod at West Greenland. ICNAF Environmental Symposium, ICNAF Spec. Publ 6, 817-819.
- Hovgård, H., Buch, E., 1990. Fluctuation in the cod biomass of the West Greenland sea ecosystem in relation to climate. In Sherman, K., Alexander, L.M., Gold, B.D., (Eds.), *Large Marine Ecosystems: Patterns, Processes, and Yields*. AAAS, Washington, D.C., 36-43
- Hurrell, J.W, Kushnir, Y., Ottersen, G., Visbeck, M., 2003. An overview of the North Atlantic Oscillation: Climatic Significance and Environmental Impact. Edited by J.W. Hurrell, Y. Kushnir, G.Ottersen and M. Visbeck, pp1-36, AGU Washington, D.C.
- Ingram, R.G., Bâcle, J, Barber, D.G., Gratton, Y., Melling, H., 2002. An overview of physical processes in the North Water. *Deep-Sea Res.*, 49, 4893-4906.
- Jones, E.P., Anderson, L.G., 1986. On the origin of the chemical properties of the Arctic Ocean halocline, *Journal of Geophysical Research*, 91, 10759-10767.
- Jones, E.P., Coote, A.R., 1980. Nutrient distributions in the Canadian Archipelago: Indicators of summer water mass and flow characteristics. *Can. J. Fish. Aquat. Sci.*, 37, 589-599.
- Jones, E.P., Dryssen, D., Coote, A.R., 1984. Nutrient regeneration in deep Baffin Bay with consequences for measurements of the conservative tracer NO and fossil Fuel CO₂ in the oceans. *Canadian J. Fish. Aquat. Sci.*, 41, 30-35.
- Jones, E.P., Levy, E.M., 1981. Oceanic CO₂ increase in Baffin Bay. *Journal of marine research*, 39 (3), 405-416.
- Killerich, A., 1943. The hydrography of the West Greenland fishing banks. *Mecd. Komm. For Danmarks Fiskeri- og Havundersogelser*, Vol II.
- Lazier, J.R.N., 1973. The renewal of Labrador Sea Water. *Deep-Sea Res.* 20, 341-353.
- Lazier, J.R.N., 1988. Temperature and salinity changes in the deep Labrador Sea, 1962-1986. *Deep-Sea Research*, 35(8), 1247-1253.
- Lazier, J.R.N, Wright, D.G., 1993. Annual velocity variations in the Labrador Current. *J. Physical Oceanography*, 23(4), 1993.

- Lee, A.J., 1968. NORWESTLANT Surveys: Physical Oceanography. ICNAF Special Pub. No. 7, Part I:31-54, Part II:38-159.
- Lemon, D.D., Fissel, D.B., 1982. Seasonal variations in currents and water properties in northwestern Baffin Bay 1978-1979. *Arctic*, 35 (1), 211-218.
- Mamayev, O.I., 1975. Temperature-salinity analysis of World Ocean waters. Elsevier, Amsterdam, 374pp.
- McLaughlin, F.A., Carmack, E., Macdonald, R., Weaver, A.J., Smith, J., 2002. The Canada Basin 1989-1995: Upstream events and far-field effects of the Barents Sea. *Journal of Geophysical Research*, 107 (C7), 10.1029/2001JC000904.
- McLaughlin, F.A., Carmack, E.C., Macdonald, R.W., Bishop, J.K.B., 1996. Physical and geochemical properties across the Atlantic-Pacific water mass front in the southern Canadian Basin. *Journal of Geochemical Research* 101 (C1), 1183-1197.
- Melling, H., 2000. Exchanges of freshwater through the shallow straits of the North American Arctic. In *The freshwater budget of the Arctic Ocean*, Lewis, E.L., Jones, E.P., Lemke, P., Prowse, T.D., Wadhams, P., editors. Kluwer Academic Publishers, pp 479-502.
- Melling, H., 1998. Hydrographic changes in the Canada Basin of the Arctic Ocean, 1979-1996. *Journal of Geophysical Research*, 101, 7637-7645.
- Melling, H., Gratton, Y., Ingram, G., 2001. Oceanic Circulation within the North Water Polynya in Baffin Bay. *Atmosphere-Ocean*, 39(3), 301-325.
- Melling, H., Lake, R.A., Topham, D.R., Fissel, D.B., 1984. Oceanic thermal structures in the western Canadian Arctic. *Continental Shelf Research* 3(3), 233-258.
- Morison, J., Steele, M., Anderson, R., 1998. Hydrography of the upper Arctic Ocean measured from the nuclear submarine USS Pargo. *Deep-Sea Research I*, 45, 15-38.
- Muench, R.D., 1990. Mesoscale phenomena in the polar oceans. In *Polar Oceanography, Part A: Physical Science*, Academic, 223-285.
- Muench, R.D., 1971. *The Physical Oceanography of northern Baffin Bay region.*

- Baffin Bay North Water Project, Arctic Institute of North America 150pp.
- Myers, R.A., Helbig, J.A., Holland, D., 1989. Seasonal and interannual variability of the Labrador Current and West Greenland Current. ICES, C.M. C(16), 10pp.
- Myers, R.A., Mertz, G., Helbig, J.A., 1990. Long period changes in the salinity of Labrador Sea Water. ICES, C.M. C(21), 8pp.
- Mysak, L.A., Manak, D.K., 1989. Arctic sea-ice extent and anomalies, 1953-1984. *Atmosphere-Ocean*, 27(2), 376-405.
- Ostlund, H.G., Hut, G., 1984. Arctic Ocean water mass balance from isotope data. *J. Geophysical Research*, 89(C4), 6373-6381.
- Palfrey, K.M., Day, C.G., 1968. Oceanography of Baffin Bay and Nares Strait in the summer of 1966, and current measurements in Smith Sound, summer 1963. US Coast Guard Oceanographic Report 16, CG-373-16, 204p.
- Proshutinsky, A.Y., Johnson, M.A., 1997. Two circulation regimes of the wind-driven Arctic Ocean. *Journal of Geophysical Research*, 102, 12493-12514.
- Rätz, H.-J., Stein, M., 1999. Variation in growth and recruitment of Atlantic cod (*Gadus morhua*) off Greenland during the second half of the twentieth century. *J. Northw. Atl. Fish. Sci.*, 25, 161-170.
- Redfield, A.C., Friedman, I., 1969. The effect of meteoric water, melt water and brine on the composition of Polar Sea water and on the deep waters of the ocean. *Deep-Sea Research*, 16 (supplement), 197-214.
- Rudels, B., 1986. The outflow of polar water through the Arctic Archipelago and the oceanographic conditions in Baffin Bay. *Polar Research*, 4, 161-180.
- Rudels, B., Fahrbach, E., Meincke, J., Budéus, G., Eriksson, P., 2002. The East Greenland Current and its contribution to the Denmark Strait overflow. *ICES Journal of Marine Science*, 59, 1133-1154.
- Ruddick, B., 1983. A practical indicator of the stability of the water column to double diffusive activity. *Deep-Sea Research*, 30, 1105-1107.
- Sadler, H.E., 1976. Water, heat and salt transports through Nares Strait, Ellesmere Island. *Journal of the Fisheries Research Board of Canada*, 33: 2286-2295. Dalhousie University, Halifax.

- Sadler, H.E., 1975. The flow of water and heat through Nares Strait. PhD thesis, Dalhousie University, Halifax.
- Schmitt, R.W., 1994. Double diffusion in oceanography. *Annual Review of Fluid Mechanics*, 26, 255-285.
- Smith, E. H., Soule, F.M., Mosby, O., 1937. The MARION expedition to Davis Strait and Baffin Bay: Part II, Physical Oceanography. United States Coast Guard Bulletin 19.
- Steele, M., Morison, J., Ermold, W., Ignatius, R., Ortmeier, M., Shimada, K., 2004. The circulation of Summer Pacific Halocline Water in the Arctic Ocean., *Journal of Geophysical Research*, 109(C02027), 10.1029/2003JC002009.
- Stein, M., 1995. Climatic conditions around Greenland—1992. *NAFO Scientific Council Studies*, 22, 33-41.
- Stein, M., Buch, E., 1986. 1983: An unusual year off West Greenland? *Arch. FischWiss.* 36(1/2):81-95.
- Sverdrup, H.U., Johnson, M.W., Fleming, R.H., 1942. *The Oceans: Their Physics, chemistry and general biology*. Prentic-Hall, Inc.
- Talley, L.D., McCartney, M.S., 1982. Distribution and Circulation of Labrador Sea Water. *Journal of Physical Oceanography* 12(11), 1189-1205.
- Talley, L.D., Yun, J.-Y., 2001. The role of cabelling and double diffusion in setting the density of the North Pacific Intermediate Water salinity minimum. *Journal of Physical Oceanography*, 31, 1538-1549.
- Tan, F.C, Strain, P.M., 1980. The distribution of sea-ice meltwater in the Eastern Canadian Arctic. *Journal of Geophysical Research*, 85 (C4), 1925-1032.
- Tomczak, M., Godfrey, J.S., 1994. *Regional Oceanography: An Introduction*. Elsevier Science Inc.
- Top, Z., Clarke, W.B., Eismont, W.C., Jones, E.P., 1980. Radiogenic helium in Baffin Bay bottom water, *J. Mar. Res.* 38 (3), 435-452.
- Walker, S.J., Weiss, R.F., Salameh, P.K., 2000. Reconstructed histories of the annual

mean atmospheric mole fractions for the halocarbons CFC-11, CFC-12, CFC-113 and carbon tetrachloride. *Journal of Geophysical Research*, 105(C6), 14285-14296.

- Wallace, W.D., 1985. A study of the ventilation of Arctic Waters using ChloroFluoroMethanes as tracers, PhD thesis, Dalhousie University, Halifax.
- Wang, J., Mysak, L.A., Ingram, R.G., 1994. Interannual variability of sea-ice cover in Hudson Bay, Baffin Bay and the Labrador Sea. *Atmosphere-Ocean*, 32(2), 421-447.
- Warner, M.J., Weiss, R.F., 1985. Solubilities of chlorofluorocarbons 11 and 12 in water and seawater. *Deep-Sea Research*, 32(12), 1485-1497.
- Wüst, G., 1936. Schichtung und Zirkulation des Atlantischen Ozeans. *Die Stratosphäre*. *Wiss Erg. D. Atl. Exp. Meteor*, 6: 1 with Atlas, Berlin.
- UNESCO, 1983. Algorithms for computation of fundamental properties of seawater. *UNESCO Technical Paper in Marine Science*, 44, 53pp.

Appendix

Hydrographic Data obtained from the Canadian Marine Environmental Data Service (MEDS)

Key:

BIO...	Bedford Institute of Oceanography
IOS...	Institute of Ocean Sciences
FRB...	Fisheries Research Board
AINA...	Arctic Institute of North America
NAFC...	North Atlantic Fisheries College
ICES...	International Council for the Exploration of the Sea
BSH...	Bundesamt für Seeschifffahrt und Hydrographie (Federal Maritime and Hydrographic Agency)

CD... Conductivity-Temperature-Depth profiling system

BO... Bottle

BT... Bathythermograph

year	Cruise ID	cruise dates (Date span from cruise catalogue)	Collection agency/country	type of instruments used for T&S	SHIP NAME
1928	3101250	1928/07/19 1928/09/11	USA	BO	MARION
	26GO28001	1928/06/11 1928/10/05	DENMARK	BO	GODTHAAB
1948	26RG48002	1948/06/26 1948/07/14	DENMARK	BO	RESEARCH VESSELS IN GREENLAND
	26RG48003	1948/08/30 1948/09/14	DENMARK	BO	RESEARCH VESSELS IN GREENLAND
	26RG48007	1948/07/24 1948/07/29	DENMARK	BO	RESEARCH VESSELS IN GREENLAND
	26RG48008	1948/07/15 1948/07/15	DENMARK	BO	RESEARCH VESSELS IN GREENLAND
	310048001	1948/07/18 1948/07/31	USA	BO	UNKNOWN
	319948001	1948/06/27 1948/06/27	USA	BO	UNKNOWN
1949	180049031	1949/06/27 1949/11/02	UNKNOWN	BT	UNKNOWN
	26RG49001	1949/07/12 1949/07/13	DENMARK	BO	RESEARCH VESSELS IN GREENLAND
	26RG49002	1949/08/26 1949/08/27	DENMARK	BO	RESEARCH VESSELS IN GREENLAND

1950	26 05350	1950/05/17 1950/09/01	DENMARK	BO	UNKNOWN
	31ED03750	1950/07/20 1950/08/25	USA	BO	EDISTO
1951	31ED51001	1951/06/08 1951/08/31	USA	BO	EDISTO
1952	26RG52001	1952/07/06 1952/08/07	DENMARK	BO	RESEARCH VESSELS IN GREENLAND
	31ED52001	1952/07/05 1952/08/29	USA	BO	EDISTO
1953	26RG53001	1953/07/03 1953/08/05	DENMARK	BO	RESEARCH VESSELS IN GREENLAND
	31AK03800	1953/01/15 1953/03/14	USA	BO	ATKA
	31PU04270	1953/08/01 1953/09/10	USA	BO	PURSUIT
1954	180354189	1954/07/28 1954/10/25	BIO, CANADA	BO	LABRADOR
	26DA08240	1954/07/05 1954/08/23	DENMARK	BO	DANA
	26RG54001	1954/07/03 1954/07/31	DENMARK	BO	RESEARCH VESSELS IN GREENLAND
1955	180355203	1955/06/03 1955/11/14	BIO, CANADA	BO	LABRADOR
	180455452	1955/07/18 1955/12/22	BIO, CANADA	BO	CALANUS
	26 08460	1955/03/31 1955/08/14	DENMARK	BO	UNKNOWN
1956	180356219	1956/07/11 1956/10/07	BIO, CANADA	BO	LABRADOR
	180456453	1956/01/09 1956/09/13	BIO, CANADA	BO	CALANIS
	26DA09990	1956/07/07 1956/08/02	DENMARK	BO	DANA
1957	180357244	1857/07/01 1957/10/01	BIO, CANADA	BO	LABRADOR
	180457237	1957/05/31 1957/09/06	BIO, CANADA	BO	CALANUS
1958	26DA09090	1958/07/09 1958/08/17	DENMARK	BO	DANA
	26RG58001	1958/07/01 1958/08/15	DENMARK	BO	RESEARCH VESSELS IN GREENLAND
1959	06GA00720	1959/08/03 1959/08/17	GERMANY	BO	GAUSS
	180359294	1959/01/15 1959/11/30	BIO, CANADA	BO	A.T.CAMERON
1960	180760329	1960/08/22 1960/09/24	BIO, CANADA	BO	THETA
	181060340	1960/08/29 1960/09/25	BIO, CANADA	BO	LABRADOR
1961	180461354	1961/07/22	FRB, CANADA	BO	CALANUS

		1961/09/10			
	182361473	1961/11/13 1961/12/24	AINA, CANADA	BO	LAND BASED PARTY
1962	181062362	1962/09/26 1962/10/20	BIO, CANADA	BO	LABRADOR
	31AK09660	1962/09/26 1962/10/13	USA	BO	ATKA
	31ER62001	1962/03/09 1962/03/21	USA	BO	ERICA DAN
	31EV01760	1962/04/01 1962/07/28	USA	BO	EVERGREEN
	58GS00920	1962/04/19 1962/07/10	NORWAY	BO	G.O.SARS
	90TP62037	1962/05/07 1962/07/05	USSR	BO	TOPSEDA
	90TP62038	1962/08/19 1962/10/23	USSR.	BO	TOPSEDA
1963	06WH00600	1963/12/07 1963/12/11	GERMANY	BO	WALTHER HERWIDG
	181063003	1963/06/30 1963/07/05	BIO, CANADA	BO	THETA
	181063005	1963/09/15 1963/10/25	BIO, CANADA	BO	LABRADOR
	26DA63003	1963/06/30 1963/08/03	DENMARK	BO	DANA
	31EV63001	1963/07/17 1963/08/04	USA	BO	EVERGREEN
	58GS63001	1963/04/09 1963/05/09	NORWAY	BO	G.O.SARS
1964	06WH00610	1964/06/19 1864/11/23	BSH, GERMANY	BO	WALTHER HERWIDG
	181064020	1964/09/05 1964/10/22	BIO, CANADA	BO	LABRADOR
	26DA64075	1964/07/13 1964/07/24	DENMARK	BO	DANA
1965	06WH00620	1965/01/25 1965/12/01	BSH, GERMANY	BO	WALTHER HERWIDG
	180565039	1965/07/12 1965/08/23	NAFC, UK	BO	A.T.CAMERON
	181065001	1965/08/28 1965/10/20	BIO, CANADA	BO	LABRADOR
	319965008	1965/08/31 1965/09/16	USA	BO	UNKNOWN
	31EV65001	1965/07/28 1965/08/06	USA	BO	EVERGREEN
1966	26DA00300	1966/06/29 1966/08/05	DENMARK	BO	DANA
	31ED66001	1966/07/30 1966/08/31	USA	BO	EDISTO
1967	06WH00820	1967/10/13 1967/11/05	GERMANY	BO	WALTHER HERWIDG

	180267013	1967/08/17 1967/09/09	IOS, CANADA	BO	LABRADOR
	90NO67022	1967/08/12 1967/12/01	USSR	BO	NVOROSIYSK
1968	06WH00830	1968/07/21 1968/08/15	GERMANY	BO	WALTHER HERWIDG
	180268013	1968/08/15 1968/09/15	IOS, CANADA	BO	LABRADOR
	31WE13780	1968/09/08 1968/09/23	USA	BO	WESTWIND
1969	06WH00710	1969/02/25 1969/03/18	BSH, GERMANY	BO	WALTHER HERWIDG
	06WH00840	1969/01/26 1969/11/12	BSH, GERMANY	BO	WALTHER HERWIDG
	90PE69002	1969/07/06 1969/09/13	USSR	BO	PERSEI III
1970	181069050	1970/01/06 1970/10/11	BIO, CANADA	BO, BT	HUDSON
1971	180271014	1971/08/18 1971/08/29	IOS, CANADA	BO	LOUIS S. ST.LAURENT
	26DA00800	1971/07/11 1971/08/24	DENMARK	BO	DANA
1972	18QU72001	1972/08/23 1972/09/25	UNKNOWN	BO	QUEST
	26RG72001	1972/02/23 1972/07/08	DENMARK	BO	RESEARCH VESSELS IN GREENLAND
	90P372010	1972/10/24 1973/01/20	USSR	BO	PERSEI III
1973	26RG73001	1973/01/18 1973/10/24	DENMARK	BO	RESEARCH VESSELS IN GREENLAND
1974	26RG74001	1974/01/08 1974/11/27	DENMARK	BO	RESEARCH VESSELS IN GREENLAND
1975	182775002	1975/04/26 1975/05/25	UNKNOWN	BO	LAND BASED PARTY
	18VA75001	1975/04/26 1975/05/25	UNKNOWN	BO	VARIOUS SMALL VESSELS
	26RG75001	1975/01/06 1975/11/27	DENMARK	BO	RESEARCH VESSELS IN GREENLAND
1976	26RG76001	1976/01/12 1976/12/02	DENMARK	BO	RESEARCH VESSELS IN GREENLAND
1977	181077999	1977/08/16- 1977/09/04	UNKNOWN	CD	UNKNOWN
	18HU77024	1977/08/23- 1977/09/16	BIO, CANADA	BO, CD	HUDSON
	26RG77001	1977/01/10- 1977/12/21	DENMARK	BO	RESEARCH VESSELS IN GREENLAND
1978	180078903	1978/07/23- 1978/10/08	NOAA, U.S.A.	CD	UNKNOWN
	18HU78026	1978/08/26- 1978/09/14	BIO, CANADA	BO	HUDSON
	26AJ78001	1978/01/02-	ICES, DENMARK	BO	A JENSEN

		1978/12/27			
1979	180078903	1978/07/23- 1979/10/12	BIO, CANADA	CD	UNKNOWN
1980	18HU80027	1980/07/14- 1980/09/10	BIO, CANADA	BO, CD	HUDSON
	18HU80028	1980/09/01- 1980/09/10	BIO, CANADA	BO, CD	HUDSON
	26AJ80001	1980/01/21- 1980/11/29	UNKNOWN	BO	ADOLF JENSEN
	26RG80001	1980/01/21- 1980/11/29	UNKNOWN	BO	RESEARCH VESSELS IN GREENLAND
	90PH80021	1980/07/31- 1980/11/09	UNKNOWN	BO	PROTSION
1981	26AJ81001	1981/03/30- 1981/12/16	UNKNOWN	BO	ADOLF JENSEN
1982	26RG82001	1982/01/14- 1982/11/11	UNKNOWN	BO	RESEARCH VESSELS IN GREENLAND
1983	181183009	1983/02/02- 1983/06/09	MEDS, CANADA	BO	UNKNOWN
	18HU83023	1983/09/06- 1983/09/14	BIO, CANADA	BO	HUDSON
	26RG83001	1983/01/03- 1983/10/28	UNKNOWN	BO	RESEARCH VESSELS IN GREENLAND
	26RG83002	1983/10/28- 1983/12/20	UNKNOWN	BO	RESEARCH VESSELS IN GREENLAND
1984	181084039	1984/09/26- 1984/10/03	BIO, CANADA	CD	BAFFIN
	18BA84031	1984/07/31- 1984/08/12	BIO, CANADA	BO, CD	BAFFIN
	26RG84002	1984/05/05- 1984/12/06	UNKNOWN	BO	RESEARCH VESSELS IN GREENLAND
1985	181085029	1985/10/03- 1985/10/15	BIO, CANADA	CD	BAFFIN
	26RG85001	1985/01/02- 1985/11/24	UNKNOWN	BO	RESEARCH VESSELS IN GREENLAND
1986	181086021	1986/07/27- 1986/08/23	BIO, CANADA	CD	HUDSON
	26RG86001	1986/04/05- 1986/08/17	UNKNOWN	BO	RESEARCH VESSELS IN GREENLAND
1987	181087031	1987/08/26- 1987/09/16	BIO, CANADA	CD	HUDSON
	26AJ87260	1987/03/05- 1987/07/21	BIO, CANADA	BO	ADOLF JENSEN
	90KS87001	1987/09/11- 1987/12/09	UNKNOWN	BT, BO	KAPITAN SHAYTANOV
1988	181088037	1988/10/01- 1988/10/15	BIO, CANADA	CD	BAFFIN
	26AJ88260	1988/06/26- 1988/11/29	BIO, CANADA	BO	ADOLF JENSEN
	90KS88012	1988/09/01- 1988/12/11	UNKNOWN	BT, BO	KAPITAN SHAYTANOV

1989	06WH89001	1989/10/18- 1989/11/22	BIO, CANADA	BO	W. HERWIG
	181089016	1989/08/06- 1989/09/28	BIO, CANADA	CD	DAWSON
	26AJ89001	1989/06/20- 1989/07/10	ICES, DENMARK	CD	ADOLF JENSEN
1990	181090022	1990/09/03- 1990/09/16	BIO, CANADA	CD	HUDSON
	26AJ90001	1990/06/07- 1990/07/03	ICES, DENMARK	CD	ADOLF JENSEN
	26MS90001	1990/07/19- 1990/09/04	ICES, DENMARK	CD	MANIITSOQ
1991	06WH91001	1991/10/23- 1991/11/21	BIO, CANADA	BO	W. HERWIG
	189191001	1991/05/17- 1991/05/18	UNKNOWN	CD	M.V.ARTIC
	Ruks91	1991/09/13- 1991/12/04	RUSSIA	BO	SHAITANOV
1992	26TU92001	1992/06/19- 1992/06/27	BIO, CANADA	CD	TULUGAQ
1993	06WH93001	1993/09/18- 1993/10/21	BIO, CANADA	BO, BT	W. HERWIG
	26TU93001	1993/07/01- 1993/07/09	BIO, CANADA	CD	TULUGAQ
1995	18SN95026	1995/08/03- 1995/09/04	IOS, CANADA	CD	LOUIS S. ST. LAURENT
	26TU95001	1995/07/02- 1995/07/08	ICES, DENMARK	CD	TULUGAQ
1996	26PA96001	1996/07/08- 1996/09/19	ICES, DENMARK	CD	PAAMIUT
	26TU96001	1996/06/28- 1996/07/04	ICES, DENMARK	CD	TULUGAQ
1997	18SN97020	1997/08/03- 1997/08/19	IOS, CANADA	CD	RB YOUNG
	18SN97021	1997/08/19- 1997/08/26	IOS, CANADA	CD	ST.LAURENT
	26PA97001	1997/08/15- 1997/09/01	ICES, DENMARK	CD	PAAMIUT
	26TU97001	1997/06/27- 1997/07/07	ICES, DENMARK	CD	TULUGAQ
1998	18RD98012	1998/04/04- 1998/07/21	IOS, CANADA	CD	PIERRE RADISSON
	26PA98001	1998/07/28- 1998/09/01	ICES, DENMARK	CD	PAAMIUT
	26TU98001	1998/06/24- 1998/07/04	ICES, DENMARK	CD	TULUGAQ
1999	06WH99211	1999/10/10- 1999/11/08	BSH, GERMANY	CD	W. HERWIG
	26PA99001	1999/07/22- 1999/08/26	ICES, DENMARK	CD	PAAMIUT
	26TY99001	1999/07/22-	ICES, DENMARK	CD	TULUGAQ

		1999/08/26			
	18RD99039	1999/08/23- 1999/10/02	IOS, CANADA	CD	PIERRE RADISSON
2001	SOI2001	August 2001	IOS, CANADA	CD	AKADEMIK IOFFE